ABSTRACT

NUMERICAL STUDIES OF UNSTEADY, TWO-DIMENSIONAL LIQUID IMPACT PHENOMENA

by

Yen-Chen Huang

Co-chairmen: Frederick G. Hammitt
Wen-Jei Yang

The dynamics of high speed impact between a compressible water droplet and a rigid solid surface is investigated analytically. The purpose of the study is to examine the environment leading to the erosion mechanism of a material due to the liquid impingement.

A Compressible-Cell-and-Marker numerical method is developed to solve the differential equations governing the unsteady, two-dimensional liquid-solid impact phenomena. The method is designed to solve this unsteadiness up until the time reasonably approaches steady state solution. The validity of the method is confirmed by comparing its numerical results with the exact solution for the classical one-dimensional liquid impact problem. The accuracy of the numerical results is found to be superior to the other existing comparable numerical methods in this type of application.

Viscosity and surface tension are neglected as compared with the magnitude of impact pressure. Pressure and velocity distribution are solved as a function of time. The deformation of a drop is also recorded for three different shapes: cylinder, sphere, and a combination of both. Two different impact Mach numbers, 0.2 and 0.5, which refer to water, are studied. Two different conditions, free-slip and non-slip, are investigated.

After the first instant of impact, the pressure build-up and

the lateral flow begin simultaneously. However, the expansion of the droplet near the contact edge due to the lateral flow is not appreciable during the early stage of impact. The calculation also indicates that a zone of negative pressure appears on the upper region of the droplets where cavitation has been observed, but shows no bursting out of the top surface, because the compression is continuously released as the drop surface is free to deform. The occurrence of the negative pressure may result from either the reflection of a compression wave from the top surface or the rarefaction from the side of the droplet. The location of the negative pressure depends upon the initial geometry of the droplet and the impact Mach number. The maximum pressure in this two-dimensional liquid impact problem is found to be less than the one-dimensional maximum pressure for all three different droplets in various degrees. As time elapses, the maximum pressure shifts from the center of the contact area radially outward, while the pressure at the center attenuates to the stagnation pressure.

THE UNIVERSITY OF MICHIGAN

College of Engineering

Department of Mechanical Engineering

Cavitation and Multiphase Flow Laboratory

Report No. UMICH 03371-8-T

NUMERICAL STUDIES OF UNSTEADY, TWO-DIMENSIONAL LIQUID IMPACT PHENOMENA

by

Yen-Chen Huang
Approved by: F. G. Hammitt

Financial Support Provided by:

National Science Foundation
Grant No. GK-730

July 1971

ACKNOWLEDGEMENTS

The author wishes to thank his thesis chairman Professor Frederick G. Hammitt for suggesting the thesis research topic and for his constant advice and support during this investigation. Deep gratitude is due to Professor Wen-Jei Yang who served as co-chairman during the period Professor Hammitt was on leave of absence in France, for his long hours of guidance often until late afternoon. Appreciation is also expressed to Professor George Springer for many of his discussion with great interests; to Dr. Robert Hickling for his valuable comments and suggestions and to Professor Clarence Siebert for serving on the doctoral committee. Special thanks are indebted to my colleague Dr. Terry M. Mitchell for his participation in numerous of the author's thesis meetings. The assistance of Virginia Wild in the preparation of the final manuscript is very much appreciated.

The author also wishes to gratefully acknowledge the project financial supports from the Naval Air Development Center and National Science Foundation; the fellowship financial supports from E. I. DuPont de Numours and Co., Inc., Air Products and Chemicals Inc., and the University of Michigan; the computing financial support from the University Computing Center, without all of these supports, the thesis would not have been possible.

TABLE OF CONTENTS

LIST OF FIGURES

NOMENCLATURE

Symbol	Description
A	Exponent in Tait's equation of state
A_1, A_2 B_1, B_2	Coefficients in equation of motion after normalization
B	Constant in Tait's equation of state
C	Shock wave velocity
C_o	Sonic Velocity
D	Diameter
E	Specific total energy
e	Specific internal energy
F_z, F_r	External forces in z- and r- direction, respectively
H_1, H_2	Dimensions of Computation Domain in z- and r- direction, respectively
I_m, J_m	Mesh indices of marker m
K	Constant
L	Length
M	Mach number
p	Pressure
p^o	$p/\rho_o C_o V_o$
R	Radius
R_m	Location of marker m in r- coordinate
r	Radial coordinate
r^o	r/R
t	Time
t_1, t_2	Durations defined in Eqs. (3-5) and (3-6)
t^o	Non-dimensional time, Ct/D
U	Marker velocity component in z-direction
u	Velocity component in z-direction
u_n	Velocity component in normal direction
V	Marker velocity component in r-direction

v	Velocity component in r-direction
v_t	Velocity component in tangential direction
V_o	Impact velocity
x_n	Coordinate in normal direction
x_t	Coordinate in tangential direction
z	Vertical coordinate
z^o	z/L
Z_m	Location of marker m in z-coordinate
α	Stability factor
ρ	Density

Subscripts

c	Characteristic parameter
i	Finite difference mesh index in z-direction
j	Finite difference mesh index in r-direction
k	$i \pm 1/2$
ℓ	$j \pm 1/2$
m	Marker index
o	Initial value

Superscripts

*	Normalized variable by characteristic parameter
o	Non-dimensional variable
n	n-th finite difference time step index

CHAPTER I
INTRODUCTION

In recent years, there is growing concern on the problem of erosion as a result of severe local pressures and pressure changes due to liquid impingement on high speed machinery and aircraft components.

The earliest attention[1, 2] for liquid impact erosion arose in hydraulic (Pelton) and wet steam turbines. When the steam turbine stages operate in the region of vapor-liquid mixture, after the steam has expanded from the high pressure state, the liquid droplets are impacted by the rotating blades at about the operating speed of the turbine[3, 4, 5]. With the higher velocities in the very large new turbine designs, it is likely that the erosion problem can no longer be met through improved materials.

Likewise, in the late 1940's when the speeds of aircraft exceeded Mach 0.5, rapid erosion was experienced by aircraft flying through rain[6] particularly on propellor blades. The problem has become increasingly severe with the present much higher speed aircraft, and also with helicopter blades. Research has been sponsored in this country[7] and also in many other countries,[8] with attention focusing now on radome, window, and structural materials of fixed-wing aircraft and helicopters, as well as missiles to avoid degraded performance and possible failure. The phenomena are similar to the liquid droplet impact erosion of steam turbines and hydraulic Pelton turbines.

It has been suggested[9, 10, etc.] that the damaging mechanism of cavitation may actually be a liquid jet impingement resulting from the non-symmetrical collapse of a bubble. Cavitation erosion is important for high speed ship propellers and other components as well as many other power plant components such as pumps, etc.[11] Erosion is also a problem in turbines[12, 13] and pumps[14, 15] of space

power plants using liquid metals as the working fluid, as well as in present sodium-cooled fast breeder reactor power plants and in many other cases involving many different fluids.[11]

Soil erosion caused by raindrop impact, a rather analogous phenomenon, also has received attention[16] in the present tide of interest in ecology.

A. Background

Liquid droplet or liquid jet impact on a solid surface has been observed for centuries. The first extensive description of this phenomena was that given by Worthington[17] around 1894. Considerable pioneering work in more recent years was conducted by Dr. Olive Engel[18] since the early 1950's. Her work[19] includes a chemical mapping of the radial water flow on the impact plane, the use of high-speed motion-picutre photography to record the motion of the impacting water drop, and the use of Schlieren photography to study details in the radial flow. Bowden and Brunton[20] reported on fundamental studies of liquid jet impact at supersonic speed. Recently, Fyall[21] used a turbine-driven Barr and Stroud CP5 rotating mirror camera (2×10^5 - 8×10^6 pps) to record photographically the collision process of a moving target with a single stationary water drop in order to study the basic mechanisms of rain erosion. The study of liquid jet impact is currently under way in this laboratory (Cavitation and Multiphase Flow Laboratory, Mechanical Engineering Department) using highly sophisticated photographic apparatus, such as a Beckman-Whitley camera. The above are merely typical citations from a very numerous and growing literature in this field.

Photographic studies[19, 20, 21] have shown that the maximum lateral velocity typically considerably exceeds the impact velocity. The resulting sheet of liquid spreads radially around the periphery of the contact zone, while the remaining portion of the drop is relatively undeformed. This suggest that compressibility effects are important

in the liquid-solid impact phenomena.

In the initial stages of the impact, the sudden deceleration of the liquid will establish a large pressure gradient. The spatial gradients of velocities are negligible compared with the large magnitude of local acceleration.

For the one-dimensional case, during the early phases of impact, the integration of the appropriate equation of motion

$$\frac{\partial v}{\partial t} = -\frac{\partial p}{\partial z} \tag{1.1}$$

yields the well-known "water hammer pressure"

$$p = \rho_o C V_o \tag{1.2}$$

where ρ_o is the density of the ambient liquid, V_o is the impact velocity, and C is the shock wave velocity with respect to the undisturbed liquid. Tait[22] in 1888 proposed the following equation of state for water:

$$\frac{p + B}{p_o + B} = \left(\frac{\rho}{\rho_o}\right)^A \tag{1.3}$$

where B and A are two empirical functions of temperature. The values of A and B will be considered in the Appendix A. The combination of Equations (1.2) and (1.3) yields the shock wave velocity[23] as

$$C^2 = \frac{p_o + B}{\rho_o} \cdot \frac{1 - \left(1 - \frac{V_o}{C}\right)^A}{\frac{V_o}{C}\left(1 - \frac{V_o}{C}\right)^A} \tag{1.4}$$

Heymann[24] derived a convenient approximation for the shock wave velocity which is an explicit function of impact velocity only

$$C = C_o (1 + 2V_o) \tag{1.5}$$

where C_o is the sonic velocity in the undisturbed liquid. The above expression is in good agreement with measured shock wave velocity data for water from various sources[25, 26, 27, 28, 29]. It is recommended for use only up to $V_o/C_o = 1.2$. In the reference[23], a

second order approximation for cold water was derived

$$\frac{C}{C_o} = 1 + 1.925 \frac{V_o}{C_o} - 0.083 \left(\frac{V_o}{C_o}\right)^2 \qquad (1.6)$$

by a least square fit computer program for V_o/C_o up to 3. Within this range, prediction for C from Equations (1.4) and (1.6) agree to within $\pm$ 2%.

The present author has now derived another second order approximation yet more convenient to estimate the shock wave velocity in water, for V/C_o also up to 3. This is

$$\frac{C}{C_o} = 1 + 2 \frac{V_o}{C_o} - 0.1 \left(\frac{V_o}{C_o}\right)^2 \qquad (1.7)$$

Savic and Boult[30] presented a mathematical analysis of the low speed impact and spreading of a spherical liquid drop on a rigid surface but did not take compressibility into account.

Engel[19] performed an approximate analysis of spherical droplet liquid-solid impact and modified the water hammer equation as follows, for the plane rigid surface,

$$p = \frac{\gamma}{2} \rho_o C_o V_o \qquad (1.8)$$

where γ is a coefficient giving the fraction of impact velocity. It approaches unity for high impact velocities.

Heymann[31] presented new quantitative results for the maximum impact pressure generated which is in some cases the order of 3 times the simple water hammer pressure. His analysis assumes that at the first instant of contact, the pressures have already built up to $\rho_o C V_o$. The present analysis shows that this assumption may not be valid.

B. Review of Solution Technique

To obtain a closed-form solution by analytically solving the general transport equations with the constitutive relations of the materials is formidable, and probably impossible, because of the unsteady, non-linear, non-homogeneous natures of the problems. The development of high speed computers has made it feasible to solve a wide variety of complex time-dependent, multi-dimensional problems by using numerical techniques. Various methods are available for solving certain classes of problems, but each of the known methods has certain limitations. A comprehensive survey of numerical methods, applications, investigators, and representative programs for transient fluid flow in two or more dimensions has been presented by Harlow.[56]

Basically, there are two numerical schemes, Eulerian and Lagrangian. The Eulerian scheme can further be classified according to choice of primary variables (pressure and velocity) method and also secondary variables (stream function and velocity) method. In all Eulerian methods, the coordinate system is fixed in the reference frame, while in Lagrangian scheme, the moving coordinate system is embedded into the configuration to be studied. The Eulerian schemes cannot easily handle free surfaces, moving boundaries or contact discontinuities which separate two materials. However, Eulerian schemes cause no difficulty for those single-phase problems in which turbulence or large distortion is encountered. On the contrary, in Lagrangian schemes, the material interfaces can be precisely followed, free surface boundary conditions can be applied, and arbitrary shape can be present. However, when the configuration becomes badly distorted, the calculation becomes less accurate. A combination of both Eulerian and Lagrangian schemes may overcome some of the difficulties of both, while offering some of the advantages. There are a number of such approaches

such as Marker-and-Cell (MAC) method[57,58], Particle-in-Cell (PIC) method[59,60], and Implicit Continuous-Fluid Eulerian (ICE) method[61]. Some were developed from those just mentioned above with modification such as SUMMAC (Stanford University Modified MAC) method[62] to studies of finite-amplitude water waves and the modification of MAC in the Reference 70 to studies of collapsing bubbles, while others developed independently such as Coupled-Eulerian-Lagrangian (CEL) method.[63] Both MAC and PIC methods have been applied to the impact of fluid drops. However, MAC is limited to incompressible fluid, while PIC appears to be applicable only to the hypervelocity impact.

The numerical method, which is developed in this study, also is a combination of both Eulerian and Lagrangian schemes. While the Lagrangian portion of the numerical calculation is used to mark the phase boundary, the modified two-step, nine-point Lax and Wendroff explicit Eulerian method[64,65,66,67] is developed to offer the compressibility which is lacking in the MAC method.

C. Objective

The bulk of prior research on liquid-solid impact has been limited to high-speed photographic studies, other experimental investigations, and relatively simple analyses. The main objective of this thesis is to analytically investigate the problem of liquid-solid impact: formulate the transient, two-dimensional governing equations plus equation of state for water and then, by using the numerical technique, to find the solution for the flow patterns and impact pressure and velocity distribution developed in a liquid drop or liquid jet following its collision with a plane rigid surface, using dimensionless parameters as far as possible to make the results as generally applicable as possible. Results will provide the information for the further understanding of the basic mechanism in the liquid impingement.

CHAPTER II

THEORETICAL INVESTIGATION

A. Formulation of the Problem

Three phases are involved in the phenomenon of liquid-solid impact: A liquid droplet which has travelled through a gaseous region strikes a solid surface. Equations and boundary conditions describing the situations are coupled. Therefore, it is a formidable task to obtain the analytical solution. However, in order to get a tractable solution, one may treat the liquid phase as a distributed system, subjected to the boundary condition at the interfase with solid and gas.

The solid target material may respond to the impact like an essentially rigid body with negligible deformation, an elastic body, a plastic body, or even like a fluid, depending upon the velocity of impact. The problem treated in its most general aspects requires a detailed investigation of the manner in which the material would behave rheologically under an impact. Some compromise must be made between the complexity of the physical problem and the practical difficulties involved in solving the equations governing the model selected. In the following analysis, the surface will be assumed to behave like a rigid body. This model, representing a limiting case, is of great practical importance, and will provide an insight into the nature of the impact phenomenon.

The compressibility of the liquid must be taken into account in any valid and realistic analysis, unless the impact velocity is extremely small (and of little practical interest). As will be seen later, compressibility effects are predominant in the liquid response. Therefore, if they are neglected, an infinitely large pressure will be produced at the first instant of impact.

However, it is reasonable to neglect the effects of surface tension and viscosity. This is especially valid for high speed impacts,

particularly when the liquid is water with its low viscosity. Body forces will also be neglected in the study. Cylindrical coordinates were selected, simply because they are most suitable to deal with the axisymmetric phenomena which will be assumed.

Under these assumptions, the equations governing the phenomena when a liquid droplet of spherical or cylindrical shape strikes a rigid solid surface are written as follows.

The equation of continuity for the liquid phase gives:

$$\frac{\partial \rho}{\partial t} + \frac{\partial(\rho u)}{\partial z} + \frac{1}{r}\frac{\partial(r\rho v)}{\partial r} = 0 \qquad (2.1)$$

The momentum equations for the liquid phase:

$$\frac{\partial(\rho u)}{\partial t} + \frac{\partial(\rho u^2)}{\partial z} + \frac{1}{r}\frac{\partial(r\rho vu)}{\partial r} = -\frac{\partial p}{\partial z} \qquad (2.2)$$

$$\frac{\partial(\rho v)}{\partial t} + \frac{\partial(\rho vu)}{\partial z} + \frac{1}{r}\frac{\partial(r\rho v^2)}{\partial r} = -\frac{\partial p}{\partial r} \qquad (2.3)$$

with the equation of state for water

$$\frac{p + B}{p_o + B} = \left(\frac{\rho}{\rho_o}\right)^A \qquad (2.4)$$

where u and v are the axial and radial velocity components respectively for the cylindrical coordinates z and r. Time t is another independent variable, and ρ and p are the fluid density and pressure. The values of the two constants in the equation of state for water are chosen (as discussed in Appendix A)

$$A = 7.15 \qquad B = 3.047 \text{ kilobars} \qquad (2.5)$$

Strictly speaking, it would require also the energy equation for the fluid

$$\frac{\partial(\rho E)}{\partial t} + \frac{\partial(\rho uE)}{\partial z} + \frac{1}{r}\frac{\partial(r\rho vE)}{\partial r} + \frac{\partial(pu)}{\partial z} + \frac{1}{r}\frac{\partial(rpv)}{\partial r} = 0$$

to complete the formulation, where $E = e + 1/2\,(u^2 + v^2)$ is the specific total energy, and e is the specific internal energy. Since the main concern here is not the energy transfer, and since the process is practically isothermal over the very short duration of impact (order of 1 μsec.), the energy balance problem in the stream will not be considered.

On the other hand, the approximate equation of motion and the kinematics relations for the marker particles used in the Lagrangian calculation are:

$$\frac{d(mU)}{dt} = \Sigma\ F_z \tag{2.6}$$

$$\frac{d(mV)}{dt} = \Sigma\ F_r \tag{2.7}$$

$$U = \frac{dZ}{dt} \tag{2.8}$$

$$V = \frac{dR}{dt} \tag{2.9}$$

where mU and mV are the momentums of a marker particle subject to external forces F_z and F_r in the z- and r- direction respectively.

One defines

$$t^* = \frac{t}{t_c}\ , \qquad z^* = \frac{z}{z_c}\ , \qquad r^* = \frac{r}{r_c}$$

$$\rho^* = \frac{\rho}{\rho_c} \qquad u^* = \frac{u}{u_c}\ , \qquad v^* = \frac{v}{v_c} \tag{2.10}$$

$$p^* = \frac{p}{p_c}\ , \qquad B^* = \frac{B}{p_c}\ ,$$

where ρ_c, u_c, v_c, p_c, t_c, z_c, r_c are the characteristic parameters of the problem. The non-dimensional governing equations, after

dropping the asterisk, *, may be expressed in normalized form for the Eulerian calculation:

$$\frac{\partial \rho}{\partial t} + A_1 \frac{\partial(\rho u)}{\partial z} + A_2 \frac{1}{r} \frac{\partial(r\rho v)}{\partial r} = 0 \qquad (2.11)$$

$$\frac{\partial(\rho u)}{\partial t} + A_1 \frac{\partial(\rho u^2)}{\partial z} + A_2 \frac{1}{r} \frac{\partial(r\rho vu)}{\partial r} = -B_1 \frac{\partial p}{\partial z} \qquad (2.12)$$

$$\frac{\partial(\rho v)}{\partial t} + A_1 \frac{\partial(\rho uv)}{\partial z} + A_2 \frac{1}{r} \frac{\partial(r\rho v^2)}{\partial r} = -B_2 \frac{\partial p}{\partial r} \qquad (2.13)$$

$$\frac{p + B}{p_o + B} = \left(\frac{\rho}{\rho_o} \right)^A \qquad (2.14)$$

and in the Lagrangian calculation:

$$\frac{d(\rho U)}{dt} \cong B_1 \frac{dp}{dz} \qquad (2.15)$$

$$\frac{d(\rho V)}{dt} \cong B_2 \frac{dp}{dr} \qquad (2.16)$$

where

$$A_1 = \frac{u_c t_c}{z_c} \quad , \quad A_2 = \frac{u_c t_c}{r_c}$$
$$B_1 = \frac{p_c t_c}{\rho_c u_c z_c} \quad , \quad B_2 = \frac{p_c t_c}{\rho_c u_c r_c} \qquad (2.17)$$

One may select the characteristic parameters ρ_c, u_c, p_c, t_c, z_c, r_c in such a way that all the coefficients A_1, A_2, B_1, and B_2 become unity. However, for convenience in the discrete numerical

computation, and for the nature of the problem, the characteristic parameters will be chosen such as the following. Characteristic density ρ_c will be the undisturbed density at 1 atm ρ_o. Characteristic velocity u_c will be the impact velocity V_o. Characteristic pressure p_c will be the simple water hammer pressure based on $\rho_o C_o V_o$. z_c and r_c are the cell size dimensions in z and r directions, respectively. It is convenient in many cases that they be chosen to be equal. There will be a definite relationship between z_c, r_c and the characteristic lengths of the problem, e.g., the length and the diameter of a cylindrical liquid droplet. Characteristic time t_c will be z_c/C, where C is the shock wave velocity defined in the Eqs. (1.4) and (1.6). After such selection of characteristic parameters, the four parameters in the governing equations: A_1, A_2, B_1, B_2 can be reduced to $A_1=A_2=M/(1+2M-0.1M^2)$, and $B_1=B_2=1/(1+2M-0.1M^2)$, where $M = V_o/C_o$.

The appropriate initial conditions over the domain of calculation are

$$p = p_o \qquad u = u_o \qquad v = v_o$$

where p_o is the environmental pressure, u_o and v_o are the initial impact velocities in z- and r- direction respectively. In the case of a normal impact (i.e., perpendicular), $v_o = 0$ of course and $V_o = u_o$. The appropriate boundary conditions are:

i) along the axisymmetric axis(z), r = 0, and symmetry requires

$$v = 0, \quad \frac{\partial u}{\partial r} = 0, \quad \frac{\partial p}{\partial r} = 0$$

ii) along the impacted rigid surfaces, z = 0, $\frac{\partial v}{\partial z} = 0$, u = 0, $\frac{\partial p}{\partial z} = 0$, for full-slip wall condition, which, strictly speaking, an assumption of zero viscosity would necessitate, and v = 0, u = 0, $\frac{\partial p}{\partial z} = 0$ for non-slip wall condition.

iii) along the free surface, incompressible continuity condition

yields $$p = p_o, \quad \frac{\partial u_n}{\partial x_n} = \frac{\partial v_t}{\partial x_t} = 0$$

where u_n and v_t are the moving velocity components of the liquid-air interface in the normal x_n and tangential x_t directions of the surface respectively.

iv) along the sides of the finite computational domain, permeable boundary conditions will be imposed, in such a way that the normal space derivative of the variable vanishes at the boundary,

$$\frac{\partial u}{\partial z} = 0, \quad \frac{\partial v}{\partial z} = 0, \quad \frac{\partial p}{\partial z} = 0 \quad \text{at } z = H_1$$

$$\frac{\partial u}{\partial r} = 0, \quad \frac{\partial v}{\partial r} = 0, \quad \frac{\partial p}{\partial r} = 0 \quad \text{at } r = H_2$$

where H_1 and H_2 are sizes of computational domain in z- and r- direction respectively.

B. Compressible Cell-and-Marker (ComCAM) Numerical Solution Method

The method begins with an Eulerian grid as shown in Figure 1. Field variables such as density and velocity are directly associated with the cells of the grid. In addition to the grid, a series of Marker particles are assigned to the liquid. These particles are necessary to mark the free surface movement. Numerical computation will start with particles located only along the surface. This arrangement is possible because of the condition that fluid particles initially on the free boundary always remain on the free boundary.[71]

The cells of the grid system are labeled with the indices i, j; further the density ρ, the pressure p, and the velocity components u and v are defined at the center of each cell as $\rho_{i,j}$, $p_{i,j}$, $u_{i,j}$, and $v_{i,j}$, respectively. The superscript n+1 indicates that the quantity

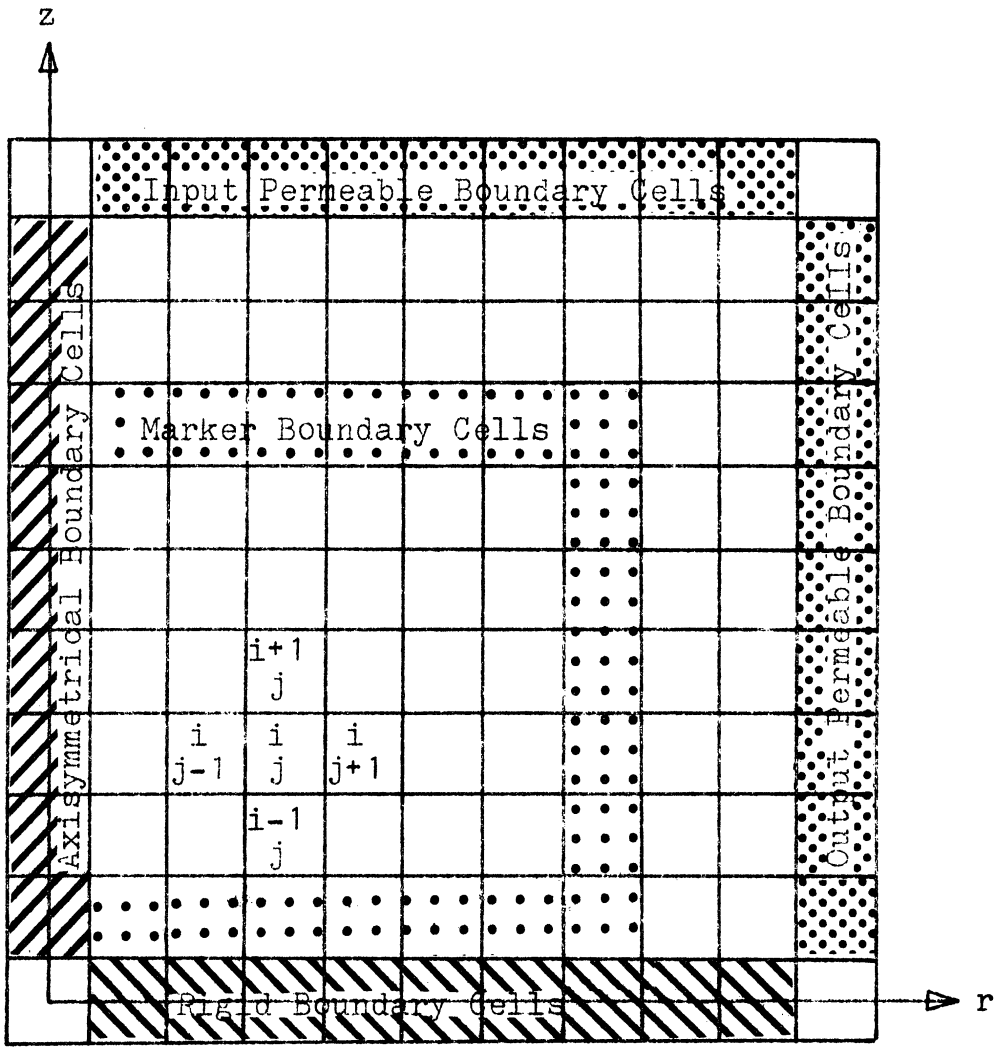

Figure 1

The Computing Mesh

is evaluated at $t = (n+1)\Delta t$, while n denotes that the evaluation is at $t = n\Delta t$. The subscript m is used for particles; the velocity and position of a Marker particle and the position of the corresponding Marker cell are represented by (U_m, V_m), (Z_m, R_m), and (I_m, J_m), respectively.

For convenience in computation, the explicit form of the finite-difference approximation is adopted--expressing the sought-for future physical quantity at m for Marker particles or at node i, j for cells in terms of the other quantities. For a Marker particle, its future velocity components U_m^{n+1} and V_m^{n+1} satisfy the equation of motion for particles. Where $\alpha = C \Delta t/\Delta r = C \Delta t/\Delta z$

$$U_m^{n+1} = U_m^n + \frac{\alpha B_1}{\rho_{i,j}^n} \left(p_{i+\frac{1}{2},j}^n - p_{i-\frac{1}{2},j}^n\right) \tag{2.18}$$

$$V_m^{n+1} = V_m^n + \frac{\alpha B_2}{\rho_{i,j}^n} \left(p_{i,j-\frac{1}{2}}^n - p_{i,j+\frac{1}{2}}^n\right) \tag{2.19}$$

The new location (Z_m^{n+1}, R_m^{n+1}) of the particle is then determined utilizing the new velocity.

$$Z_m^{n+1} = Z_m^n - \frac{\alpha A_1}{2} \left(U_m^{n+1} + U_m^n\right) \tag{2.20}$$

$$R_m^{n+1} = R_m^n + \frac{\alpha A_2}{2} \left(V_m^{n+1} + V_m^n\right) \tag{2.21}$$

It is followed by the relocation of the corresponding Marker cell (I_m^{n+1}, J_m^{n+1}) based on the new particle location.

$$I_m^{n+1} = \text{Integer of } (Z_m^{n+1} + 0.5) \tag{2.22}$$

$$J_m^{n+1} = \text{Integer of } (R_m^{n+1} + 0.5) \tag{2.23}$$

The future density $\rho_{i,j}^{n+1}$ and pressure $p_{i,j}^{n+1}$ of a Marker cell on the free surface are assumed to take the reference values ρ_o and p_o, respectively. On the other hand, its velocity components $u_{i,j}^{n+1}$ and

$v_{i,j}^{n+1}$ are equated to those of the corresponding Marker particle, U_m^{n+1} and V_m^{n+1}, respectively. For interior cells, their future density $\rho_{i,j}^{n+1}$ and momentum components $(\rho u)_{k,\ell}^{n+1}$ and $(\rho v)_{k,\ell}^{n+1}$ are determined using the modified two-step nine-point Lax-Wendroff Eulerian scheme[64]. The scheme is essentially an explicit formulation through which a differential equation can be solved by finite-difference approximation without iteration procedure. The forward-and-central-difference representations are employed for the time and space derivatives, respectively. The first step of the Lax-Wendroff scheme is to compute the future density and momentum components at a corner of a cell ($k = i \pm 1/2$, $\ell = j \pm 1/2$) using the finite difference form of the continuity and momentum equations (2.24) through (2.26) written in terms of the present values at points $(k, \ell - 1/2)$, $(k, \ell + 1/2)$, $(k - 1/2, \ell)$ and $(k + 1/2, \ell)$. The basic structure for the first-step computation of the Lax Wendroff scheme is depicted in Fig. 2. The new velocity components $u_{k,\ell}^{n+1}$ and $v_{k,\ell}^{n+1}$ are then determined by dividing the new corresponding momentum components by the new density at the same cell k, ℓ Equations (2.27) and (2.28) the new location pressure $p_{k,\ell}^{n+1}$ is evaluated using the thermodynamic equation of state (2.29),

$$\rho_{k,\ell}^{n+1} = (\rho_{k+1/2,\ell+1/2}^{n} + \rho_{k-1/2,\ell+1/2}^{n} + \rho_{k+1/2,\ell-1/2}^{n} + \rho_{k-1/2,\ell-1/2}^{n}) / 4$$

$$+\alpha A_1 \left((\rho u)_{k+1/2,\ell}^{n} - (\rho u)_{k-1/2,\ell}^{n} \right)$$

$$+\alpha A_2 \left((\ell - 1/4)(\rho v)_{k,\ell-1/2}^{n} - (\ell + 1/4)(\rho v)_{k,\ell+1/2}^{n} \right) / \ell \qquad (2.24)$$

$$(\rho u)^{n+1}_{k,\ell} = \left((\rho u)^{n}_{k+1/2,\,\ell+1/2} + (\rho u)^{n}_{k-1/2,\,\ell+1/2} + (\rho u)^{n}_{k+1/2,\,\ell-1/2} + (\rho u)^{n}_{k-1/2,\,\ell-1/2} \right) / 4$$

$$+ \alpha A_1 \left((\rho u)^{n}_{k+1/2,\ell}\; u^{n}_{k+1/2,\ell} - (\rho u)^{n}_{k-1/2,\ell}\; u^{n}_{k-1/2,\ell} \right)$$

$$+ \alpha A_2 \left((\ell - 1/2)\,(\rho v)^{n}_{k,\,\ell-1/2}\; u^{n}_{k,\,\ell-1/2} - (\ell + 1/4)\,(\rho v)^{n}_{k,\,\ell+1/2}\; u^{n}_{k,\,\ell+1/2} \right) / \ell$$

$$+ \alpha B_1 \left(p^{n}_{k+1/2,\ell} - p^{n}_{k-1/2,\ell} \right) \qquad (2.25)$$

$$(\rho v)^{n+1}_{k,\ell} = \left((\rho v)^{n}_{k+1/2,\,\ell+1/2} + (\rho v)^{n}_{k-1/2,\,\ell+1/2} + (\rho v)^{n}_{k+1/2,\,\ell-1/2} + (\rho v)^{n}_{k-1/2,\,\ell-1/2} \right) / 4$$

$$+ \alpha A_1 \left((\rho u)^{n}_{k+1/2,\,\ell}\; v^{n}_{k+1/2,\ell} - (\rho u)^{n}_{k-1/2,\ell}\; v^{n}_{k-1/2,\ell} \right)$$

$$+ \alpha A_2 \left((\ell - 1/4)\,(\rho v)^{n}_{k,\,\ell-1/2}\; v^{n}_{k,\,\ell-1/2} - (\ell + 1/4)\,(\rho v)^{n}_{k,\,\ell+1/2}\; v^{n}_{k,\,\ell+1/2} \right) / \ell$$

$$+ \alpha B_2 \left(p^{n}_{k,\,\ell-1/2} - p^{n}_{k,\,\ell+1/2} \right) \qquad (2.26)$$

$$u^{n+1}_{k,\ell} = (\rho u)^{n+1}_{k,\ell} \;/\; \rho^{n+1}_{k,\,\ell} \qquad (2.27)$$

$$v^{n+1}_{k,\ell} = (\rho v)^{n+1}_{k,\ell} \;/\; \rho^{n+1}_{k,\ell} \qquad (2.28)$$

$$p^{n+1}_{k,\,\ell} = \left(\rho^{n+1}_{k,\ell} \;/\; \rho_o \right)^{A} (p_o + B) - B \qquad (2.29)$$

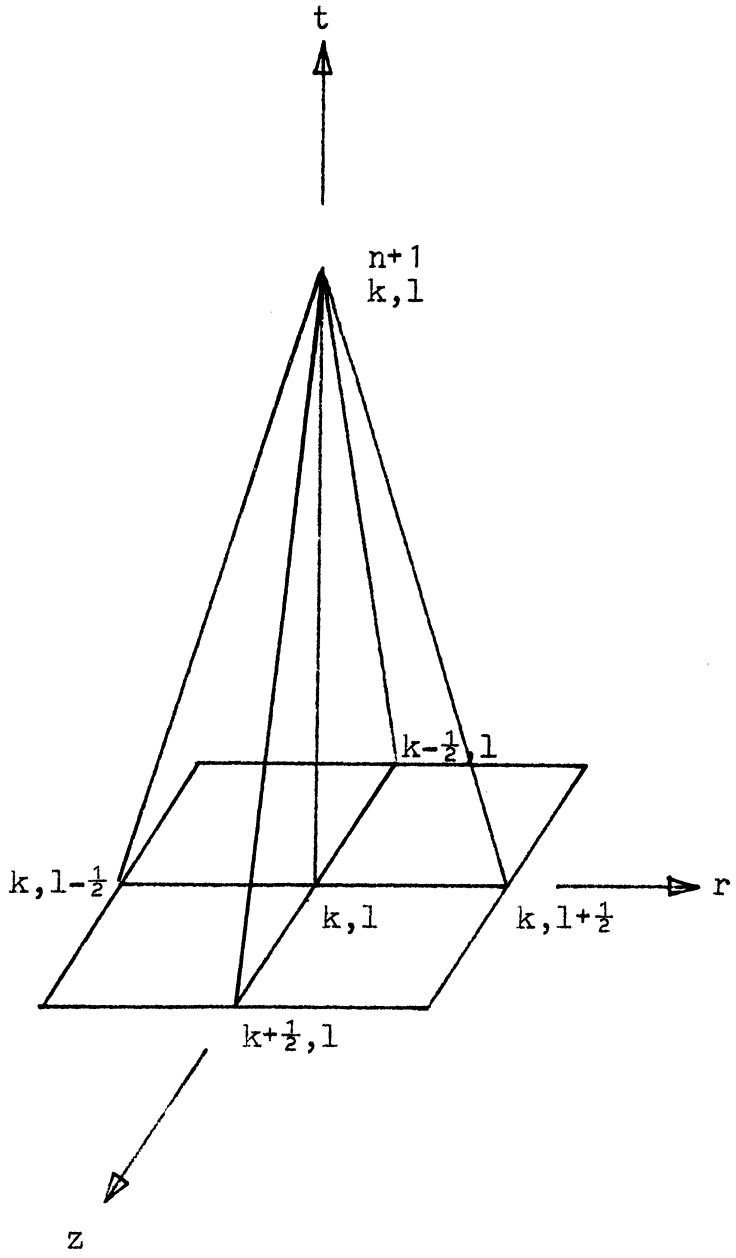

Figure 2

The Basic Structure for the First Step Computation of Modified Lax-Wendroff Scheme in the ComCAM Method

The second step of the Lax-Wendroff scheme is to calculate the new density and momentum components at cell center (i, j) using the finite-difference form of the continuity and momentum equations (2.30) through (2.32) expressed in terms of the new quantities at (i+1/2, j), (i-1/2, j), (i, j+1/2) and (i, j-1/2) determined in the first step of the Lax-Wendroff scheme and the old quantities at (i+1, j), (i-1, j), (i, j+1) and (i, j-1). The basic structure for the second-step computation of the Lax-Wendroff scheme is illustrated in Figure 3. It is followed by the determination of the new velocity components and pressure at cell center (i, j) by the same procedure as employed in the first-step computation. Equations (2.33) through (2.35)

$$
\begin{aligned}
\rho_{i,j}^{n+1} = \Bigg\{ & \rho_{i,j}^{n} + \left(\rho_{i+1/2,j}^{n+1} + \rho_{i-1/2,j}^{n+1} + \rho_{i,j-1/2}^{n+1} + \rho_{i,j+1/2}^{n+1}\right)/4 \\
& + \rho_{i,j}^{n} + \left(\rho_{i+1,j}^{n} + \rho_{i-1,j}^{n} + \rho_{i,j-1}^{n} + \rho_{i,j+1}^{n}\right)/4 \Bigg\} /4 \\
& + \alpha A_1 \Bigg\{ \left[(\rho u)_{i+1/2,j}^{n+1} - (\rho u)_{i-1/2,j}^{n+1} \right] - \left[(\rho u)_{i+1,j}^{n} \right. \\
& \left. - (\rho u)_{i-1,j}^{n} \right] /2 \Bigg\} /2 \\
& + \alpha A_2 \Bigg\{ \left[(j-1/4)\,(\rho v)_{i,j-1/2}^{n+1} - (j+1/4)\,(\rho v)_{i,j+1/2}^{n+1} \right] \\
& + \left[(j-1/2)\,(\rho v)_{i,j-1}^{n} - (j+1/2)\,(\rho v)_{i,j+1}^{n} \right] /2 \Bigg\} /2_j
\end{aligned}
\tag{2.30}
$$

$$
\begin{aligned}
(\rho u)_{i,j}^{n+1} = \Bigg\{ & (\rho u)_{i,j}^{n} + \left[(\rho u)_{i+1/2,j}^{n+1} + (\rho u)_{i-1/2,j}^{n+1} + (\rho u)_{i,j-1/2}^{n+1} \right. \\
& \left. + (\rho u)_{i,j+1/2}^{n+1} \right] /4 \\
& + (\rho u)_{i,j}^{n} + \left[(\rho u)_{i+1,j}^{n} + (\rho u)_{i-1,j}^{n} + (\rho u)_{i,j-1}^{n} + (\rho u)_{i,j+1}^{n} \right] /4 \Bigg\} /4
\end{aligned}
$$

$$+\alpha A_1 \left\{ \left[(\rho u)^{n+1}_{i+1/2,j} \; u^{n+1}_{i+1/2,j} - (\rho u)^{n+1}_{i-1/2,j} \; u^{n+1}_{i-1/2,j} \right] \right.$$

$$\left. + \left[(\rho u)^{n}_{i+1,j} \; u^{n}_{i+1,j} - (\rho u)^{n}_{i-1,j} \; u^{n}_{i-1,j} \right] /2 \right\} /2$$

$$+\alpha A_2 \left\{ (j-1/4) \; (\rho v)^{n+1}_{i,j-1/2} \; u^{n+1}_{i,j-1/2} - (j+1/4) \; (\rho v)^{n+1}_{i,j+1/2} \right.$$

$$u^{n+1}_{i,j+1/2}$$

$$\left. + \left[(j-1/2) \; (\rho v)^{n}_{i,j-1} \; u^{n}_{i,j-1} - (j+1/2) \; (\rho v)^{n}_{i,j+1} \; u^{n}_{i,j+1} \right] /2 \right\} /2j$$

$$+\alpha B_1 \left\{ (p^{n+1}_{i+1/2,j} - p^{n+1}_{i-1/2,j}) + (p^{n}_{i+1,j} - p^{n}_{i-1,j}) \; /2 \right\} /2$$

(2.31)

$$(\rho v)^{n+1}_{i,j} = \left\{ (\rho v)^{n}_{i,j} + \left[(\rho v)^{n+1}_{i+1/2,j} + (\rho v)^{n+1}_{i-1/2,j} + (\rho v)^{n+1}_{i,j-1/2} \right.\right.$$

$$\left. + (\rho v)^{n+1}_{i,j+1/2} \right] /4$$

$$+ (\rho v)^{n}_{i,j} + \left[(\rho v)^{n}_{i+1,j} + (\rho v)^{n}_{i-1,j} + (\rho v)^{n}_{i,j-1} \right.$$

$$\left.\left. + (\rho v)^{n}_{i,j+1} \right] /4 \right\} /4$$

$$+\alpha A_1 \left\{ \left[(\rho u)^{n+1}_{i+1/2,j} \; v^{n+1}_{i+1/2,j} - (\rho u)^{n+1}_{i-1/2,j} \; v^{n+1}_{i-1/2,j} \right] \right.$$

$$\left. + \left[(\rho u)^{n}_{i+1,j} \; v^{n}_{i+1,j} - (\rho u)^{n}_{i-1,j} \; v^{n}_{i-1,j} \right] /2 \right\} /2$$

$$+\alpha A_2 \left\{ \left[(j-1/4)\ (\rho v)^{n+1}_{i,j-1/2}\ v^{n+1}_{i,j-1} - (j+1/4)\ (\rho v)^{n+1}_{i,j+1/2}\ v^{n+1}_{i,j+1/2} \right] \right.$$

$$\left. +\left[(j-1/2)\ (\rho v)^{n}_{i,j-1}\ v^{n}_{i,j-1} - (j+1/2)\ (\rho v)^{n}_{i,j+1}\ v^{n}_{i,j+1} \right] /2 \right\} /2\, j$$

$$+\alpha B_2 \left\{ (p^{n+1}_{i,j-1/2} - p^{n}_{i,j+1/2}) + (p^{n}_{i,j-1} - p^{n}_{i,j+1}) /2 \right\} /2 \qquad (2.32)$$

$$u^{n+1}_{i,j} = (\rho u)^{n+1}_{i,j} \ / \ \rho^{n+1}_{i,j} \qquad (2.33)$$

$$v^{n+1}_{i,j} = (\rho v)^{n+1}_{i,j} \ / \ \rho^{n+1}_{i,j} \qquad (2.34)$$

$$p^{n+1}_{i,j} = (\rho^{n+1}_{i,j} \ / \ \rho_o)^{A} \ (\rho_o + B) - B \qquad (2.35)$$

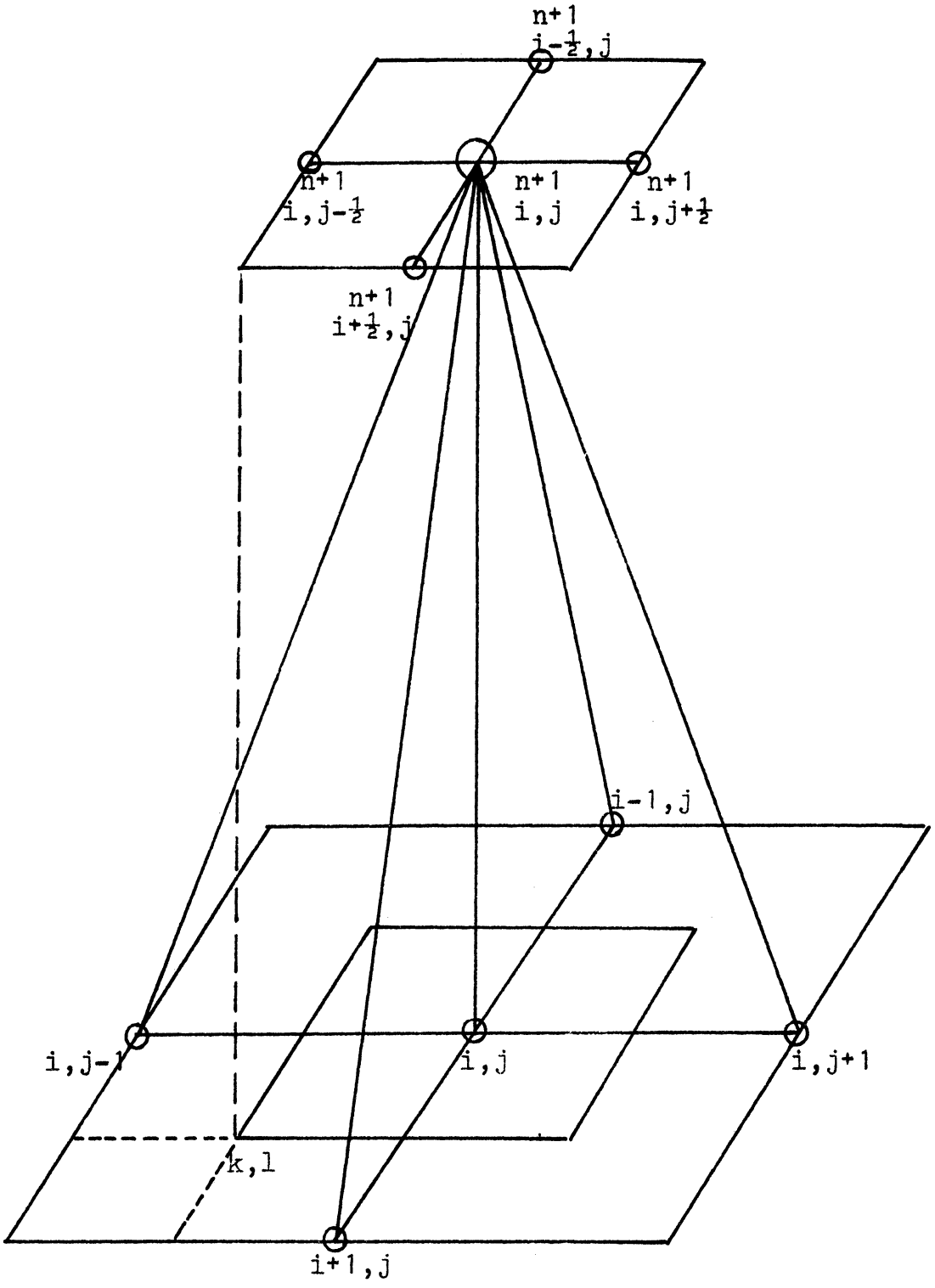

Figure 3

The Basic Structure for the Second Step Computation of Modified Lax-Wendroff Scheme in the ComCAM Method

The new quantities at the midpoints on the cell boundaries $(i, j-1/2)$, $(i, j+1/2)$, $(i+1/2, j)$ and $(i-1/2, j)$ are evaluated by taking the simple average of the new values at two adjacent corners of the cell.

The marker particles, which are regularly spaced initially along the fluid interface, do not always retain that regular spacing. After many cycles of calculation, parts of the interface may be crowded with particles, while in another section of the interface the particles may be widely separated. Since neither extreme is desired, when the particle separations are too small, minor fluctuations may cause one particle to overpass the neighboring particles. When the particle separations are too large, the interface geometry is not well resolved. The following modification is adopted for the numerical computation. If more than one particle resides in the same Marker cell, a new particle will be created to represent the average of the previous group, which is then deleted. If two particles are separated by more than one cell and that cell has no inhabiting particle, a new particle is inserted between them, having properties which are the average of both. The facility of deleting and adding Marker particles has the desired smoothing effect.

At the end of computations at each time instant, one must update the values of the flow variables in fictitious cells outside the Eulerian grid before a new round of computations is started for the interior cells at the next time increment. This can be accomplished through the use of the appropriate boundary conditions (2.36) through (2.39) which are expressed in finite difference form. The difference equations include those for the symmetrical boundary cell, permeable boundary cell, rigid boundary cell and the boundary cell at liquid-gas interface.

1. Symmetrical Boundary Cell, $j = 1$

The reflective condition at the axis of symmetry gives the following difference equations

$$
\begin{aligned}
&\rho_{i,j} = \rho_{i,j+1} \\
&u_{i,j} = u_{i,j+1}, \qquad (\rho u)_{i,j} = (\rho u)_{i,j+1} \\
&v_{i,j} = 0, \qquad (\rho v)_{i,j} = 0 \\
&p_{i,1} = p_{i,2}
\end{aligned}
\tag{2.36}
$$

2. Permeable Boundary Cell

The conditions in these fictitious boundary cells are provided to satisfy the vanishing normal space derivatives of the variables at the boundary. In finite-difference numerical calculation, this merely reduces to setting the variables in each fictitious boundary cell equal to the value in the adjacent interior cell. As an example for right-hand output permeable boundary, $j = j_{max}$ which is the largest index in the r- direction,

$$
\begin{aligned}
&\rho_{i,j} = \rho_{i,j-1} \\
&u_{i,j} = u_{i,j-1}, \qquad (\rho u)_{i,j} = (\rho u)_{i,j-1} \\
&v_{i,j} = v_{i,j-1}, \qquad (\rho v)_{i,j} = (\rho v)_{i,j-1} \\
&p_{i,j} = p_{i,j-1}
\end{aligned}
\tag{2.37}
$$

The same is true for upper input permeable boundary, except the direction is changed and $i = i_{max}$ which is the largest index in the z-direction.

3. Rigid Boundary Cell, i = 1

For this fictitious boundary cell to represent a rigid obstacle, it is required that the normal flow quantities be zero and that the reflective condition be satisfied. Two extreme cases are given as follows:

free-slip condition non-slip condition

$$\rho_{i,j} = \rho_{i+1,j}$$

$$p_{i,j} = p_{i+1,j}$$

$$u_{i,j} = 0$$

$$(\rho u)_{i,j} = 0$$

$$v_{i,j} = v_{i+1,j} \qquad v_{i,j} = 0$$

$$(\rho v)_{i,j} = (\rho v)_{i+1,j} \qquad (\rho v)_{i,j} = 0 \tag{2.38}$$

4. Atmospheric Boundary Cell

The quantities just outside the fluid region are needed to carry out the difference computations in the interior cells near the free surface and to move the marker particles. It is a special permeable boundary condition with the exception of constant atmospheric pressure being imposed.

$$\rho_{i,j} = \rho_{air}$$

$$p_{i,j} = p_o$$

$$u_{i,j} = u_{i\pm1,j} \quad , \quad (\rho u)_{i,j} = (\rho u)_{i\pm1,j} \tag{2.39}$$

$$v_{i,j} = v_{i,j\pm1} \quad , \quad (\rho v)_{i,j} = (\rho v)_{i,j\pm1}$$

where ± 1 depends upon the relative position of the fictitious boundary cell with respect to its adjacent Marker cell.

The numerical method represents an approximate solution to the original differential equations, since derivatives are replaced by finite differences. Terms of the order of the square of the time increment and spatial step size are neglected. The convergence of the

finite difference representation, i.e., the degree to which the approximate solution approaches the exact solution, must be examined by numerical experiments using different spatial-and-time step sizes.

It is known that although the explicit formulation avoids the need of iterative or matrix inversion techniques, certain stability requirements must be satisfied. The only stability criterion to be satisfied is the Courant condition[68], i.e., the distance a wave travels in the time increment Δt must be less than the spatial step size Δz or Δr. Or

$$\Delta t < \frac{\text{min.}(\Delta z, \Delta r)}{C} \tag{2.40}$$

where C is the shock wave velocity in the liquid phase. With the definition of the stability factor

$$\alpha = \frac{C\,\Delta t}{\text{min.}(\Delta z, \Delta r)} \tag{2.41}$$

one can satisfy the stability criterion by selecting a value of α less than unity.

CHAPTER III

RESULTS AND DISCUSSION

A. One Dimensional Test Problem

The same computer program as used to solve the two-dimensional axisymmetrical droplet impact problems was modified by imposing rigid tube shell boundary cells to solve classical one-dimensional water-hammer problems and hence to test the accuracy of numerical solution as well as the validity of numerical method.

Fig. 4a* shows the typical pressure profiles by three different methods at the impact Mach number of 0.2. It is significant that numerical oscillation is practically unnoticed in the ComCAM results as compared with results obtained by other Eulerian numerical methods[65, 67, e.g.] which exhibit substantial fluctuations. Fig. 4b shows the pressure-time history on the impacted plane surface. Again, the correct solution of water hammer pressure is obtained by the ComCAM method without numerical oscillations.

B. Problem Selection

Numerical computations for the normal impact of a water droplet on a rigid solid surface are performed for three typical geometrical configurations of droplet: cylindrical, spherical and composite forms, for two typical Mach numbers: 0.2 and 0.5, and for two typical boundary conditions: free-slip and non-slip. Seven different problems were solved.

1. Initially cylindrical droplet with L/D = 1 at Mach number 0.2 for free-slip boundary condition.
2. Initially spherical droplet at Mach number of 0.2 for free-slip boundary condition.
3. Initially cylindrical-spherical composite droplet at Mach number of 0.2 for free-slip boundary condition.

*Since there are too many figures to insert on quite a few occasions in this Chapter, they are placed in order at the end of the Chapter.

4. Initially cylindrical droplet with L/D = 1 at Mach number = 0.2 for non slip boundary condition.
5. Initially cylindrical droplet with L/D = 1 at Mach number = 0.5 for non-slip boundary condition.
6. Initially spherical droplet at Mach number = 0.2 for non-slip boundary condition.
7. Initially spherical droplet at Mach number = 0.5 for non-slip boundary condition.

The first problem was selected to study the effect of two dimensionality with axisymmetry. The second problem was selected to compare with the experimental results in the photographic investigation[20]. The third problem was to see the impact of cylindrical-spherical composite drop. This shape is especially interesting, because it simulated the shape of an initially spherical drop which has deformed due to the resistance of air stream before the normal impact on a rigid solid surface. The last four problems were chosen to investigate the effect of Mach number and boundary condition using the cylinder and spherical geometries. M = 0.2 and 0.5 are selected because they represented typical impact velocities of water drops in steam turbines and future supersonic transports, respectively.

Solutions of the problems were obtained by using the new ComCAM method. Numerical experiments were carried out to determine the stability factor and cell numbers until the convergence of solution was reasonably assured, in regard to magnitudes, timing, and wave shapes. It is very encouraging to mention here that unlike the reports[65,67] which experience the occurrence of negative densities, there is no single occurrence of negative density in the present study, even though the stability factor has exceeded the theoretical limit 0.408, according to Burtein[65]. As an example, when α = 0.5 was used for a relatively coarse mesh (10 x 20), the minimum density was found to be 0.777. In the present study stability factor α = 0.1 and 20 x 40 mesh were used in the calculation of cylindrical and spherical droplets, while α = 0.1 and 25 x 40 mesh were employed for the calculation of a

cylindrical-spherical composite droplet.

C. Two-Dimensional Axisymmetrical Problems

In examining the following results, one must keep in mind those boundary conditions at the interfaces of the axisymmetrical liquid droplets. Constant atmospheric pressure at the water-air free surface is imposed. The impact plane which is perfectly rigid and smooth has no movement. The properties of water are inviscid, no surface tension, but compressible as well as elastic. The tensile strength of water is taken to be -270 atm. of negative pressure, an experimental result measured by Briggs[54]. Of course, water will rupture in many circumstances at much smaller tensions, but perhaps not for the very short duration of tension involved. The two constants in the Tait's equation of state for water are A = 7.15 and B = 3008 atm.

1. Initially Cylindrical Droplet with L/D = 1 for Impact Mach Number of 0.2 and for Free-Slip Boundary Condition

Fig. 6 shows how the shape of the droplet deforms as a function of time. The top of the droplet retains its original flat shape up to the nondimensional time $t^o = Ct/D = 1$ (about equivalent to 1 μ sec for an impact Mach no. = 0.2 of a 2 mm droplet) beyond which moment it begins concave downward. It is interesting to point out that the liquid in the droplet dashes out radially over the surface without contacting it.

Fig. 7a through 7e depict the isobar distribution in the droplet at various instants, 0.125, 0.25, 0.5, 1, and 2.5, respectively. The figures illustrate how the pressure waves propagate with time from the impacted surface toward the air-water free surface. Due to constant atmospheric pressure at this free surface, all the isobaric surfaces at small times appear in a glass-cup shape resting upside down but coaxially upon the impacted surface as shown in Fig. 7a. As time progresses and the droplet shrinks in height accompained by radial-expansion, Fig. 76 shows each cup-shaped isobaric surface growing in size

both depth and width. Fig. 7c corresponds to the situation at $t^o = 0.5$. While the isobaric surfaces for small values of $p^o = p/\rho_o C_o V_o$ still retain the glass-cup shape in the outer region of the droplet, those for medium pressure in the inner region form the egg-shape surfaces which are coaxially arranged with the protruding edges pointing toward the impacted surface. In the center region of the droplet, however, the isobaric surfaces for larger pressure appear like the round-edged discs which are arranged concentrically with the major axes parallel to the impacted surface. The above-mentioned pressure pattern in the droplet is due to the interaction of the rarefaction waves from the air-water free surface at the impacted edge. The pressure at the stagnation point ($r = 0$, $z = 0$) is released not from the top of the droplet but from the contact edge of the solid liquid interface. The mechanism is explained in the following.

Let us assume that the compression wave travels along the symmetrical axis at wave speed of C[24]

$$C = C_o + KV_o \tag{3.1}$$

where C_o is sonic velocity in the undisturbed liquid,

V_o is the impact velocity, and

K is some constant (about 2 for water). Further assume the rarefaction wave velocity is C_o. The minimum diameter D_{min} of the cylindrical droplet of length L for the wave pattern at the axis of symmetry ($r = 0$) remains in the one-dimensional sense for a finite time is

$$D_{min} = 2\ L\ \left(\frac{2 + KM}{1 + KM}\right) \tag{3.2}$$

and

$$D_{min} = 4\ L \quad \text{if } M \ll 1 \tag{3.3}$$

where Mach number $M = V_o/C_o$.

The Eq. (3.3) means that for a very weak impact, the geometry of a cylindrical droplet is $L/D = 1/4$, when rarefaction waves reach the stagnation point from the top of the drop and from the edge of

the drop at the same time. The maximum pressure at the stagnation point will be one-dimensional water-hammer pressure, if the diameter D of a cylindrical droplet is greater than 2 L (2 + KM/1 + KM).

The above Eqs. (3.2) and (3.3) are only approximations without correction for the change of geometry. The deviation is simply the manipulation of the following equations:

$$R = C\,t = \frac{D}{2} \tag{3.4}$$

$$L = C\,t_1 \tag{3.5}$$

$$L = C_o t_2 \tag{3.6}$$

$$t = t_1 + t_2 \tag{3.7}$$

Substitution of Eqs. (3.4), (3.5) and (3.6) into (3.7) will yield Eq. (3.2).

Fig. 7d for $t^o = 1.0$ shows the possibility of cavitation in the region of negative pressure enclosed by the zero isobaric surface as a result of rarefaction of a pressure wave from the top of the cylindrical drop. There is no bursting out of the top surface because the compression is continually released. The isobaric surface of $p^o = 0.05$ forms a half-sliced doughnut shape surface which houses the region of high compressive pressure.

Fig. 7e for $t^o = 2.5$ illustrates that the droplet resembles a military helmet. The isobaric surfaces around the z-axis region changes from concave downward to upward as the value of p^o increases. At a certain value of p^o, however, part of the isobaric surface around the z-axis region coincides with the solid surface. The higher p^o is confined in the half-sliced doughnut shape region over the solid surface near $r^o = r/R$ of unity.

Better illustration of the pressure distribution on the impacted surface and along the axis of symmetry are given in Figs. 8 and 9 respectively. Fig. 8 shows that the the first few moments following impact the pressures build up rather uniformly over the entire impacted surface except near the vicinity of contact edge where the

boundary condition of atmospheric pressure has been satisfied. Fig. 9 depicts how the pressure waves propagate along the symmetrical axis starting from the impacted surface. These waves reach the top of the droplet at about $t^o = 0.5$ and then rebound resulting in creating a huge region of negative pressure behind. It is interesting to observe the distribution of negative pressure along the z axis at $t^o = 1.0$. The pressure at the stagnation point (0 , 0) is positive or compressive until the rarefaction waves reach that point along the axis of symmetry (r=0) or along the impact surface (z=0). Its magnitude increases continually until the time t^o of about 0.25 at a much greater rate than the pressures over the rest of the impacted surface. At the same time, the rarefaction wave starts to affect the pressure within the contact line between the droplet and the impacted surface as can be seen in Fig. 8 as well as Fig. 9. The pressure at the stagnation point then decreases and actually becomes negative at time about 1.25 as shown in Fig. 10. It then rebounds and oscillates about the normalized steady-state stagnation pressure which is $\frac{\rho_o V_o^2}{2} / \rho_o C_o V_o = M/2 = 0.1$ for M = 0.2. The numerical computation was terminated at $t^o = 2.5$, since the steady state has been reasonably approached and also most of the important features regarding the liquid-solid impact have been disclosed up to that instant. Fig. 10 also shows the pressure-time history at two other locations (0, 0.5) and (0.75, 0). The pressure at point "a" (0, 0.5) has exceeded the rupture pressure during the time t^o between 1 and 1.5. This indicates the occurrence of cavitation at the location. The cavity thus created may not stay long since it will be subject to compression after $t^o = 1.5$. Since the pressure gradient on the impacted surface is the greatest near the contact edge as shown in Fig. 8, the instantaneous radial velocity increment at the location must be correspondingly the largest as demonstrated in Fig. 11.

Fig. 11 shows the radial velocity distribution on the impacted surface. The dotted portion of the curves indicate regions where the jetting liquid does not remain in contact with the impacted surface. The jetting velocity exceeds the impact velocity at

the time about 0.2, then the net effect of rarefaction wave starts toward the center line of symmetry along the liquid-solid contact surface, reducing the pressure. Actually, the wave pattern is two-dimensional, and it depends very much upon the geometry of a drop. Suppose a cylinder of length L and diameter D is impacted by a rigid plane. If the diameter of cylinder D is infinitely large, the problem becomes one-dimensional, provided the end effect could be neglected. The maximum pressure under this condition is the one-dimensional water hammer pressure corrected for the shock wave velocity as Heymann suggested[24], and the release wave will come from the top. On the other hand, if the diameter of cylinder D is infinitesimal, the pressure at the stagnation point will also be stagnation pressure since the compression will be instantaneously released. However, most cases lie in between these two extremes. The release waves, which will come from the sides first for the cases of large L/D and will come from the top first for the cases of small L/D will interact with the compression waves two-dimensionally.

The positive pressure gradient in the radial direction (dp/dr) results in a positive time-rate change in the radial velocity, Therefore, as pressure gradients on the impacted surface change from a positive value to a negative one as shown in Fig. 8, the radial velocities on the impacted surface change correspondingly from an increasing to a decreasing mode as illustrated in Fig. 11. The maximum pressure gradient and its corresponding location on the impacted surface are given in Fig. 12. The pressure gradient is calculated by taking the pressure difference between two adjacent cells at their common cell boundary. These calculations were systematically carried out by the computer. Maximum pressure gradients on the impacted surface may occur at the same radial location over a certain period of time. The curve for the locus of the maximum pressure gradient shown in Fig. 12 was obtained by drawing a line through these data points. It is seen in Fig. 12 that the maximum

pressure gradient reaches its peak at the time of about 0.2, and at the location just inside the initial contact edge. It then decreases to its steady-state value as the location of the maximum pressure gradient moves outward. It is conjectured that the erosion mechanism may be caused by the maximum pressure gradients on the impacted surface.

2. Initially Spherical Droplet for Impact Mach Number of 0.2 and for Free-Slip Boundary Condition

Fig. 13 shows the deformation of an initially spherical droplet at various time instants following an impact on a rigid plane with Mach number = 0.2 for free-slip boundary condition. The upper half of the droplet remains relatively undeformed up to the time of $t^{o} = 1$, while the deformation near the contact edge is not apparent for at least up to $t^{o} = 0.25$.

Fig. 14a through 14e show the isobar distribution at various instants. The major pressure release comes mostly from the radial flow along the impacted surface and less from the rebound on the top of the drop. While the liquid-solid interface acts like a pressure source the liquid-air free surface serves as a pressure sink. These two effects interfuse with each other. The exact consequence depends upon both location and time.

Fig. 15 shows the pressure distribution on the impacted surface (z=0) at various time instants. From these curves, one can see that the time-rate change of pressure as well as the spatial pressure gradient are greater near the contact edge than those at the center (0,0) of the contact area during the period dominated by compression.

Fig. 16 shows the pressure distribution on the symmetrical axis (r=0) at several time instants. It is the compression that predominates over the entire portion of symmetrical axis during the early stage of impact up to the time of about 0.25. By comparing the two curves at times of 0.25 and 0.5, one can see that while the pressures on upper portion continue to increase, the pressures near the solid

plane (z=0) start to fall. As the effect of rarefaction propagates from the stagnation point toward the top of the droplet, the pressures diminish everywhere toward the stagnation pressure along the symmetrical axis.

Fig. 17 shows the pressure at three given locations as a function of time. The pressure at the stagnation point b reaches its peak value at time (Ct/D) = 0.2, and then subsides to about the final steady-state stagnation pressure(0.1). The pressure at the location on a symmetrical axis, (r=0, z=.45R) behaves in a similar manner except with phase lag. Since this location lies between the stagnation point and the top of the droplet, it is conceivable for this pressure-time curve to lie within the pressure-time curve for the stagnation point. The pressure at the "c" on the impacted surface (z=0, r=0.4R) remains unaffected until contact ring reaches that point "c". The time-rate change in pressure for the rising portion of the curve "c" is about the same as that of the curve "b" for the stagnation point. The pressure at "c" rises and eventually the pressure of the stagnation point "b" before it starts to fall in parallel with the latter.

Fig. 18 shows the radial velocity distribution on the impacted surface (z=0). Again, the dotted lines signify the portion of the liquid which is very close to but not actually in contact with the impacted plane (z=0). The overhanging liquid can be either the incoming liquid outside of contact line which is just about to impinge the solid or the re bounding liquid from the impacted surface. The velocity and the location indicated by the end of a dotted line are those photographic observations of the impacted droplet would indicate. However, the maximum radial velocity at any given instant occurs at a location between the tip of jetting and the center line (r=0), as illustrated in the figure. For the Mach number of 0.2, the maximum radial velocity ever attained is 2.65 (at 2.5 μsec) times the impacting velocity V_o in the case of free-slip boundary condition and is 2.86 (at 2 μsec) times V_o in the case of non-slip boundary condition. These calculations

are in good agreement with the following experimental results. Fyall [21] used the techniques of high speed photography and observed that the wash velocity during the first three microseconds was 3056 ft/sec for an impact speed of 990 ft/sec with 2 mm waterdrop. Perspex was used as a target material in his case.

There are two opinions about lateral flow. One proposed by Engel [19, 73] assumes that lateral outflow begins immediately following an impact. The other shared by Heymann [31], Bowden and Field [74] and others considers that the flow cannot begin before the impact pressure wave moves ahead of the circle or line of contact between drop and solid. The present study indicates that the lateral flow begins simultaneously as the pressure proceeds to build-up, but the jetting is not appreciable during the early stage of impact, as depicted in Fig. 13 and 14. For the convenience of discussion and comparison, we shall provide the following example with some physical quantities. For a spherical droplet of 2.077 mm in diamter and with the impact Mach number of 0.2(V_o = 980 ft/sec, C_o = 4900 ft/sec, $C = 1.396\ C_o$), the time to reach the critical angle, according to the analysis by Bowden and Field [74] is 0.035237×10^{-6} sec. However, before the critical angle is reached, at the time of 0.025×10^{-6} sec, the pressure distribution is such that it is highest at the center of the contact area and decreases to atmospheric pressure at the edge where it is just about to be contacted by the rigid plane. Due to the presence of this radial pressure gradient, the liquid flows radially to expand the contact area by 0.04% at this instant the normalized instantaneous maximum particle radial velocity V/V_o within the contact area is 0.03 already, according to the calculation. The radial velocity at the contact edge is often slowed down by the liquid rushing to contact the rigid plane. However, the protrusion in the contact periphery is so slight that it is almost impossible to detect or measure by experiments or photographical means. The fact that compression and rarefaction take place simultaneously from the very beginning of impact is strictly in accordance with the governing equations. It is only an approximation

that assumes no gross flow or splashing at the very beginning of impact. Since the boundary condition of atmospheric pressure on the contact edge should be satisfied at all times, the pressure is released by the lateral flow from the first instant of contact, and hence, the impact pressure becomes less than the theoretical one-dimensional maximum pressure, as depicted in Figs. 15, 16 and 17.

Fig. 19 shows the magnitude and location of the maximum radial pressure gradient on the impacted surface. Although the maximum pressure in the case of a spherical drop is less than that of a cylindrical drop, the peak of the curve for the maximum radial pressure gradient as well as the area under the curve are greater than those of the cylindrical droplet case.

3. Initially Cylindrical-Spherical Composite Droplet for Mach Number of 0.2 and for Free-Slip Boundary Condition

It is quite conceivable that not a single rain droplet resembles exactly a perfect sphere. However, a cylindrical-spherical composite shape shown in Fig. 20 seems to be closer to the actual shape of a droplet just before impact. It is very interesting to learn that the results for this cylindrical-spherical composite droplet lie in-between those for a cylindrical droplet and a spherical droplet.

Fig. 20 shows the deformation history of the composite droplet. Fig. 21a through 21e illustrate the isobar distributions at various time instants. By comparing the results presented in Figs. 7, 14, and 21, one can see that the wave propagates faster in the composite droplet than in the spherical droplet but slower than in the cylindrical droplet. This is because the effect of radial flow on immediate release of compressive pressure is greater in the composite droplet than in the spherical one, but smaller than in the cylindrical one.

Fig. 21d for $t^{o} = 1.5$ depicts a very interesting phenomenon. There are two cavity regions coexistant in the upper half portion of the droplet. The middle cavity region is created by the reflection of compression waves from the top of the droplet. While the region is in the process of shrinking it induces the formation of the additional cavity

region in a form at annular ring.

Fig. 21e shows the isobar distribution at $t^{o} = 2.5$. The maximum pressure on the impacted surface has shifted from the stagnation point to the point where a vertical line which is tangent to the initial shape of the drop intersects with the rigid surface line. This shifting of the maximum pressure on the impacted surface is caused by the convergency of impacting liquid and radial flow.

Fig. 22 and 23 show the pressure distribution on the impacted surface (z=0) and on the symmetrical axis (r=0) respectively. Again, one can see that both the greater radial pressure gradient and the greater time-rate change in pressure occur near the contact line. The negative pressure (at $Ct/D = 1.5$) in the shaded area results from the reflection of compression wave from the top of the droplet.

Fig. 24 shows the pressure variations at points a, b, and c as a function of time. The maximum pressure p^{o} at the stagnation point is about 0.9 in magnitude which is between 0.69 for spherical drop and 1.16 for cylindrical drop.

Fig. 25 shows the radial velocity distribution. Again, the maximum radial velocity at any given time is located inside the contact line. The radial velocity will increase for the positive pressure gradient and will decrease for the negative pressure gradient. Therefore, as the maximum pressure shifts outward radially, to the right of where the maximum pressure is, the radial velocities continue to increase, and to the left, the radial velocities start to decrease.

Fig. 26 shows the maximum radial pressure gradients and its corresponding location. Among the three different configurations investigated here this composite cylindrical-spherical droplet has the highest peak value of the maximum radial pressure gradients.

D. The Effect of Impact Mach Number

Figs. 27 and 34 show the deformation of a cylindrical and a spherical droplet respectively, following an impact on a rigid plane for M = 0.2 and 0.5. It is seen in the figures that the higher the impact Mach number, the greater the compressibility effects, as evidenced by greater shape deformation.

The isobar distributions at various times t^{o} = 0.125, 0.25, 1.0 and 2.5 are shown in Figs. 28a through 28d respectively for a cylindrical drop and in Figs. 35a through 35d respectively for a spherical drop. One finds that the higher the impact Mach number, the steeper the compression wave and the greater the impact pressure. Negative pressures are seen to occur in the upper region of the drop and near the tip of the jetting liquid in the case of cylindrical drop with Mach = 0.2 but not with Mach = 0.5. The negative pressure regions are also indicated by the shaded areas in Figs. 29 and 30.

Figs. 31 and 38 show the effect of Mach number on the impact pressure. It is seen that the greater the Mach number, the greater the normalized pressure at the given corresponding point, i.e., the actual pressure increases more than in proportion to the impact velocity.

It is revealed by Figs. 32 and 39 that the lower Mach number has the higher ratio of radial velocity to the impact velocity. Therefore, it is conceivable that cavitation may occur in the spherical drop also, but for smaller impact Mach numbers (which results are not available in this thesis) when the radial velocity becomes much greater than the velocity of incoming liquid normal to the impacted surface, so that the liquid is in tension and cavitation becomes possible.

The effect of Mach number on the maximum pressure gradient on the impacted surface is insignificant for a cylindrical drop but becomes important for a spherical drop because of curvature effects, as seen in Figs. 33 and 40.

E. The Effect of Non-Slip Boundary Condition

As was expected, the non-slip boundary condition retards the flow. However, it also contributes to a build-up in pressure inside the droplet. Accordingly, the instantaneous peak radial velocity is higher than the free-slip case discussed previously. For example, for a spherical drop the peak pressure at the stagnation point under the non-slip boundary condition is 0.8 as compared to 0.7 under the free-slip boundary condition. The corresponding value is 1.2 as compared to 1.16 for a cylindrical water drop. Otherwise, the patterns of pressure and velocity responses for the non-slip and free-slip cases are essentially analogous.

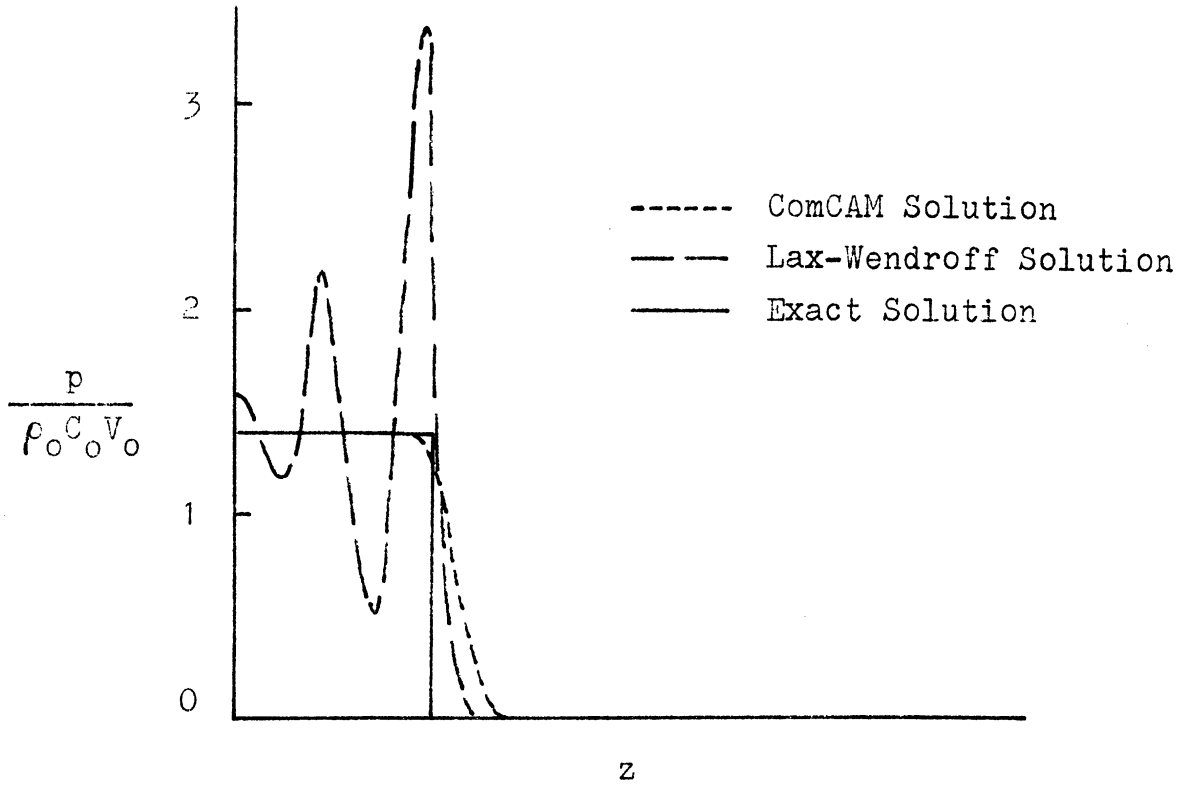

Fig. 4a. Typical Pressure Profiles for One-Dimensional Water Impact on a Solid Surface with Mach=0.2, Stability Factor = 0.2

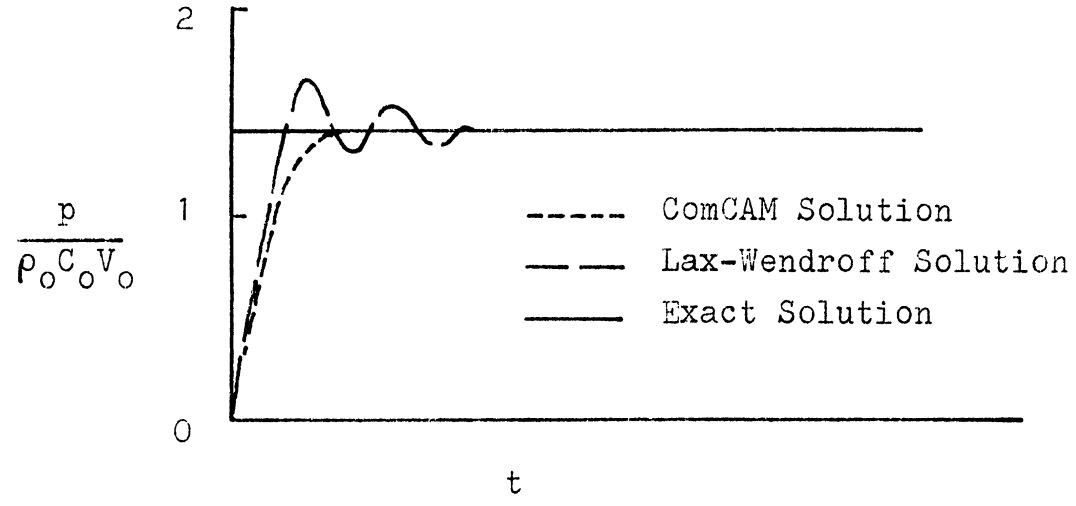

Fig. 4b. Typical Pressure Histories for One-Dimensional Water Impact on a Solid Surface with Mach=0.2, Stability Factor = 0.2

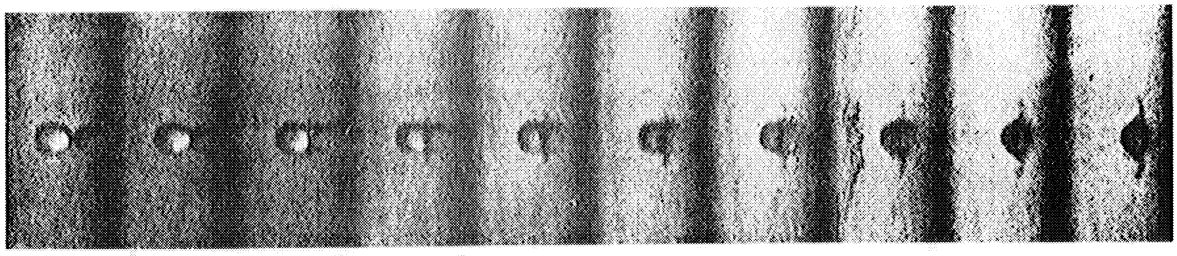

Fig. 5a. Photographs of the Deformation Stages for a Water Droplet Following an Impact on a Solid Plane (Engel[19])

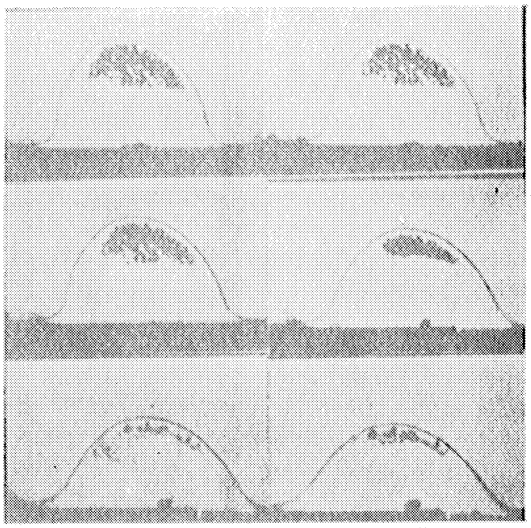

Fig. 5b. Photographs of the Cavitation for a Water Droplet Following an Impact on a Solid Plane (Brunton[75])

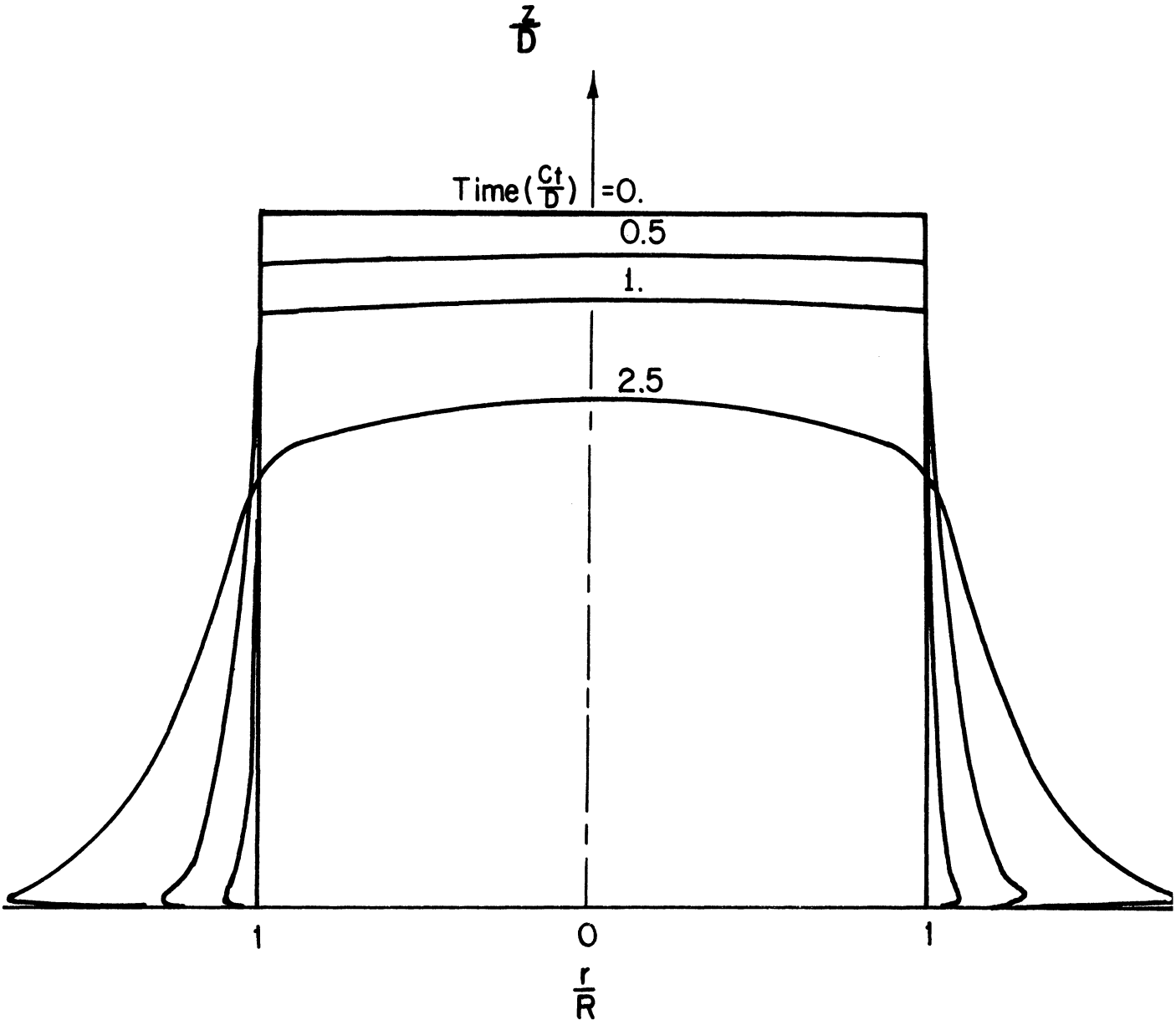

Fig. 6. Shape-Time History of an Initially Cylindrical Droplet with L/D = 1, at Mach Number = 0.2, for Free-Slip Boundary Condition.

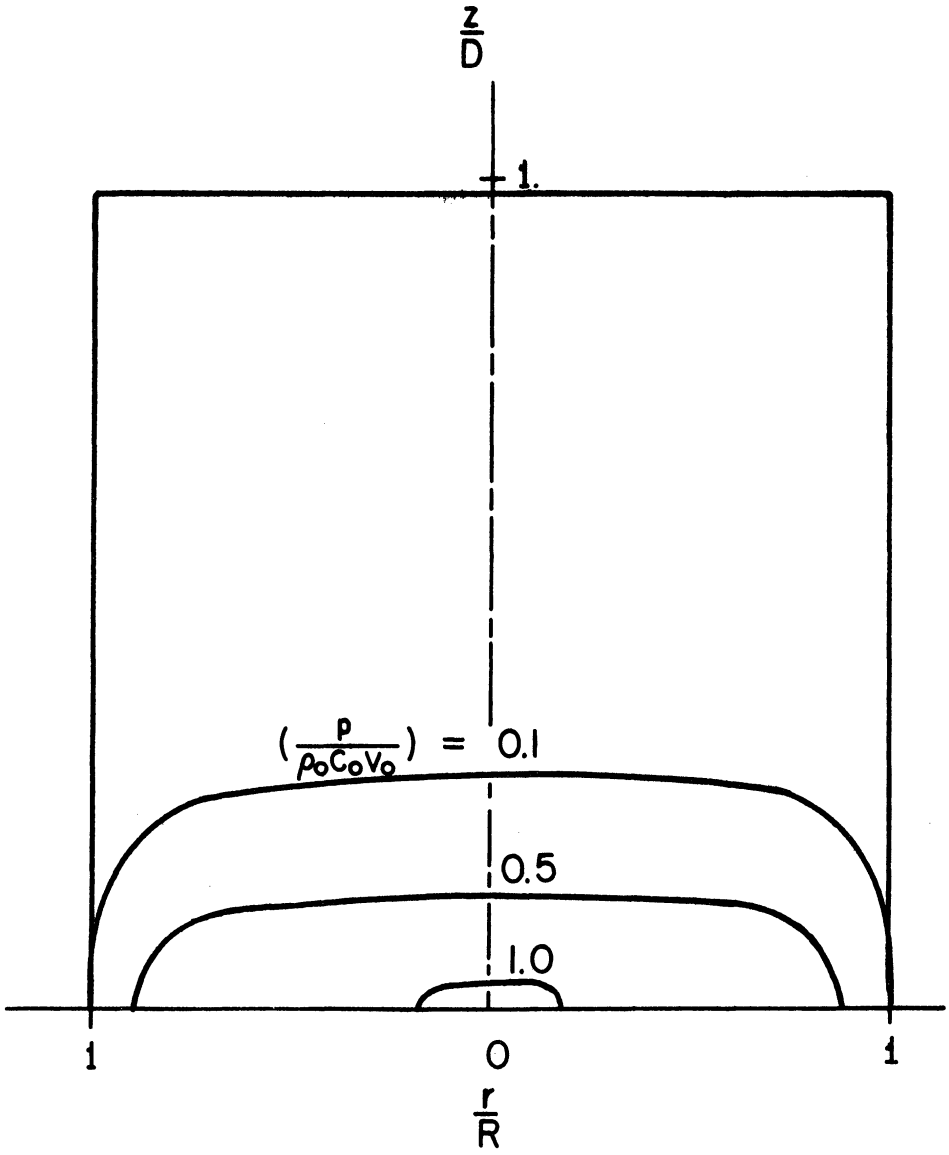

Fig. 7a. Isobar Distribution in an Initially Cylindrical Droplet with L/D = 1, at Time (Ct/D) = 0.125, for Impact Mach Number of 0.2 and for Free-Slip Boundary Condition.

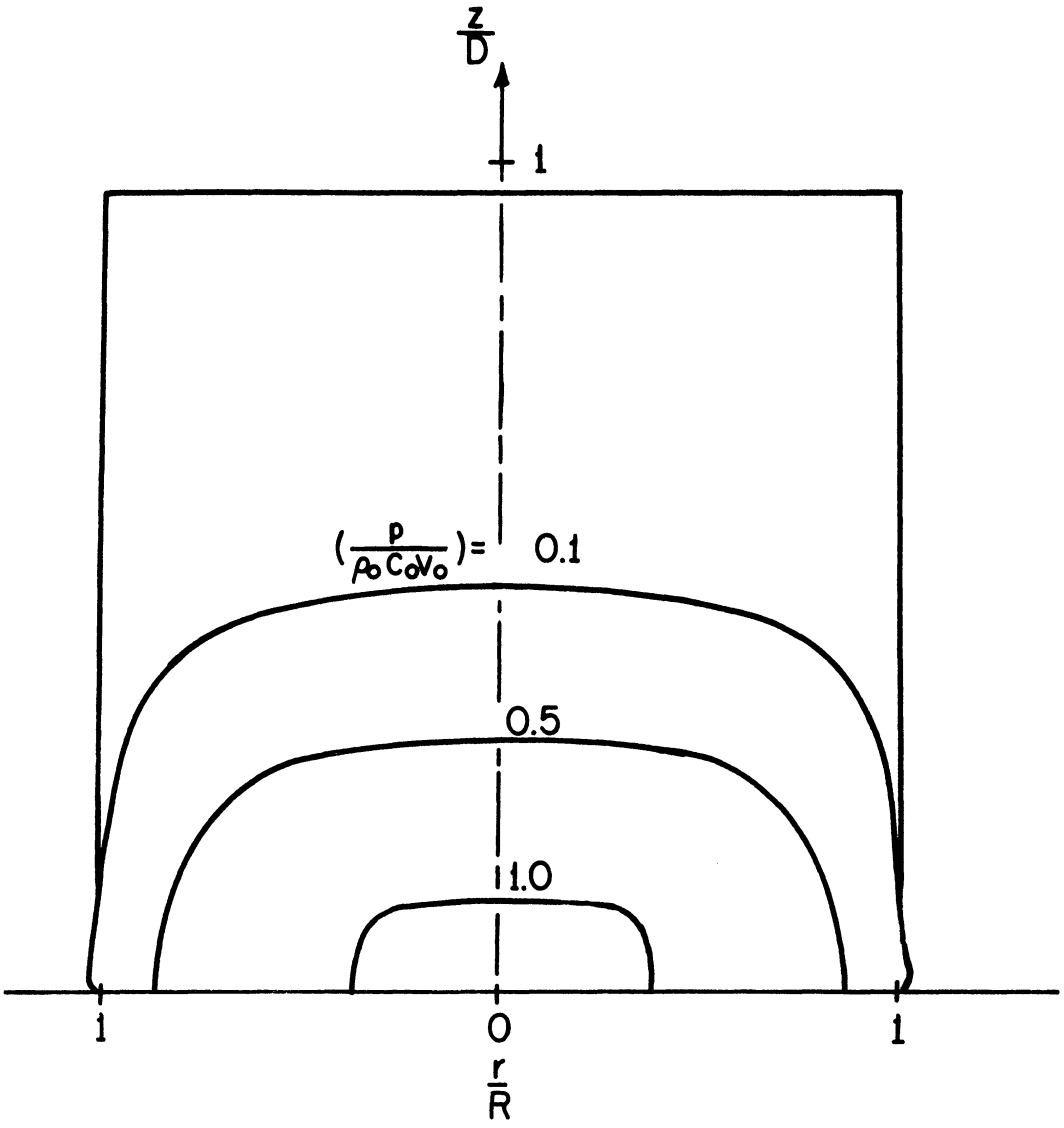

Fig. 7b. Isobar Distribution in an Initially Cylindrical Droplet with L/D = 1, at Time (Ct/D) = 0.25, for Impact Mach Number of 0.2 and for Free-Slip Boundary Condition.

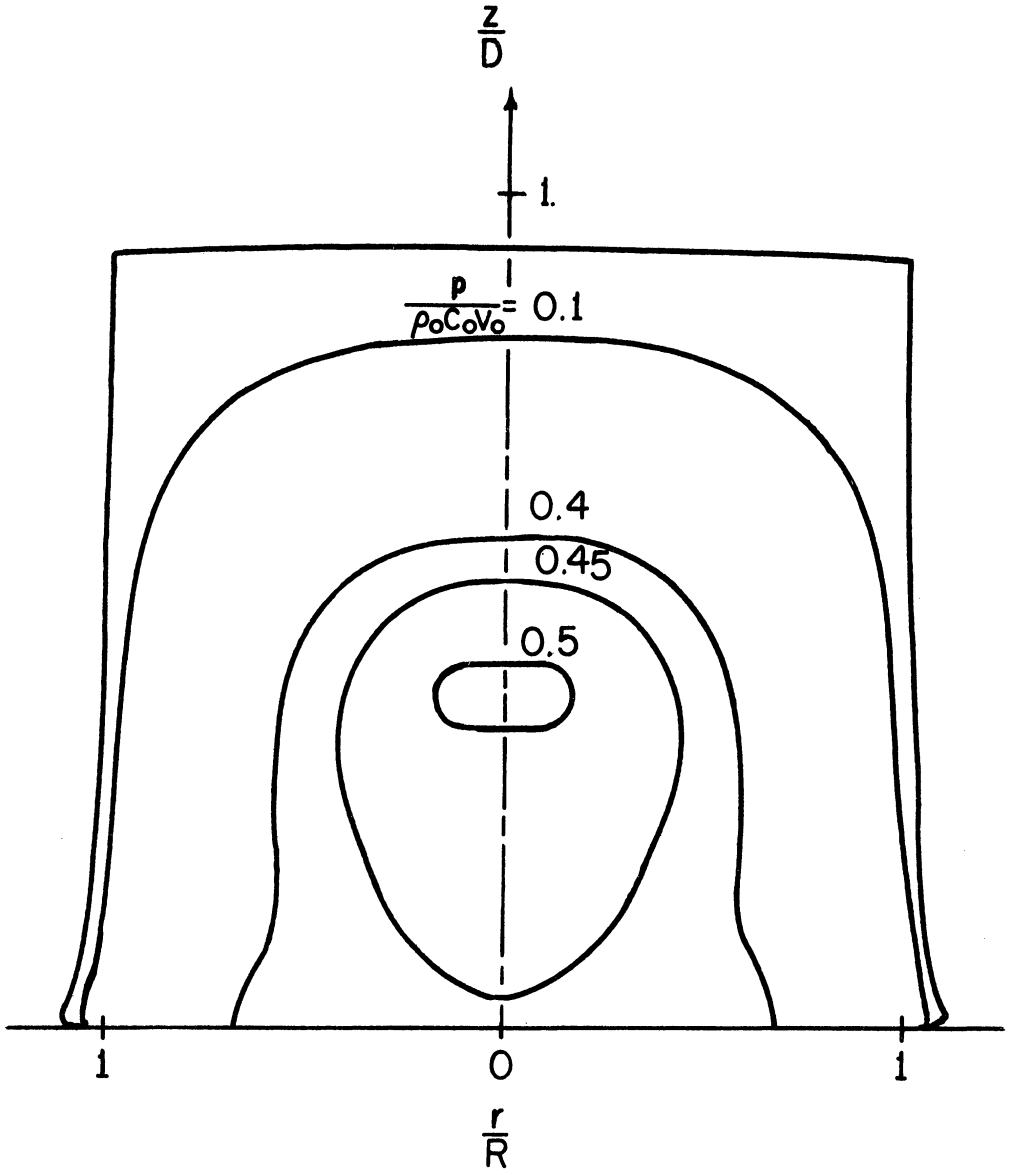

Fig. 7c. Isobar Distribution in an Initially Cylindrical Droplet with L/D = 1, at Time (Ct/D) = 0.5, for Impact Mach Number of 0.2 and for Free-Slip Boundary Condition.

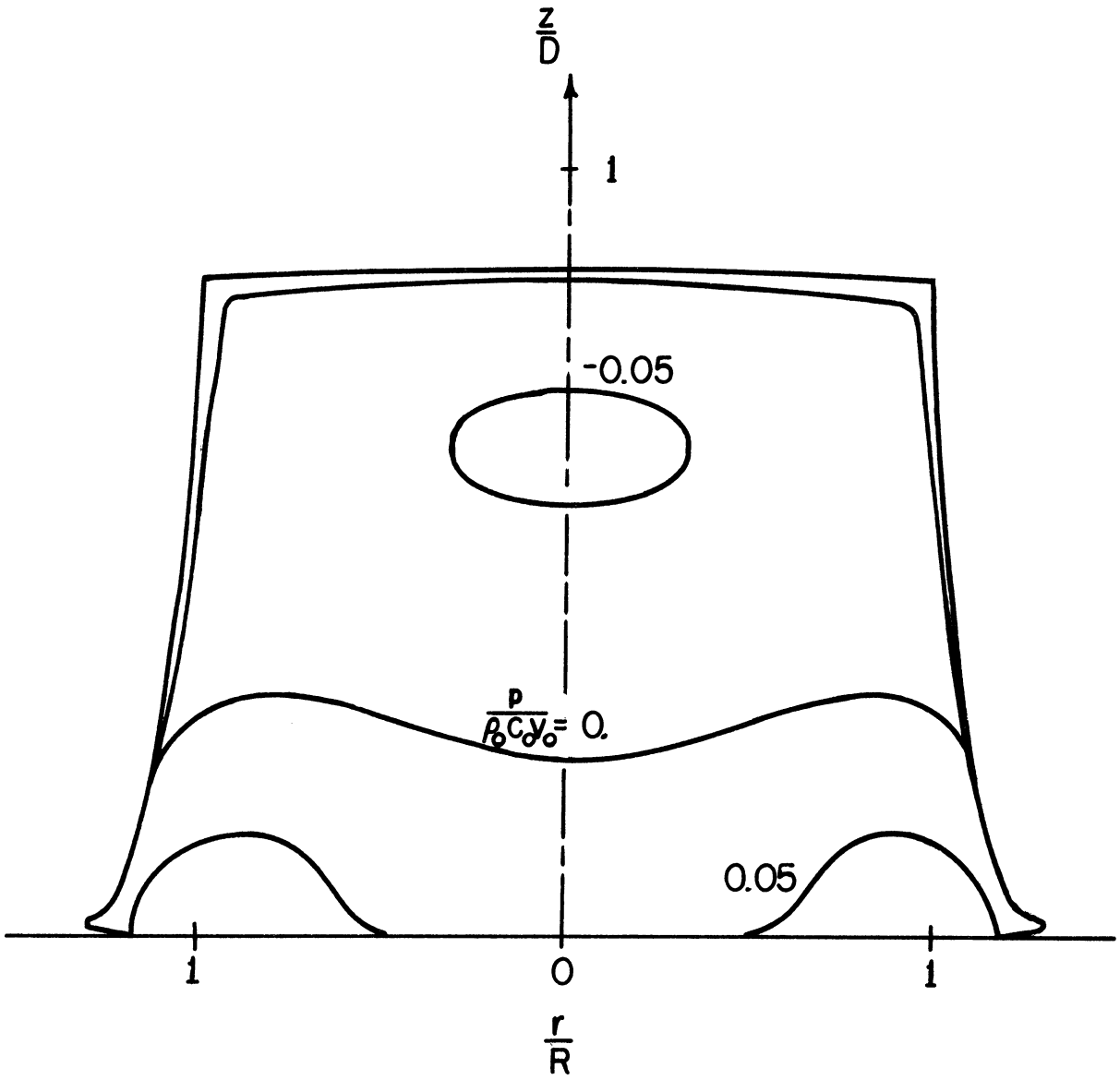

Fig. 7d. Isobar Distribution in an Initially Cylindrical Droplet with L/D = 1, at Time (Ct/D) = 1, for Impact Mach Number of 0.2 and for Free-Slip Boundary Condition.

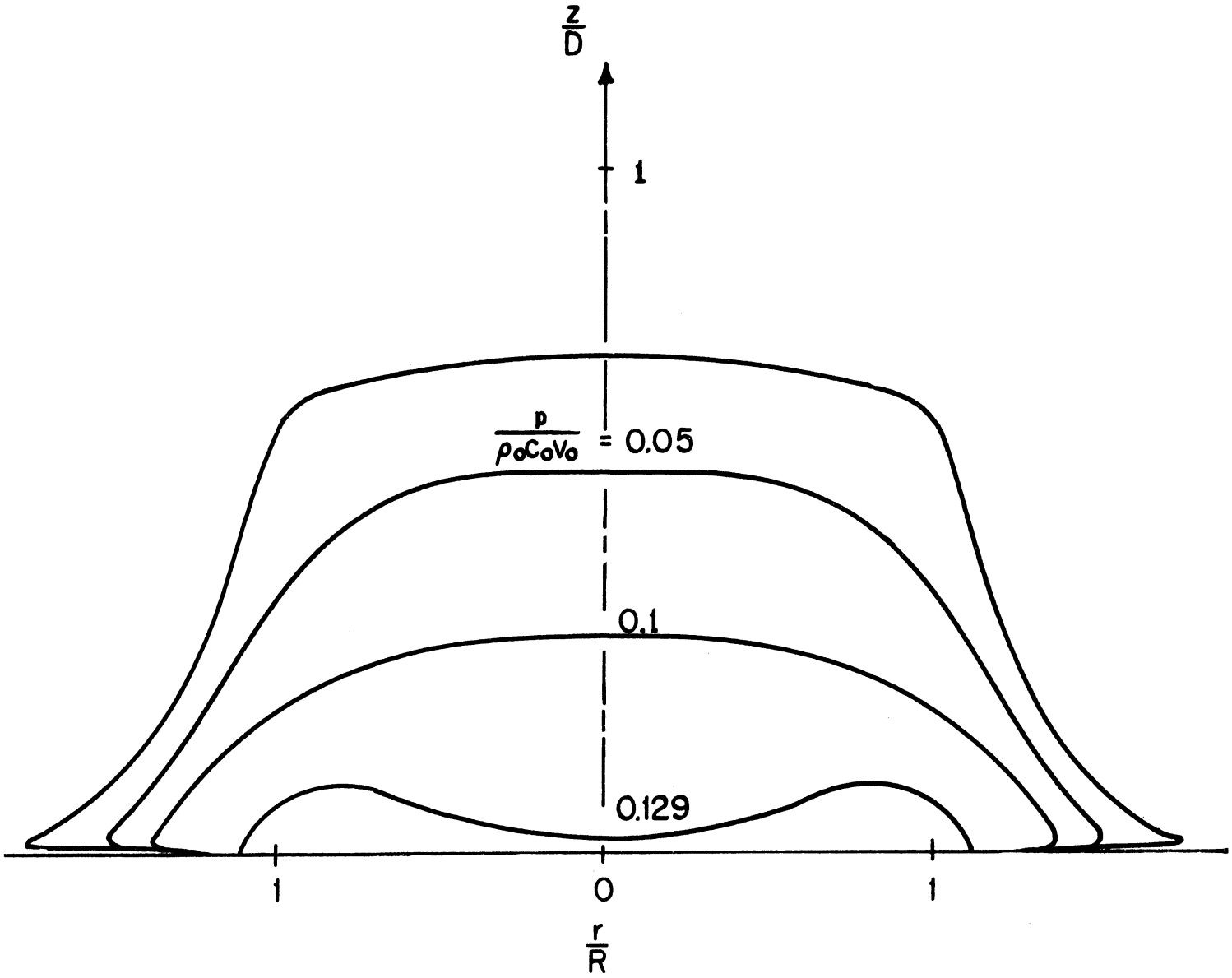

Fig. 7e. Isobar Distribution in an Initially Cylindrical Droplet with L/D = 1, at Time (Ct/D) = 2.5, for Impact Mach Number of 0.2 and for Free-Slip Boundary Condition.

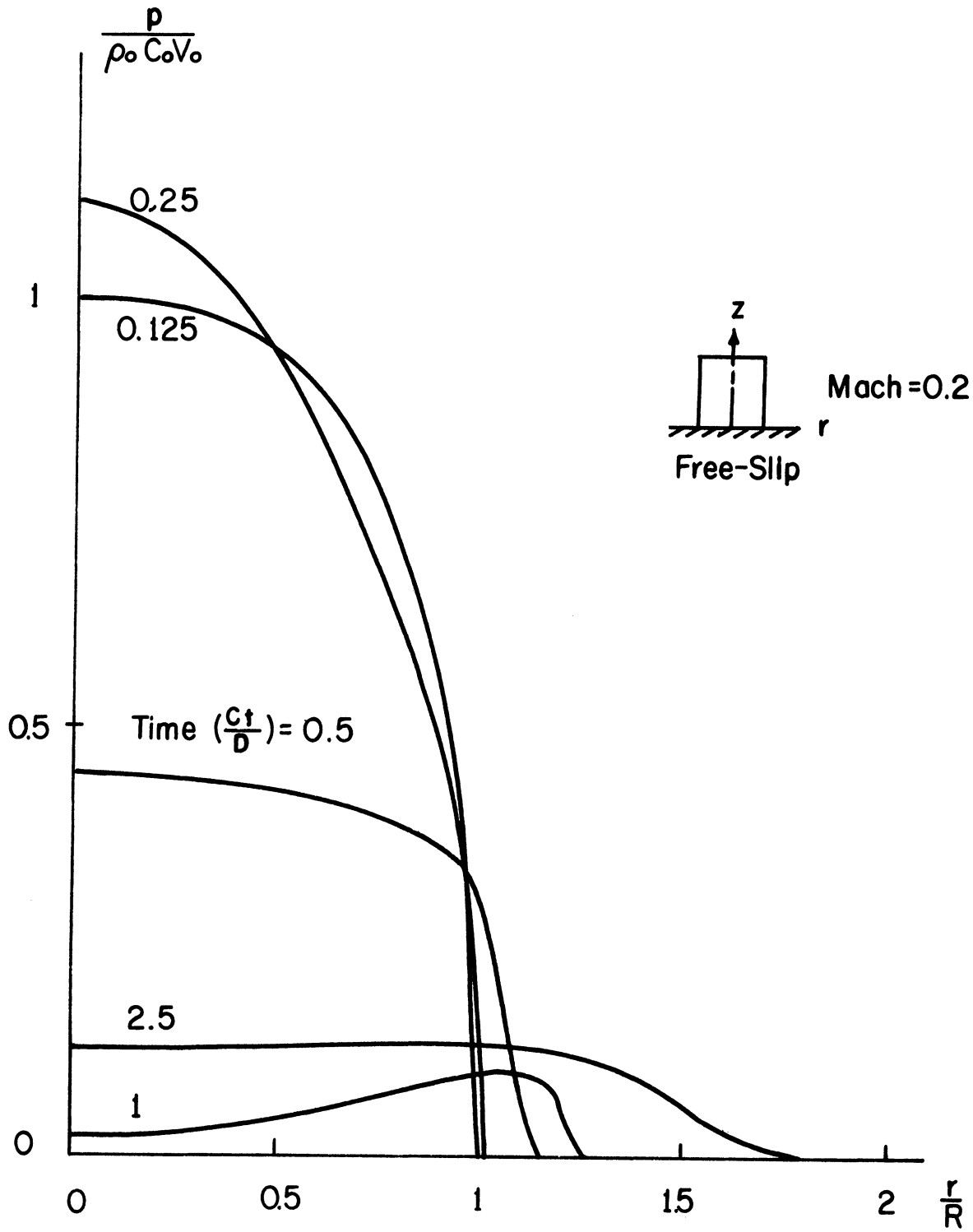

Fig. 8. Pressure-Time History at Liquid-Solid Interface (z = 0) of an Initially Cylindrical Droplet with L/D = 1, for Impact Mach Number of 0.2 and for Free-Slip Boundary Condition.

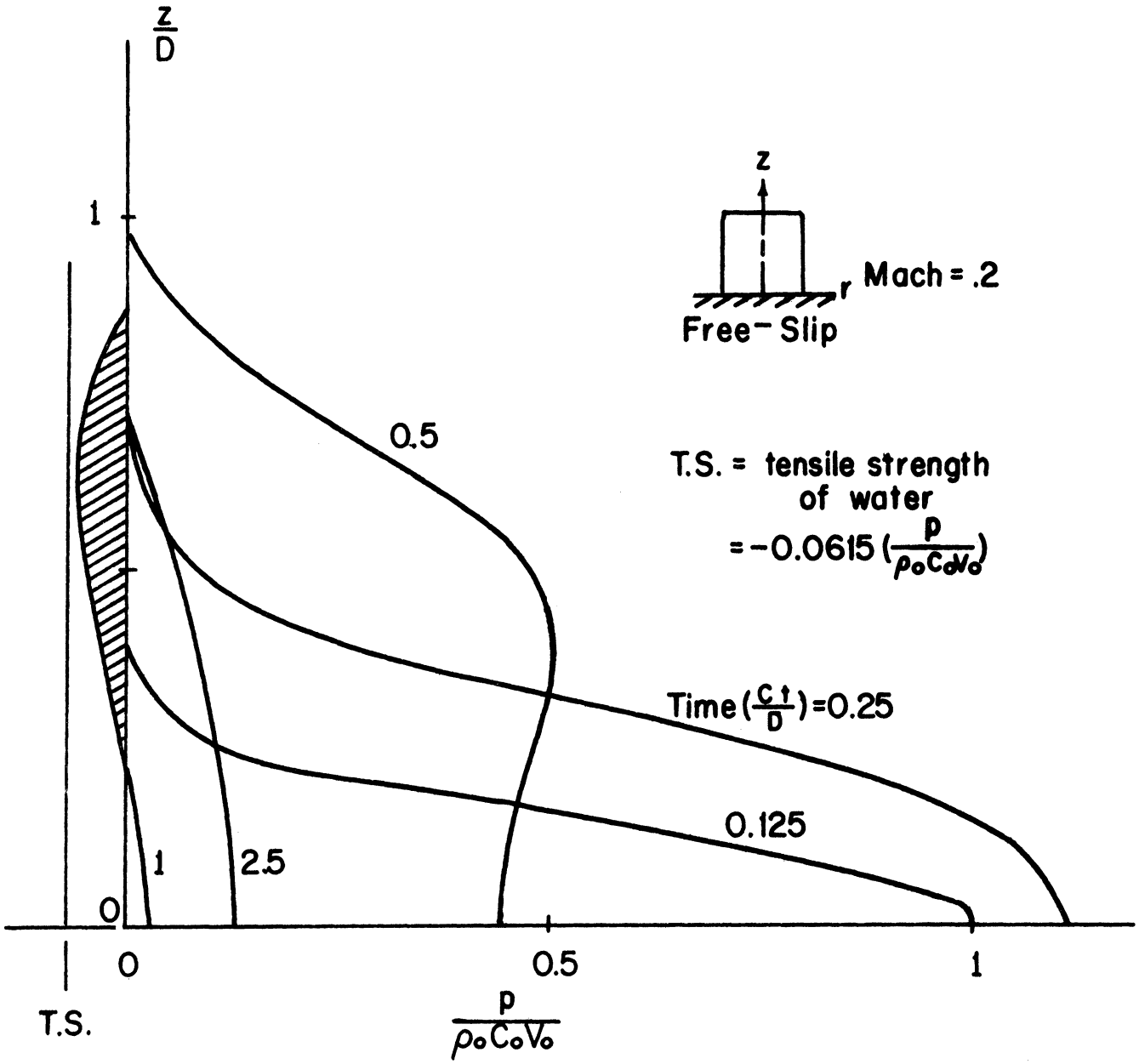

Fig. 9. Pressure-Time History along the Symmetrical Axis (r = 0) of an Initially Cylindrical Droplet with L/D = 1, for Impact Mach Number of 0.2 and for Free-Slip Boundary Condition.

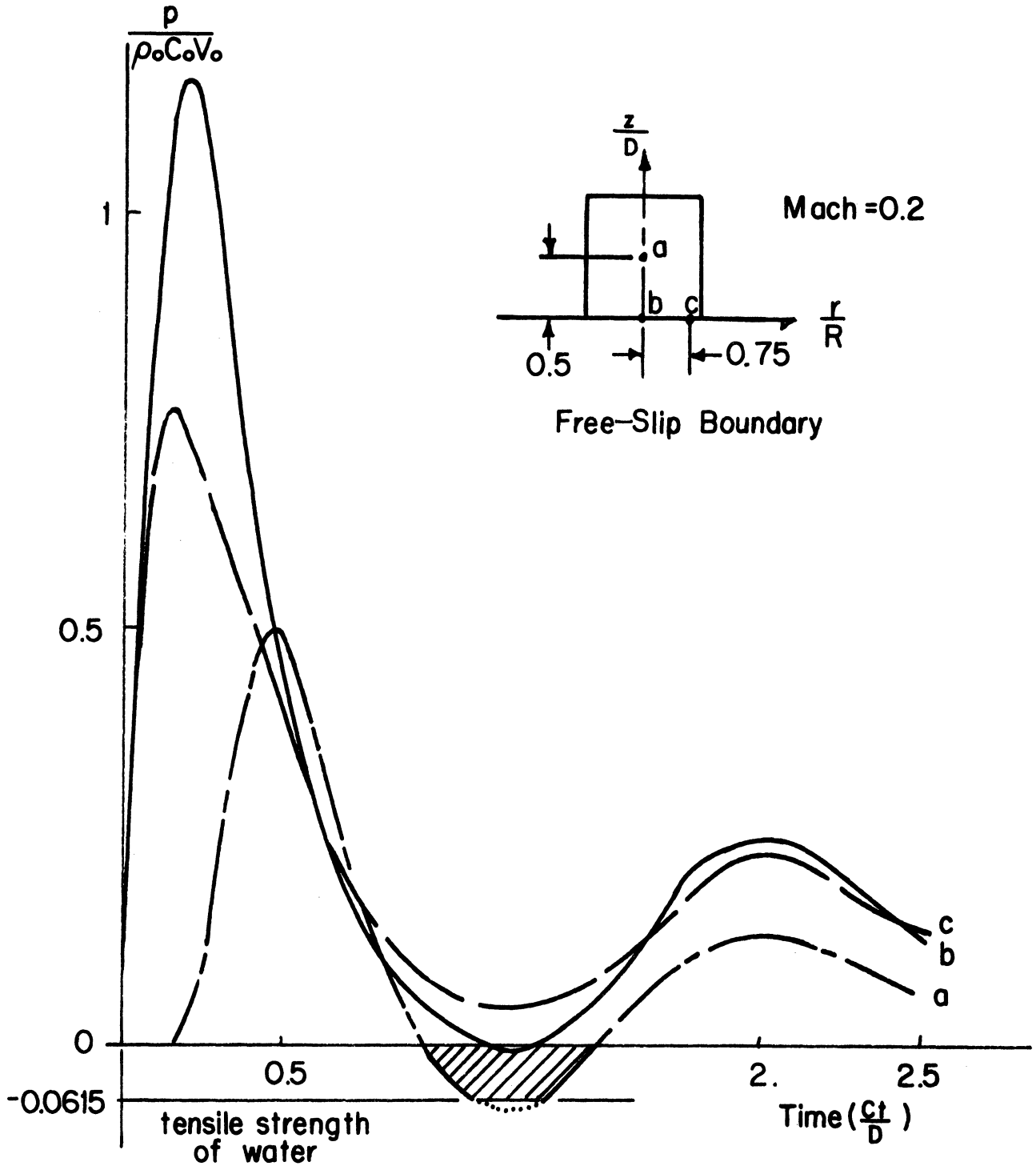

Fig. 10. Local Pressure-Time History at a (r = 0, z = 0.5L), b (r = 0, z = 0), and c (r = 0.75R, z = 0), in an Initially Cylindrical Droplet with L/D = 1, for Impact Mach Number of 0.2 and for Free-Slip Boundary Condition.

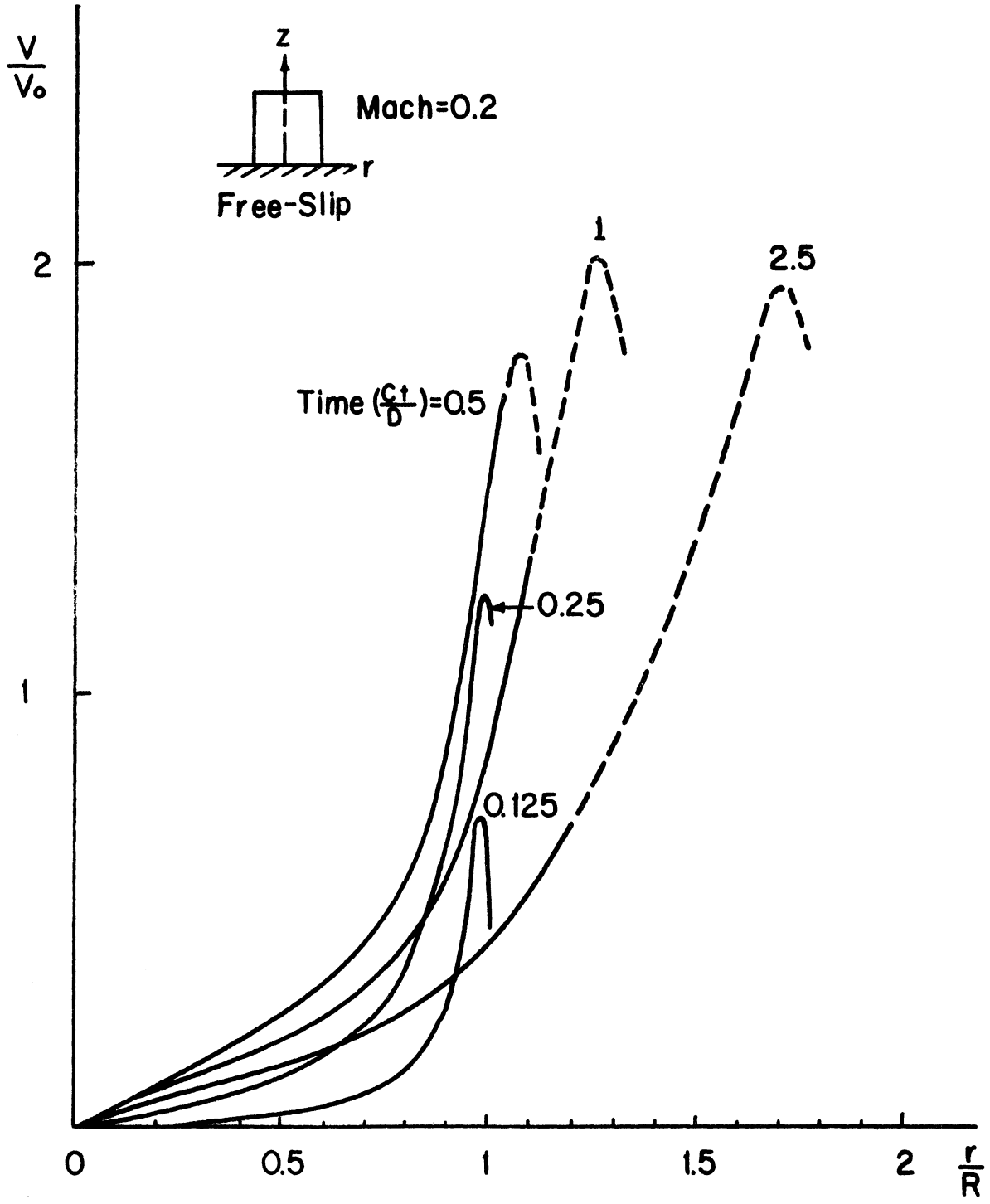

Fig. 11. Radial Velocity-Time History at Liquid-Solid Interface (r = 0) of an Initially Cylindrical Droplet with L/D = 1, for Impact Mach Number of 0.2 and for Free-Slip Boundary Condition.

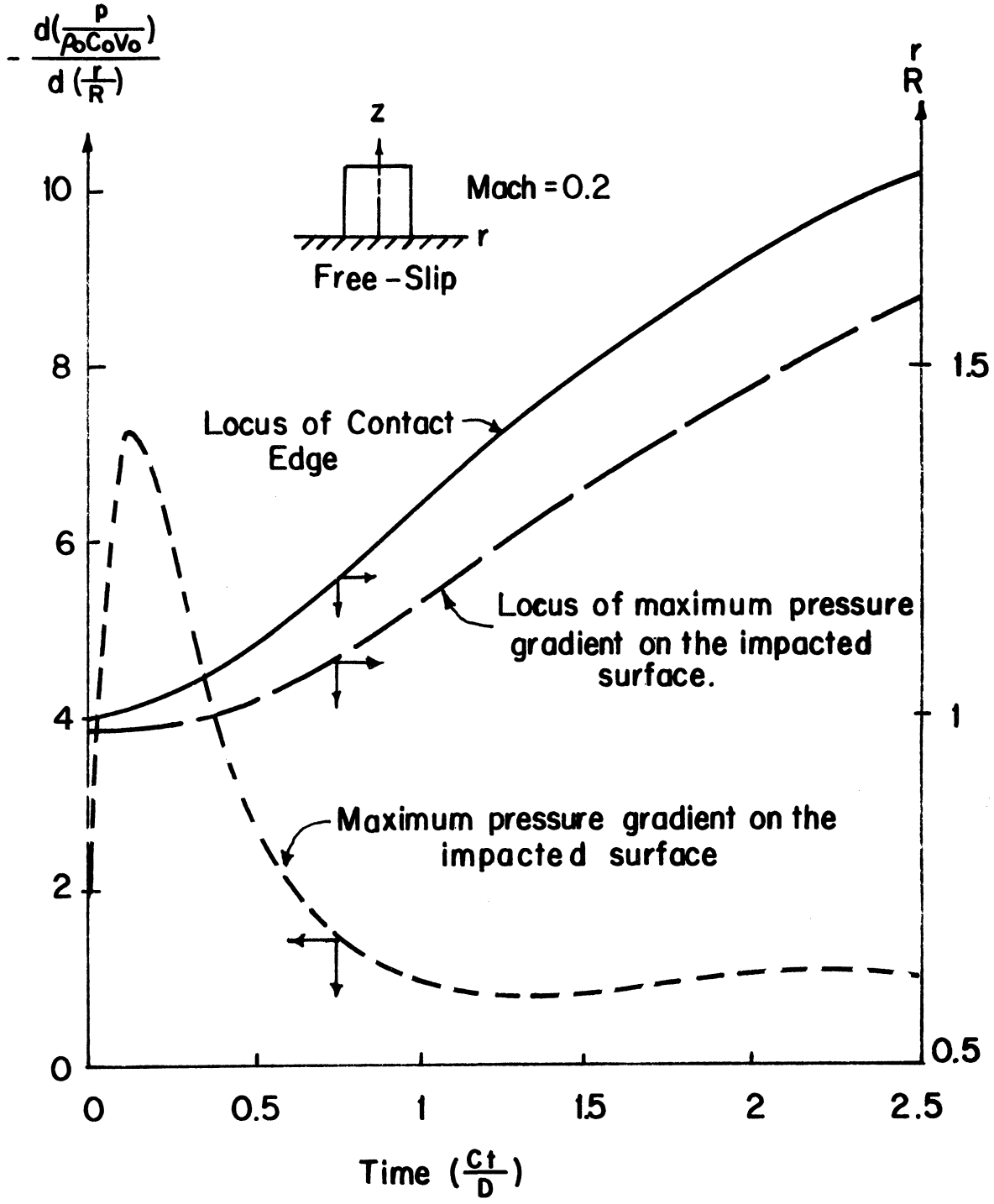

Fig. 12. Maximum Pressure Gradient-Time and -Location Relation and Contact Edge-Time History of an Initially Cylindrical Droplet with L/D = 1, for Impact Mach Number of 0.2 and for Free-Slip Boundary Condition.

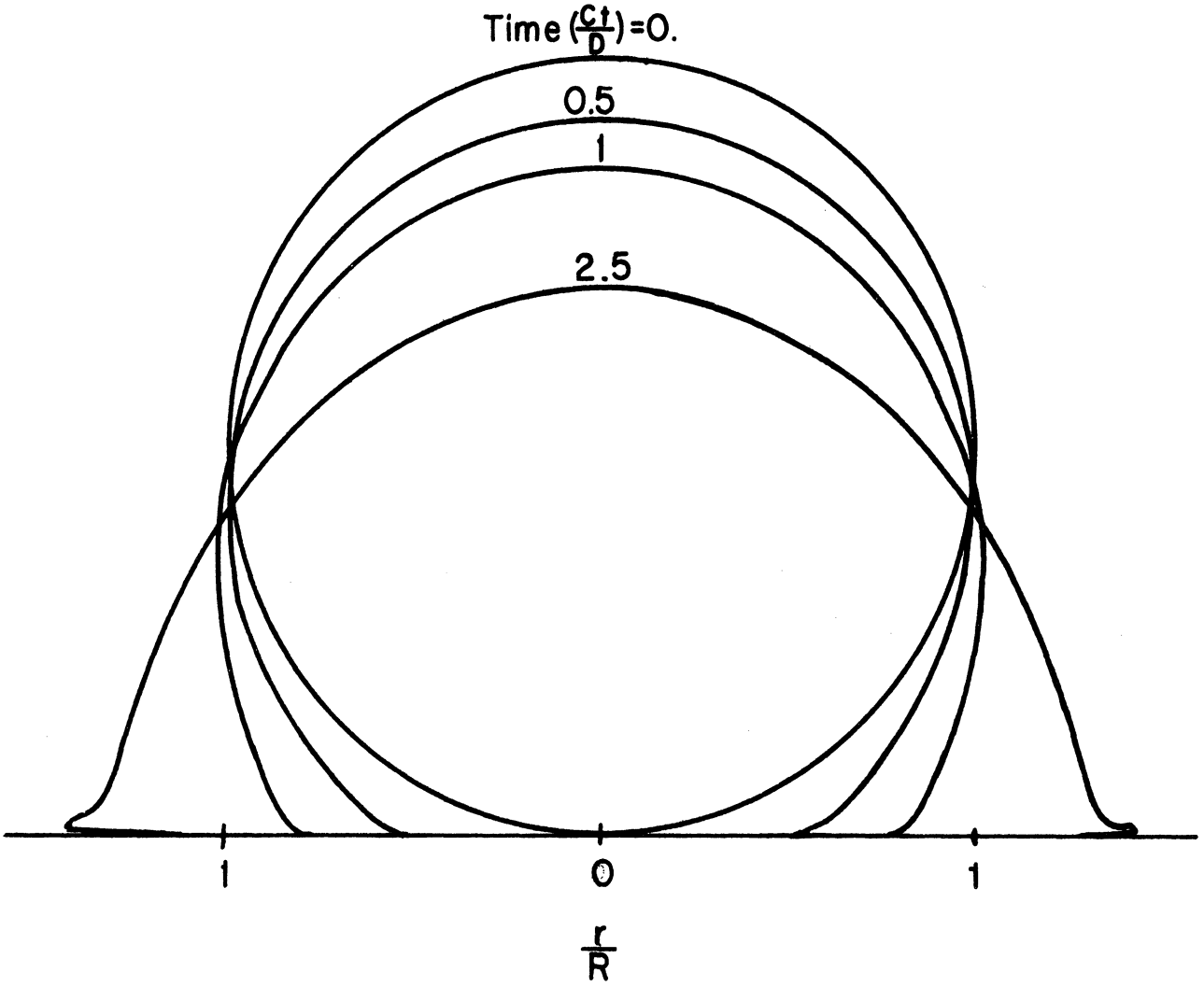

Fig. 13. Shape-Time History of an Initially Spherical Droplet at Mach Number = 0.2, for Free-Slip Boundary Condition.

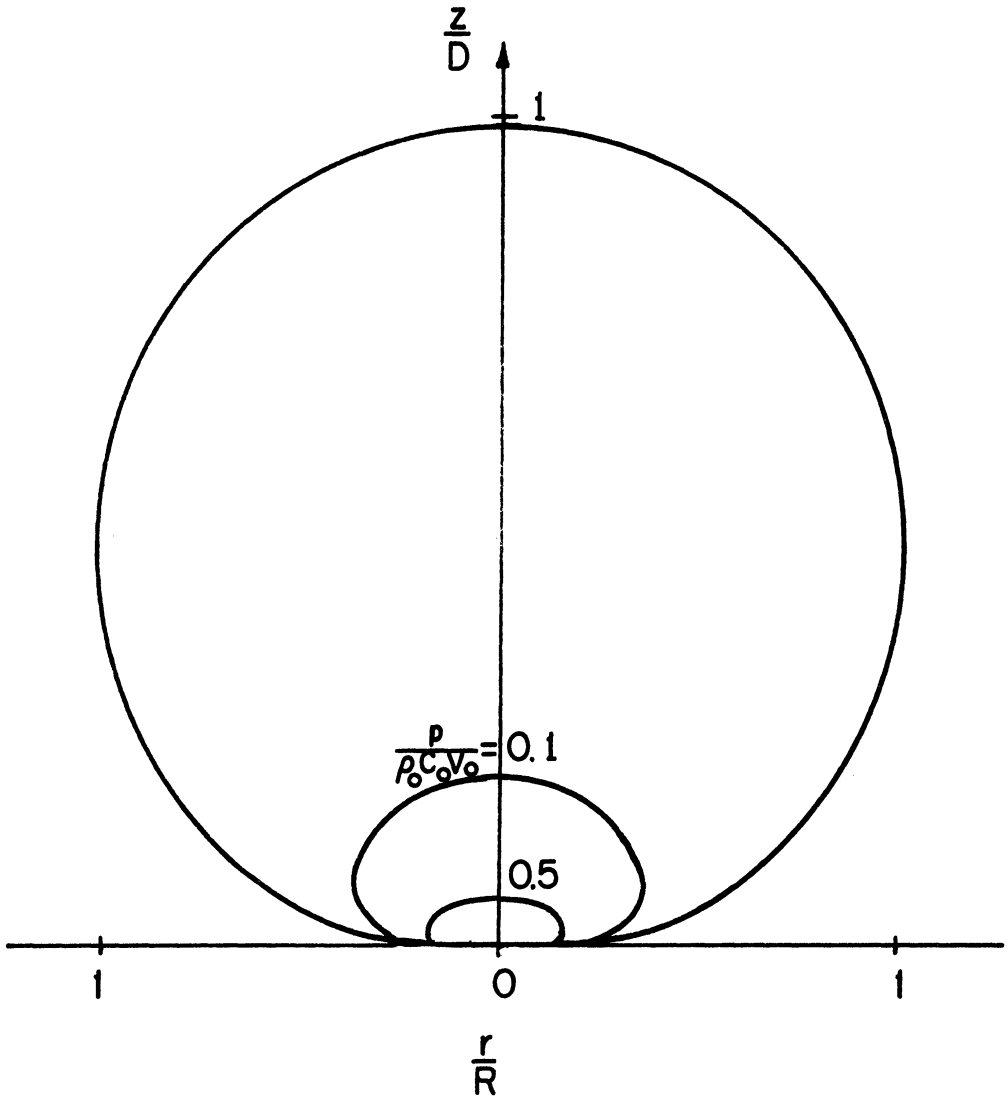

Fig. 14a. Isobar Distribution in an Initially Spherical Droplet at Time (Ct/D) = 0.125, for Impact Mach Number of 0.2 and for Free-Slip Boundary Condition.

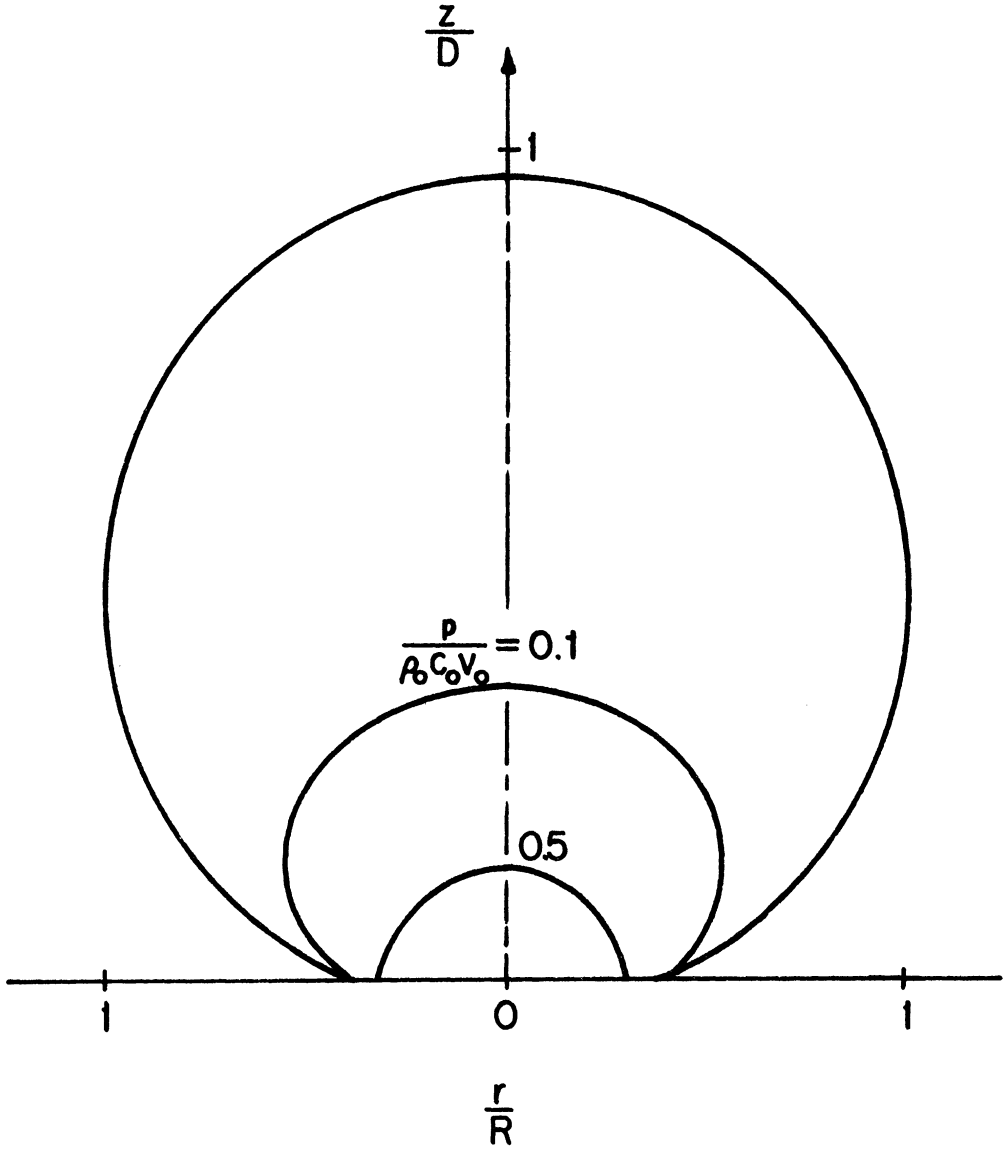

Fig. 14b. Isobar Distribution in an Initially Spherical Droplet at Time (Ct/D) = 0.25, for Impact Mach Number of 0.2 and for Free-Slip Boundary Condition.

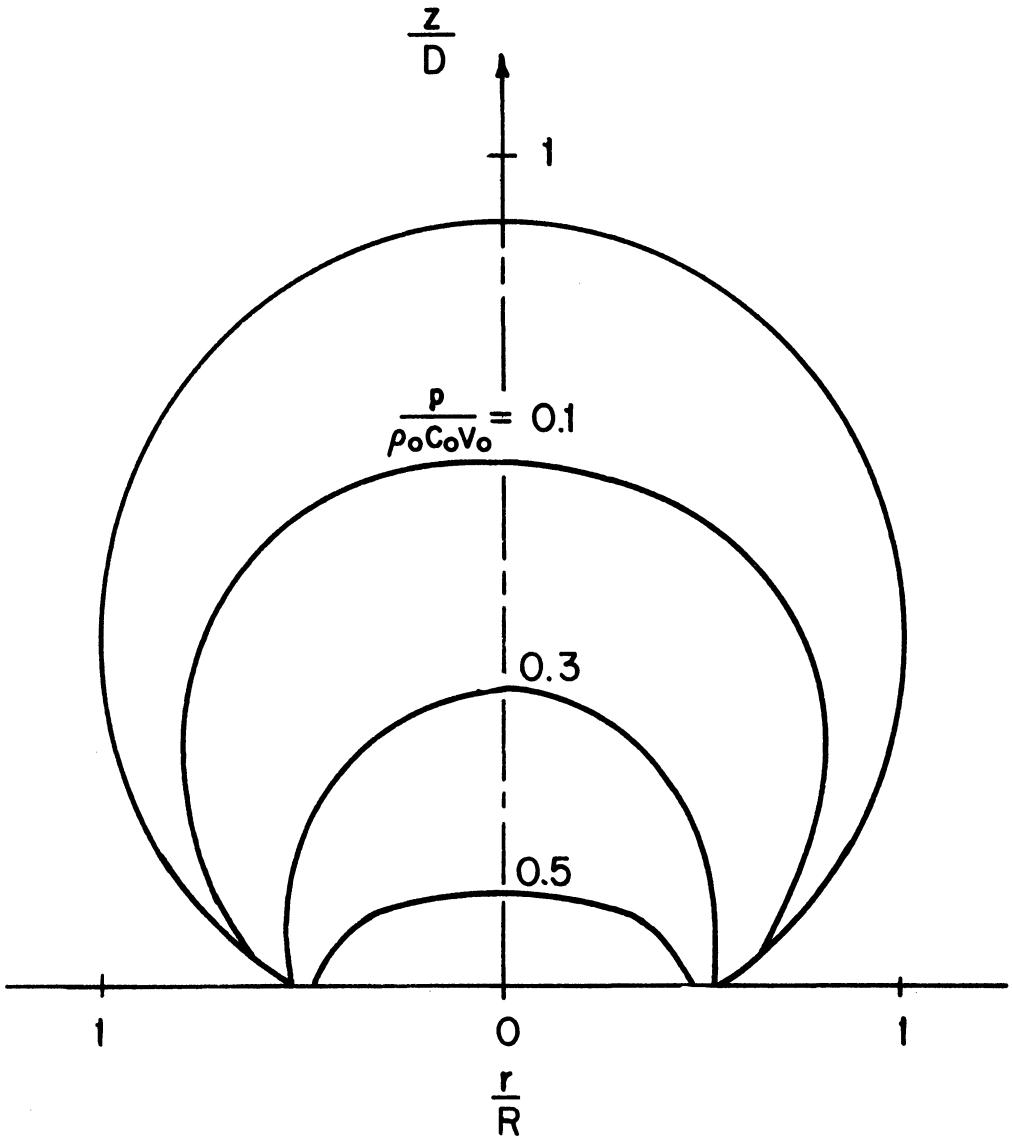

Fig. 14c. Isobar Distribution in an Initially Spherical Droplet at Time (Ct/D) = 0.5, for Impact Mach Number of 0.2 and for Free-Slip Boundary Condition.

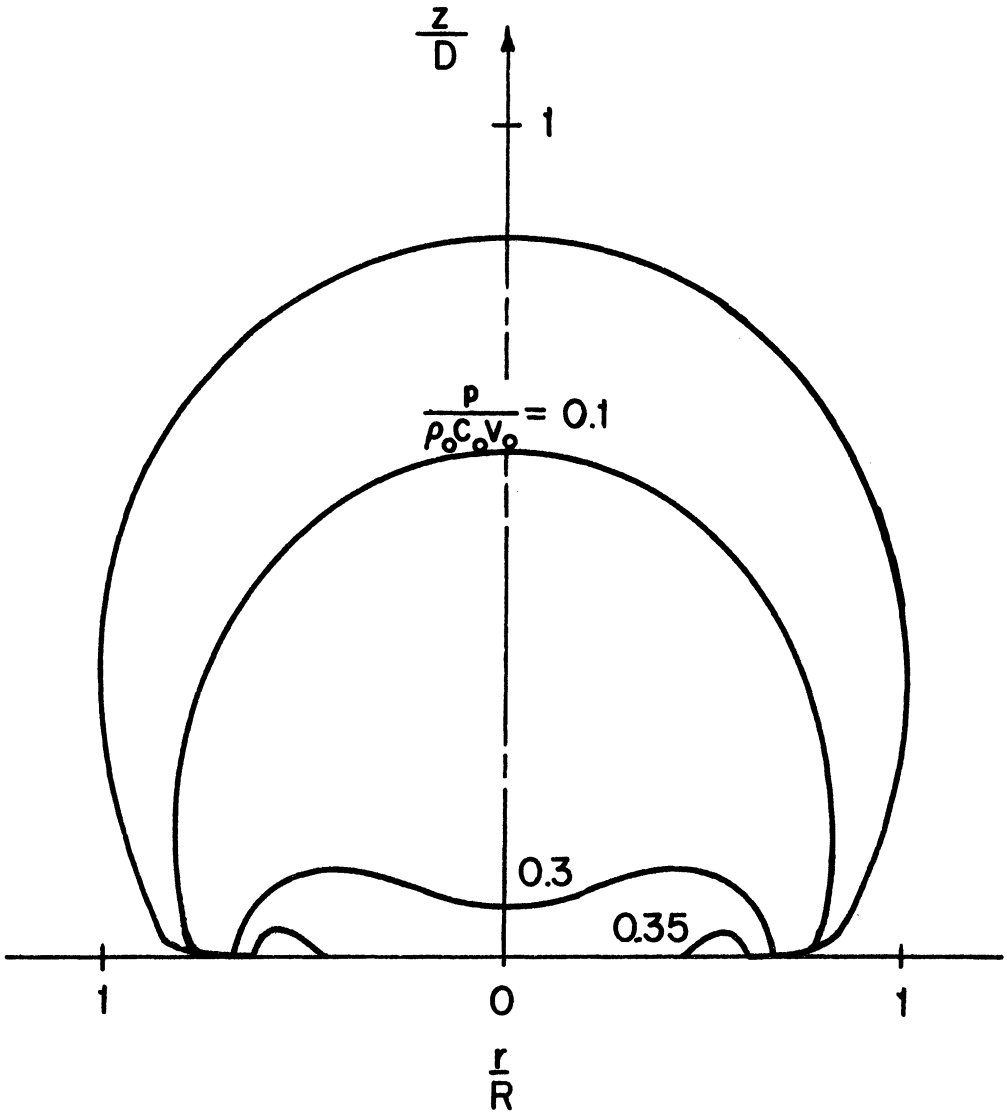

Fig. 14d. Isobar Distribution in an Initially Spherical Droplet at Time (Ct/D) = 1, for Impact Mach Number of 0.2 and for Free-Slip Boundary Condition.

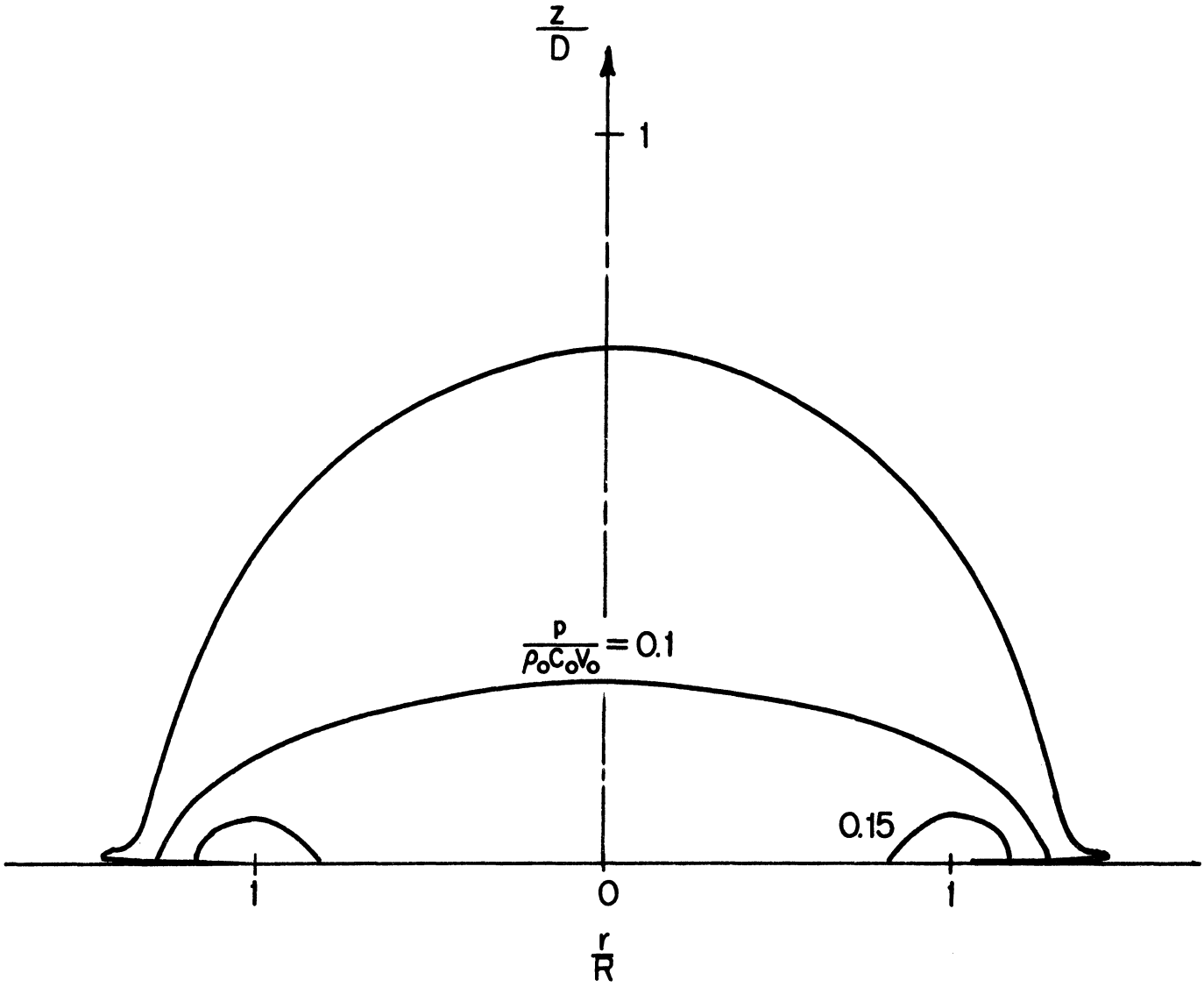

Fig. 14e. Isobar Distribution in an Initially Spherical Droplet at Time (Ct/D) = 2.5, for Impact Mach Number of 0.2 and for Free-Slip Boundary Condition.

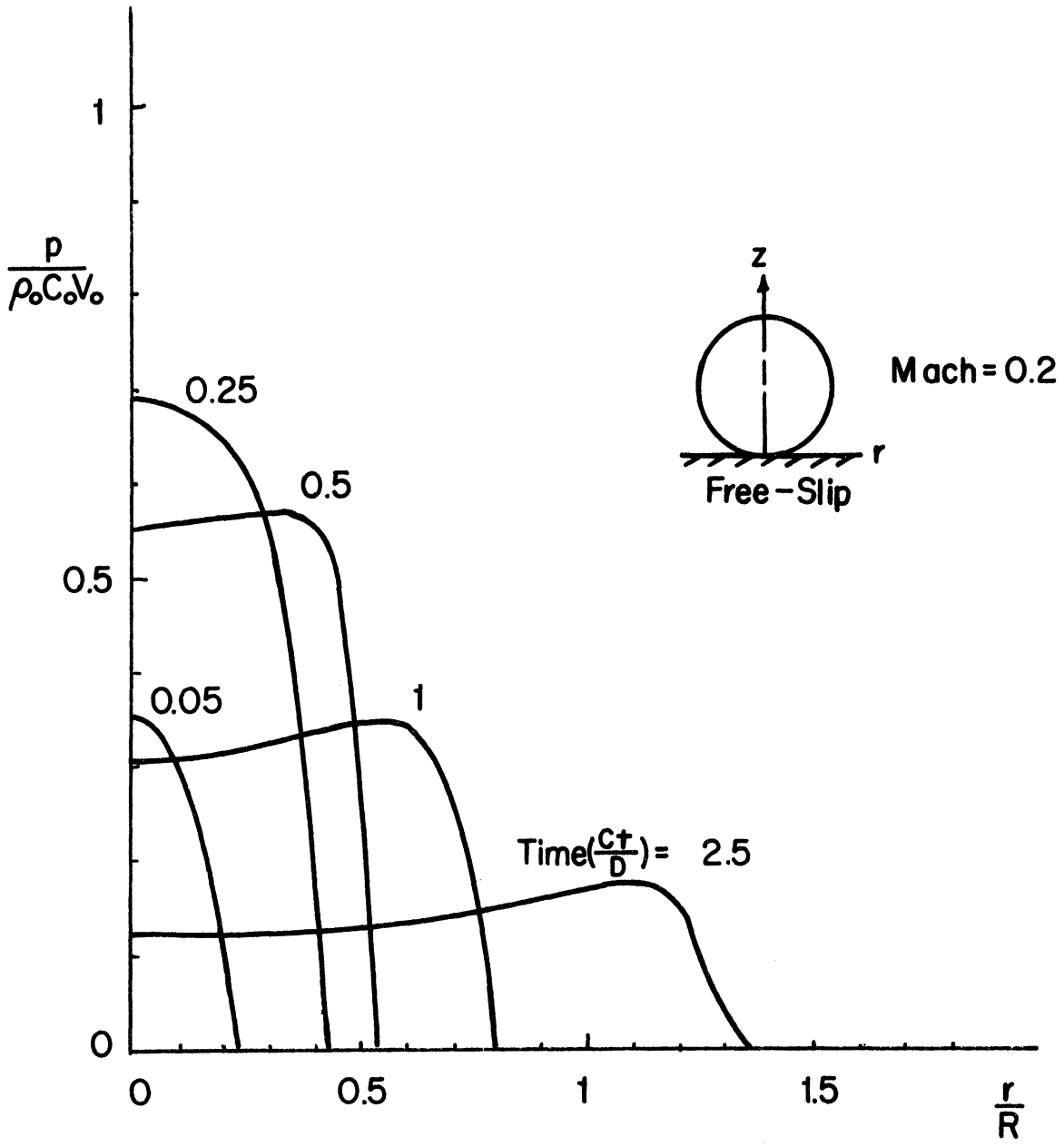

Fig. 15. Pressure-Time History at Liquid-Solid Interface (z = 0) of an Initially Spherical Droplet for Impact Mach Number of 0.2 and for Free-Slip Boundary Condition.

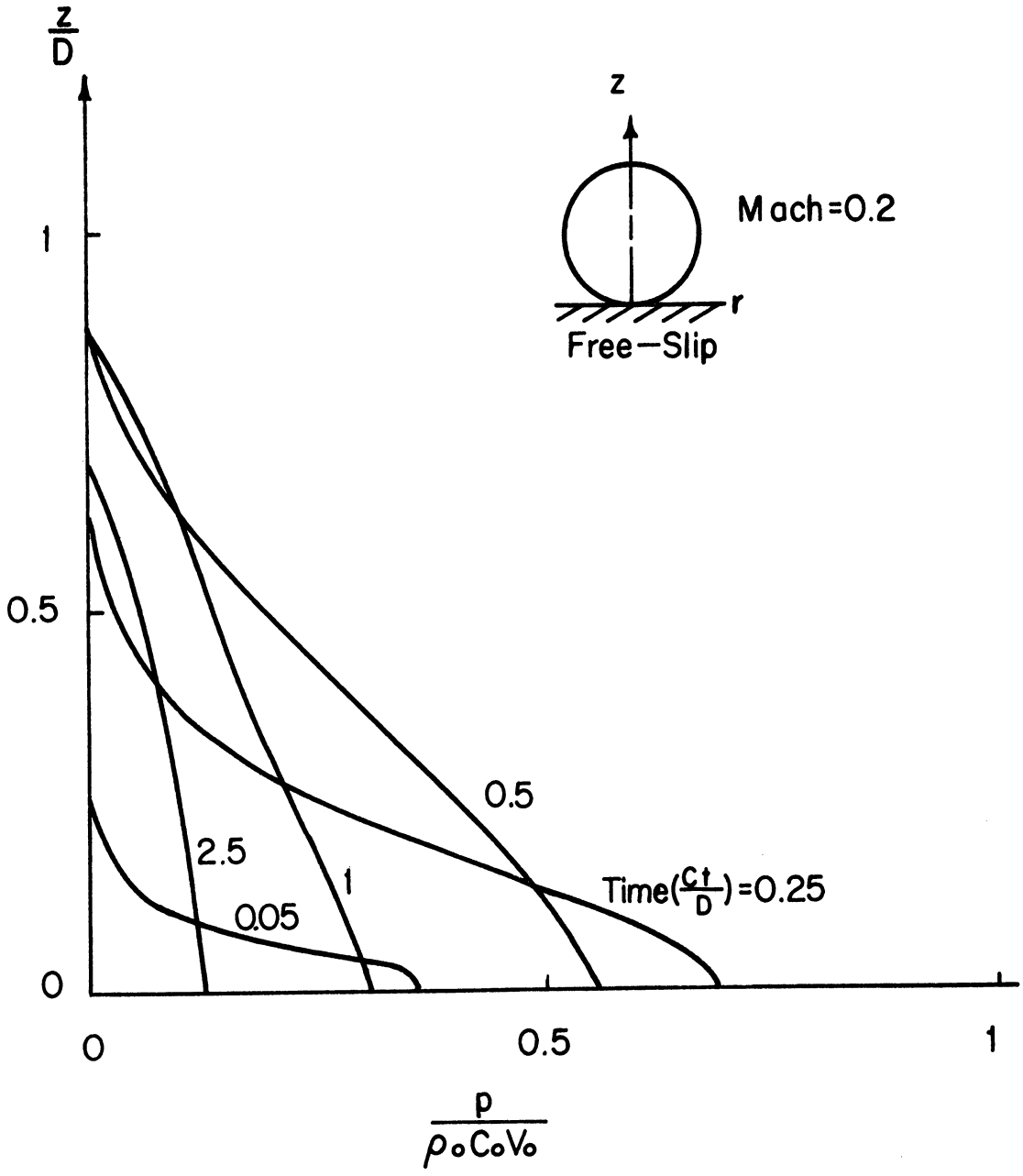

Fig. 16. Pressure-Time History along the Symmetrical Axis (r = 0) of an Initially Spherical Droplet for Impact Mach Number of 0.2 and for Free-Slip Boundary Condition.

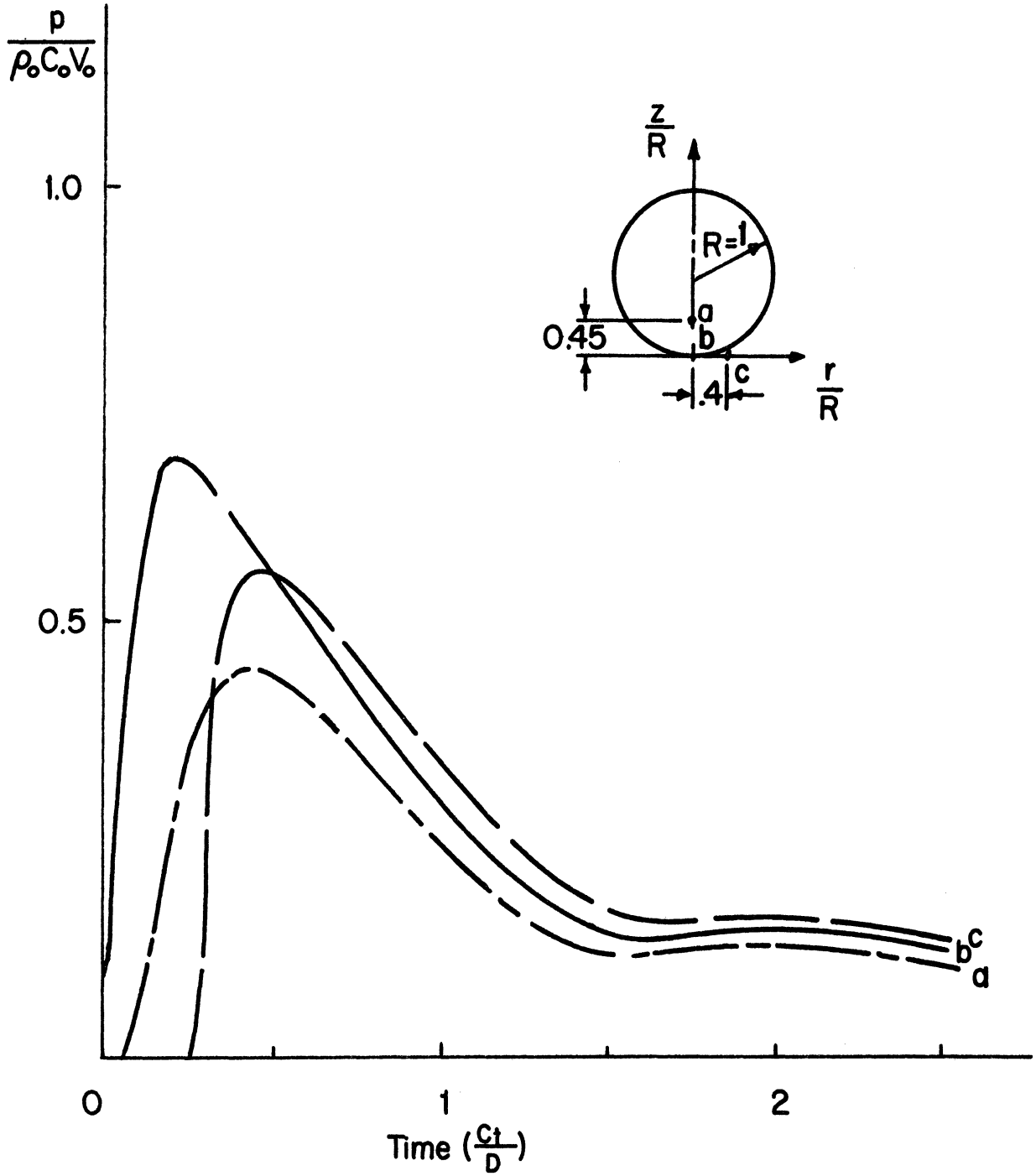

Fig. 17. Local Pressure-Time History at a (r = 0, z = 0.5L), b (r = 0, z = 0), and c (r = 0.75R, z = 0), in an Initially Spherical Droplet for Impact Mach Number of 0.2 and for Free-Slip Boundary Condition.

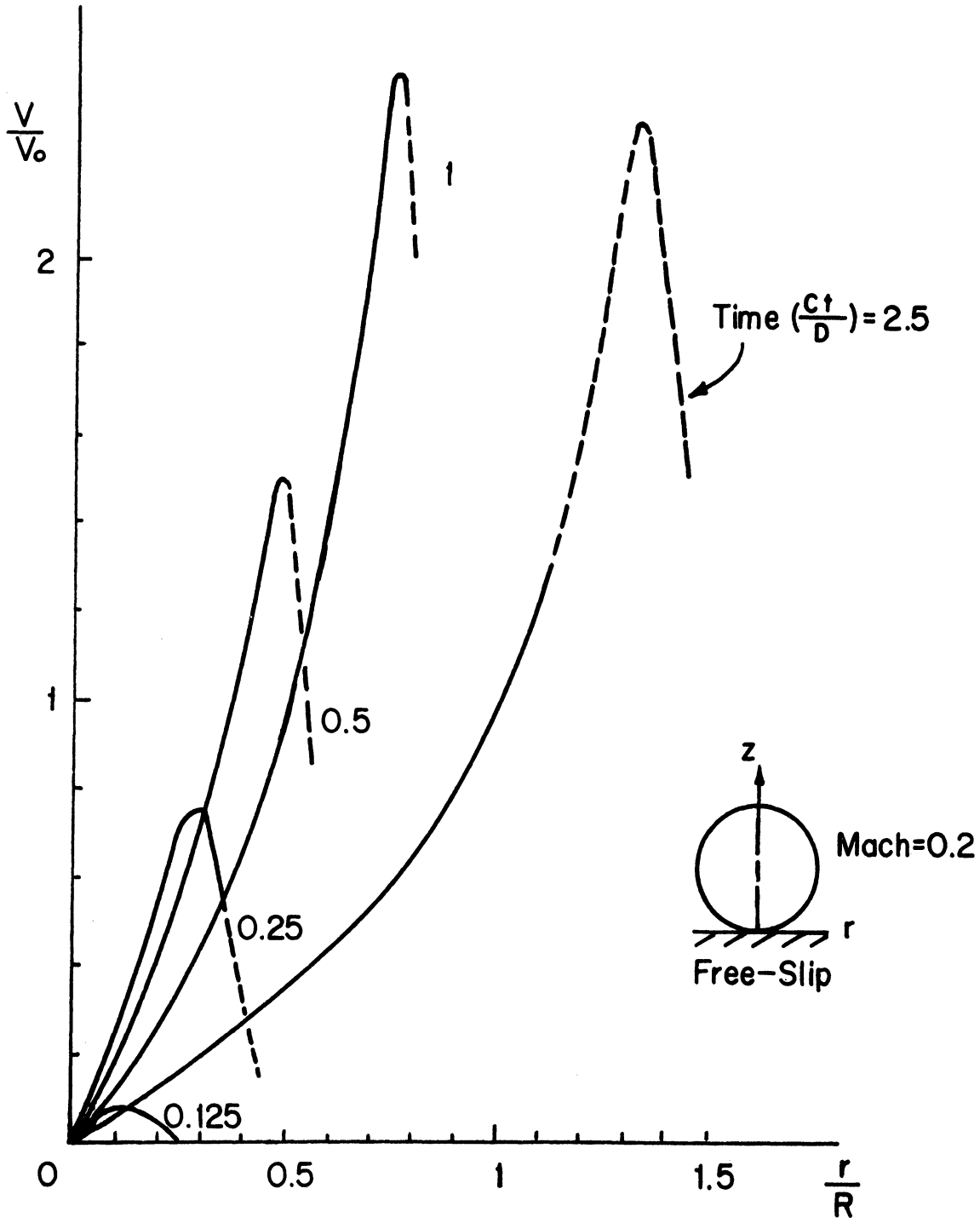

Fig. 18. Radial Velocity-Time History at Liquid-Solid Interface (r = 0) of an Initially Spherical Droplet for Impact Mach Number of 0.2 and for Free-Slip Boundary Condition.

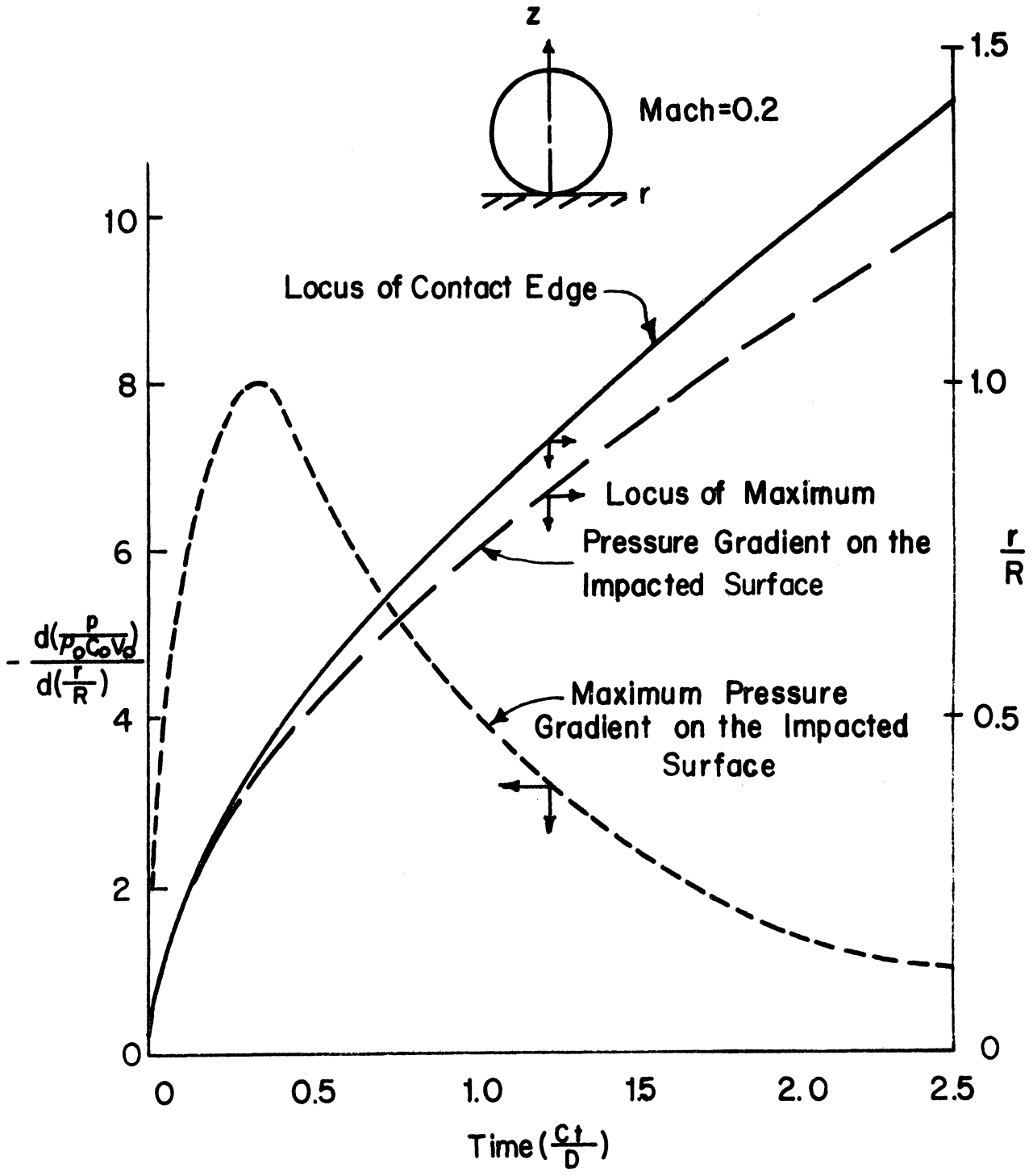

Fig. 19. Maximum Pressure Gradient-Time and -Location Relation and Contact Edge-Time History of an Initially Spherical Droplet for Impact Mach Number of 0.2 and for Free-Slip Boundary Condition.

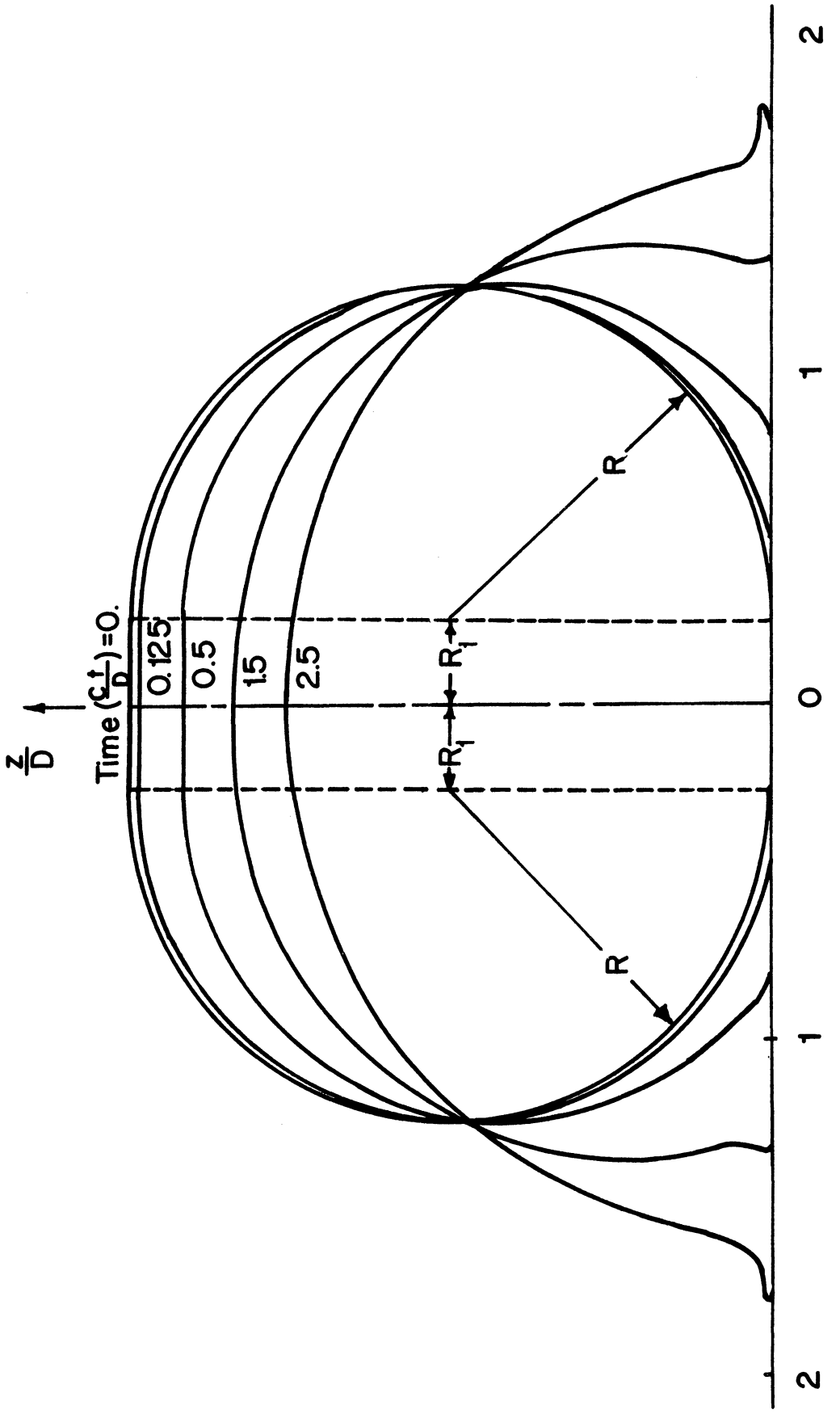

Fig. 20. Shape-Time History of an Initially Cylindrical-Spherical Composite Droplet with $R_1/R = 0.25$ and $L/D = 1$, at Mach Number = 0.2, for Free-Slip Boundary Condition.

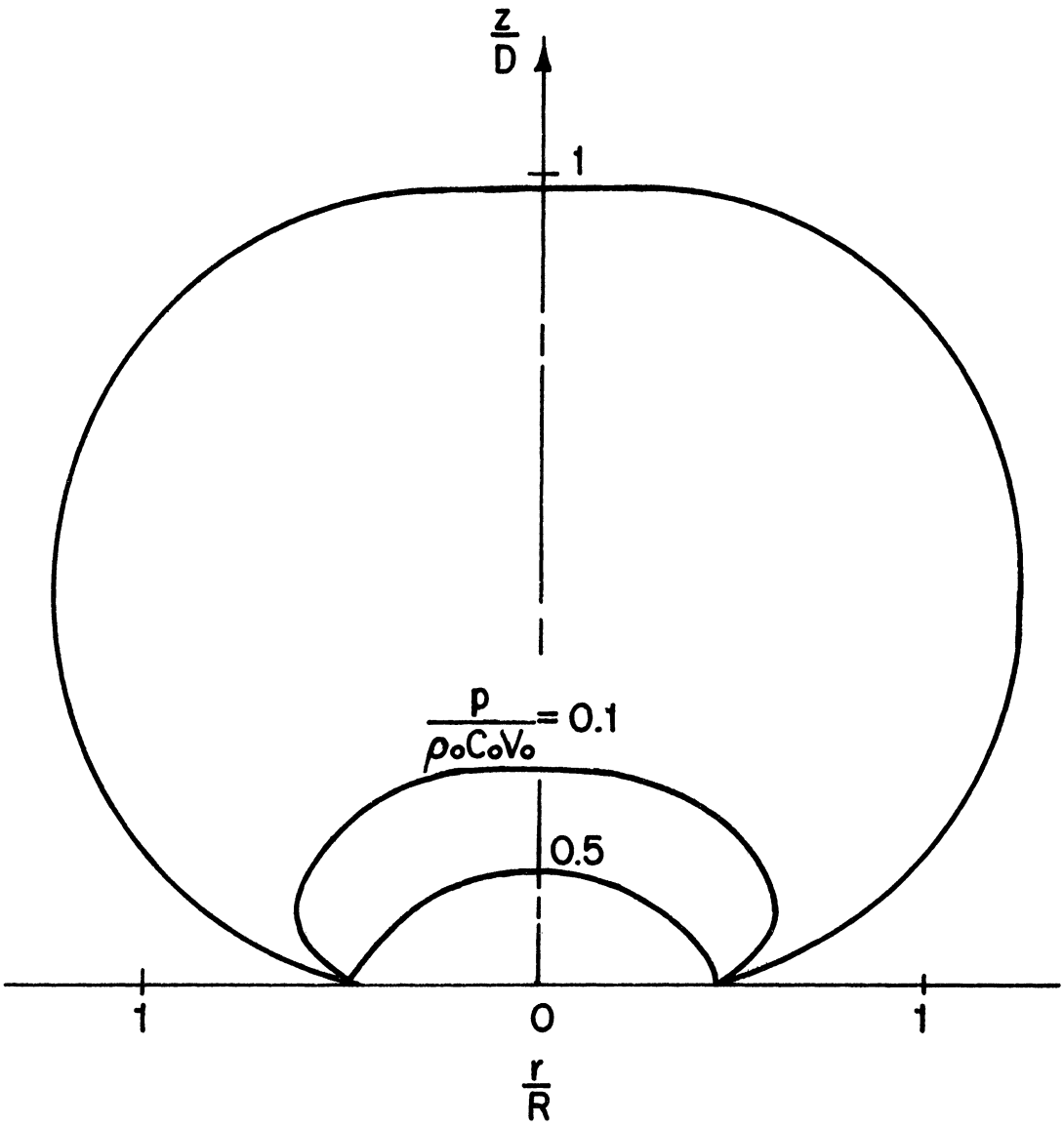

Fig. 21a. Isobar Distribution in an Initially Cylindrical-Spherical Composite Droplet with $R_1/R = 0.25$ and $L/D = 1$, at Time $(Ct/D) = 0.125$, for Impact Mach Number of 0.2 and for Free-Slip Boundary Condition.

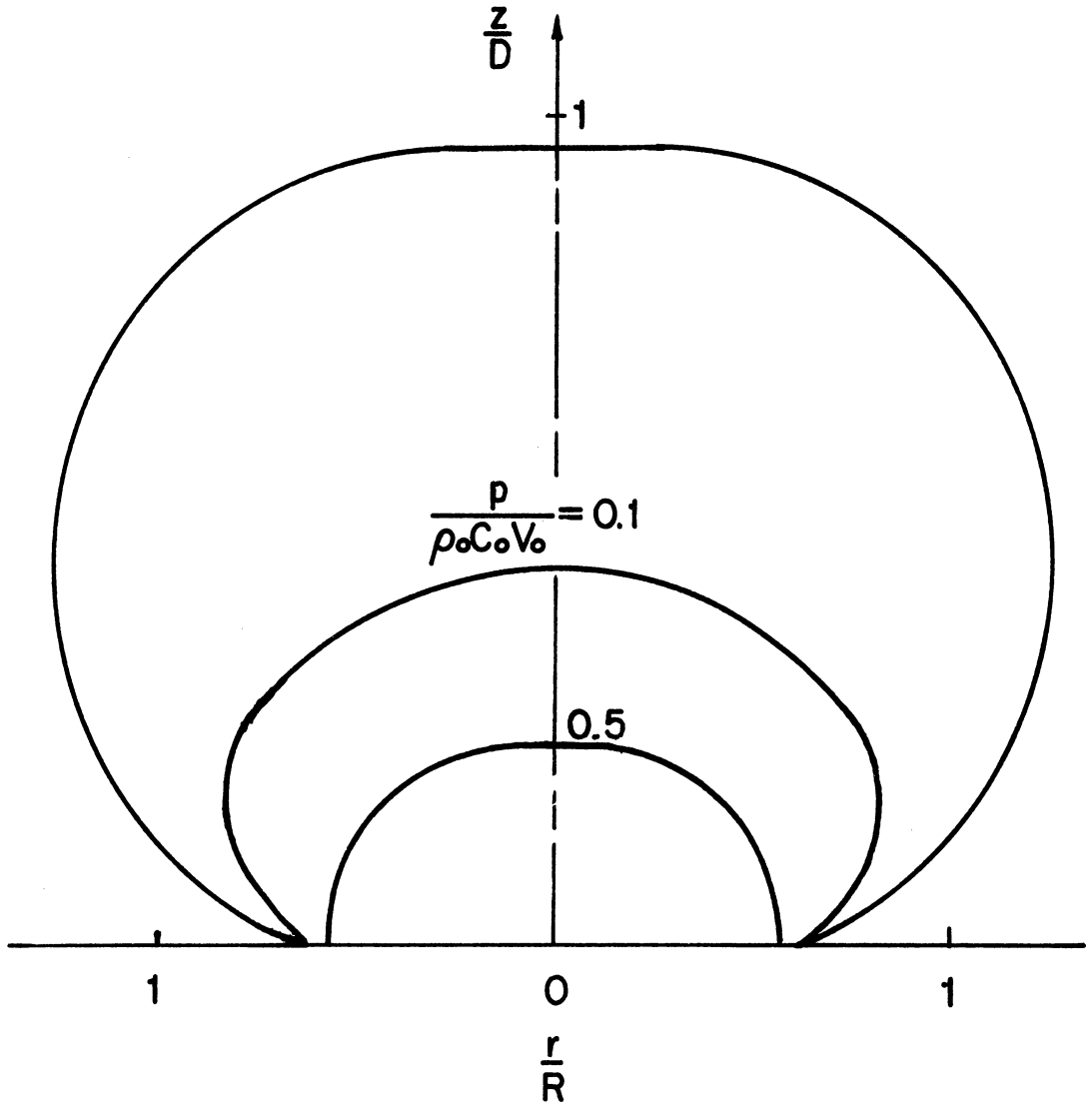

Fig. 21b. Isobar Distribution in an Initially Cylindrical-Spherical Composite Droplet with $R_1/R = 0.25$ and $L/D = 1$, at Time $(Ct/D) = 0.25$, for Impact Mach Number of 0.2 and for Free-Slip Boundary Condition.

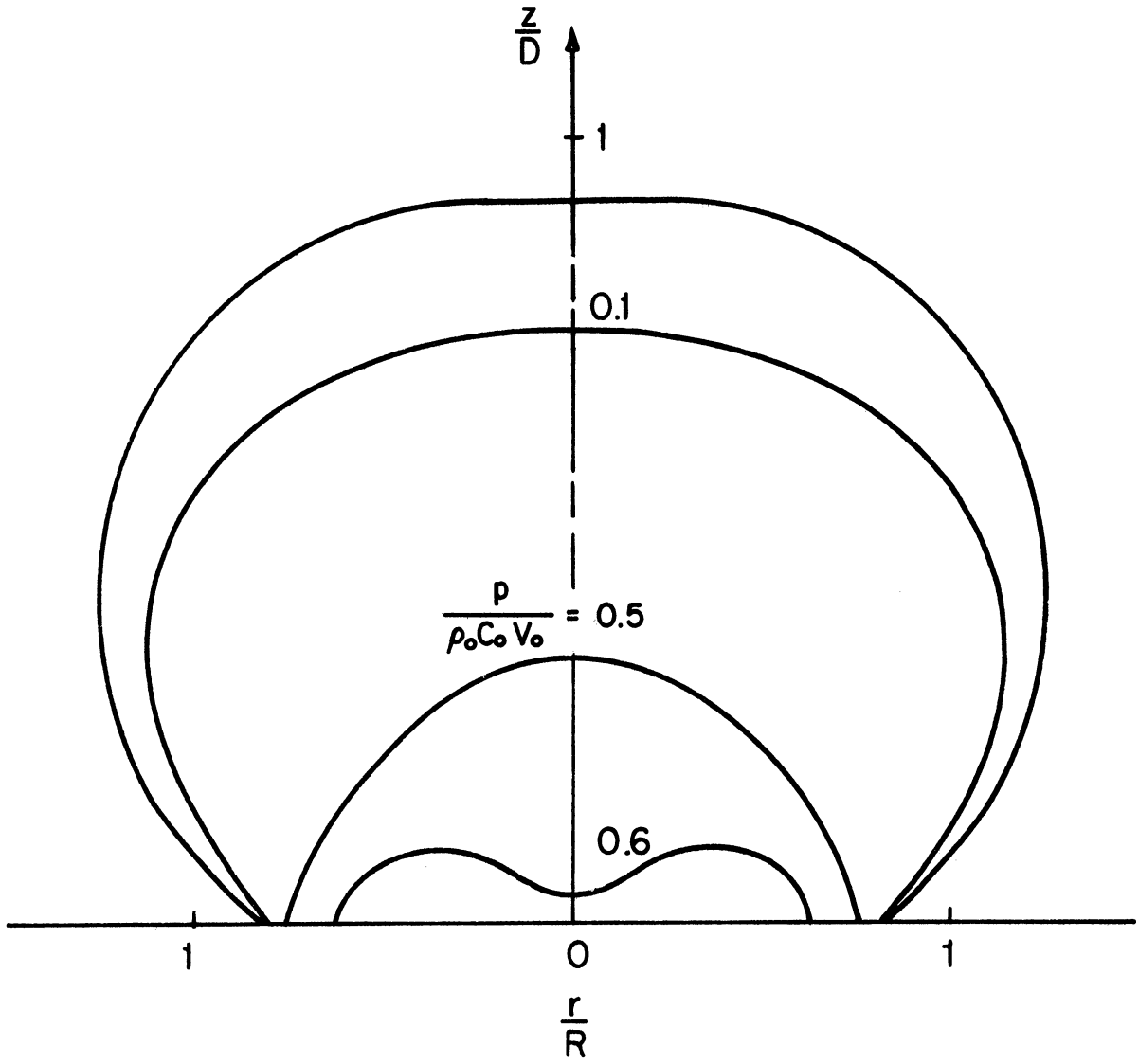

Fig. 21c. Isobar Distribution in an Initially Cylindrical-Spherical Composite Droplet with $R_1/R = 0.25$ and $L/D = 1$, at Time $(Ct/D) = 0.5$, for Impact Mach Number of 0.2 and for Free-Slip Boundary Condition.

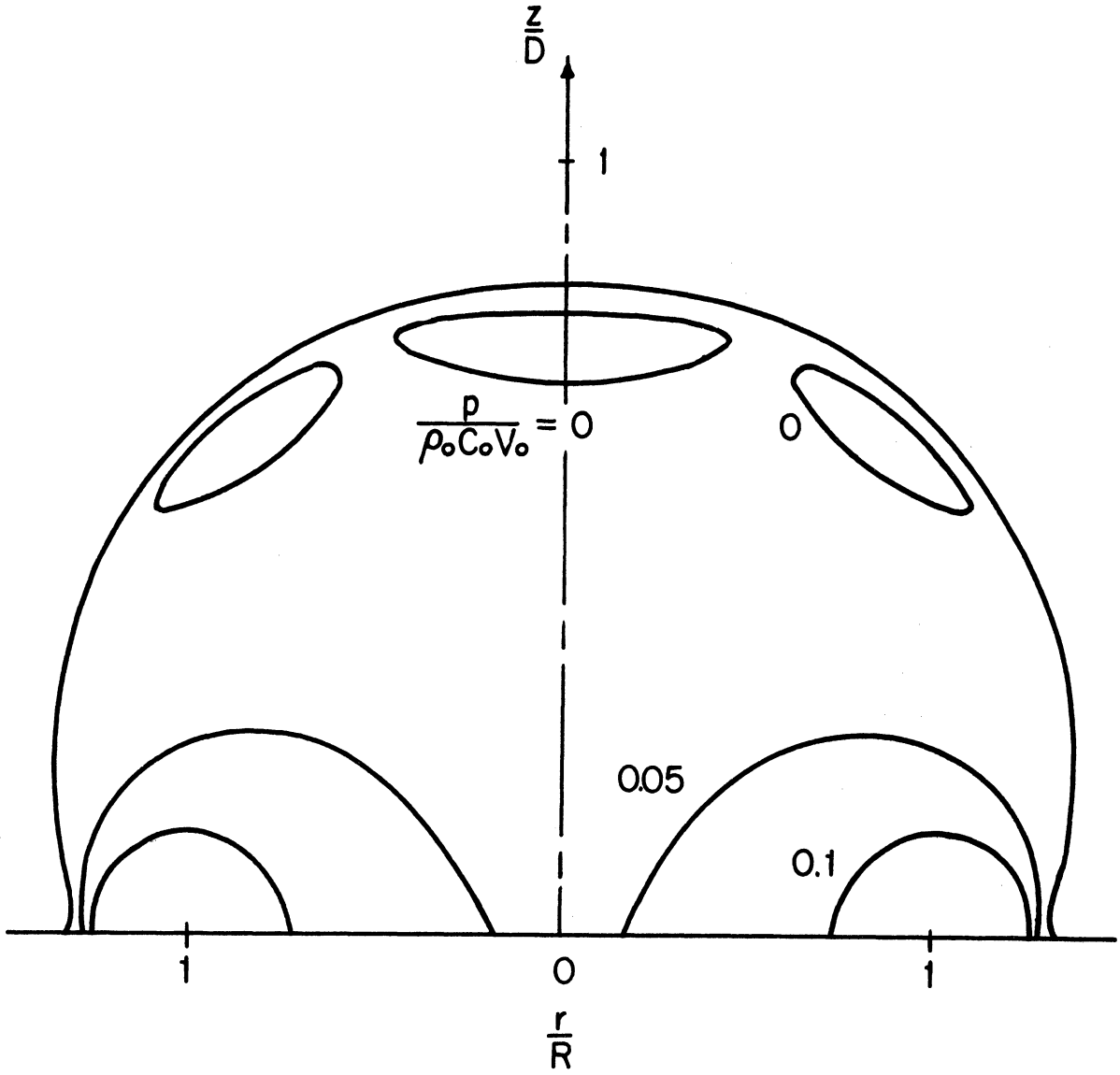

Fig. 21d. Isobar Distribution in an Initially Cylindrical-Spherical Composite Droplet with $R_1/R = 0.25$ and $L/D = 1$, at Time $(Ct/D) = 1.5$ for Impact Mach Number of 0.2 and for Free-Slip Boundary Condition.

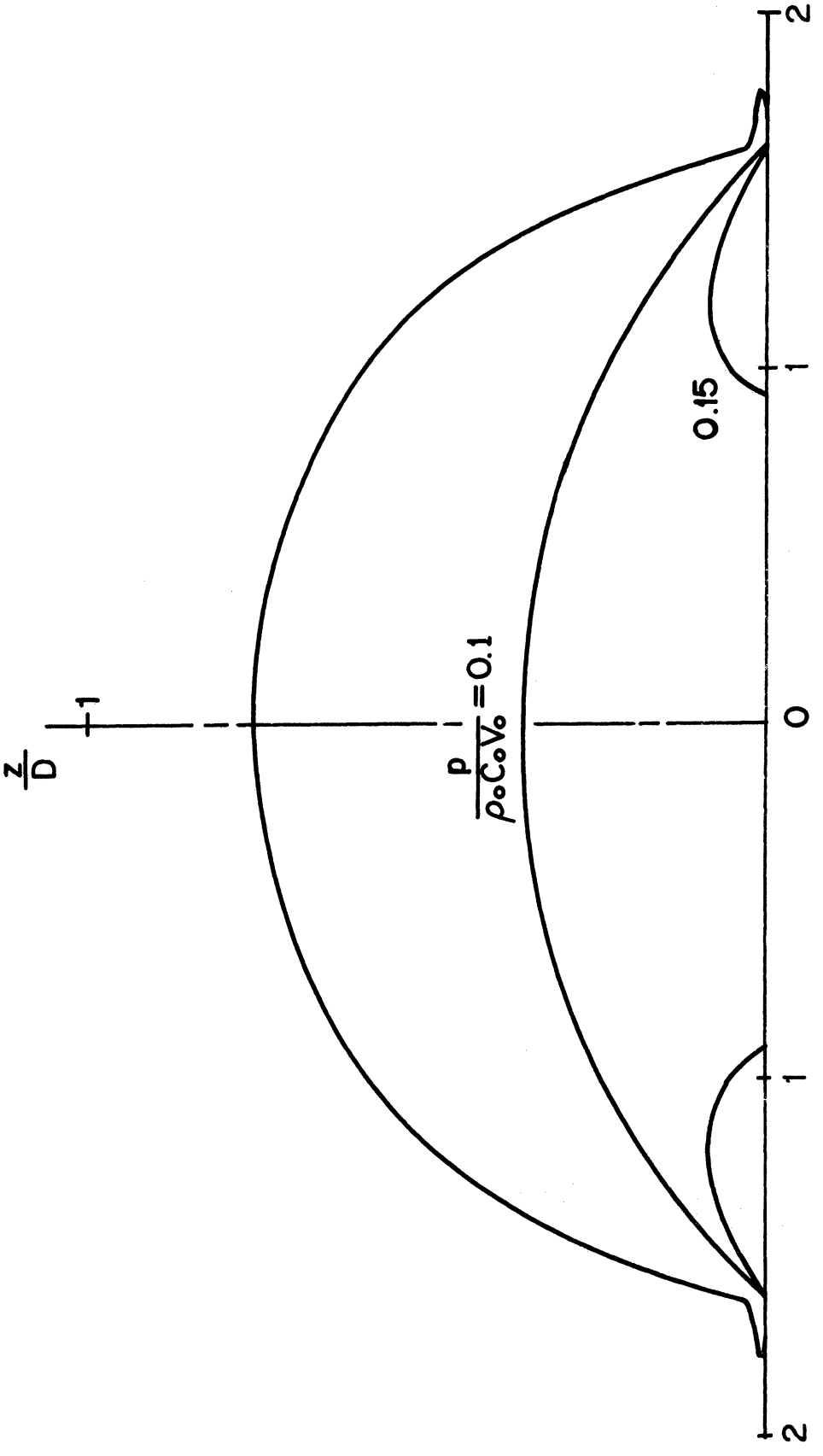

Fig. 21e. Isobar Distribution in an Initially Cylindrical-Spherical Composite Droplet with R_1/R = 0.25 and L/D = 1, at Time (Ct/D) = 2.5, for Impact Mach Number of 0.2 and for Free-Slip Boundary Condition.

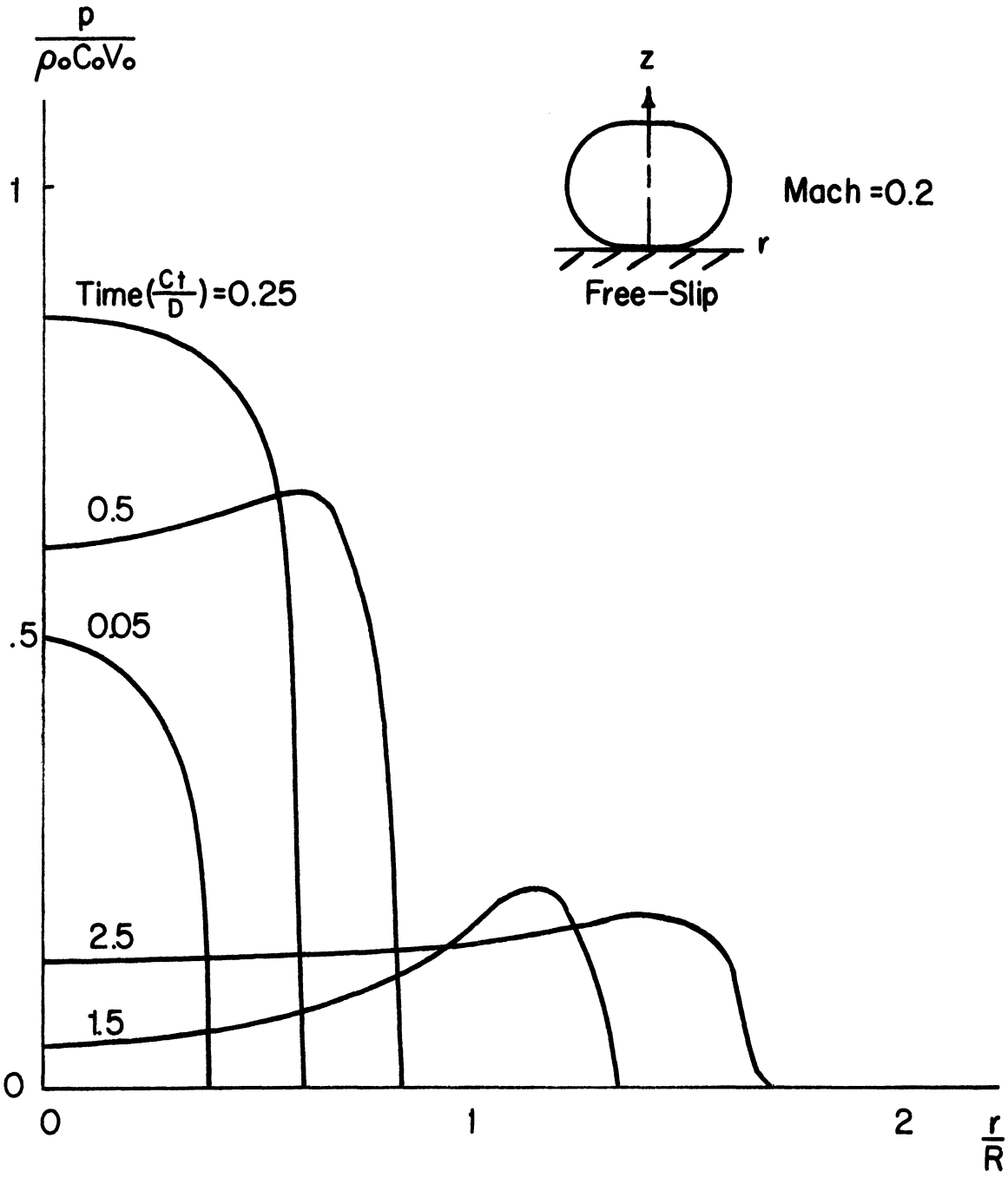

Fig. 22. Pressure-Time History at Liquid-Solid Interface (z = 0) of an Initially Cylindrical-Spherical Composite Droplet with R_1/R = 0.25 and L/D = 1, for Impact Mach Number of 0.2 and for Free-Slip Boundary Condition.

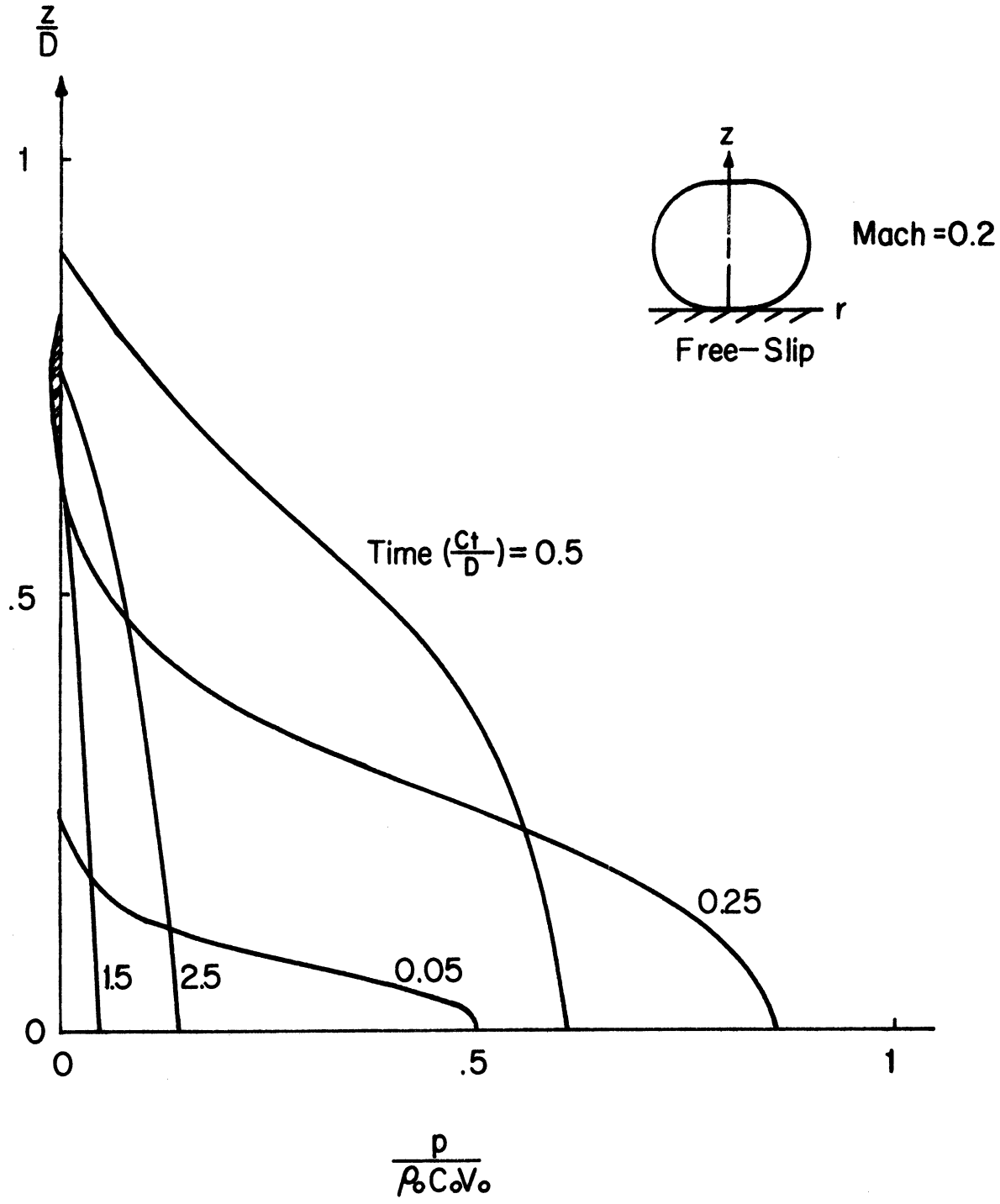

Fig. 23. Pressure-Time History along the Symmetrical Axis (r = 0) of an Initially Cylindrical-Spherical Composite Droplet with $R_1/R = 0.25$ and L/D = 1, for Impact Mach Number of 0.2 and for Free-Slip Boundary Condition.

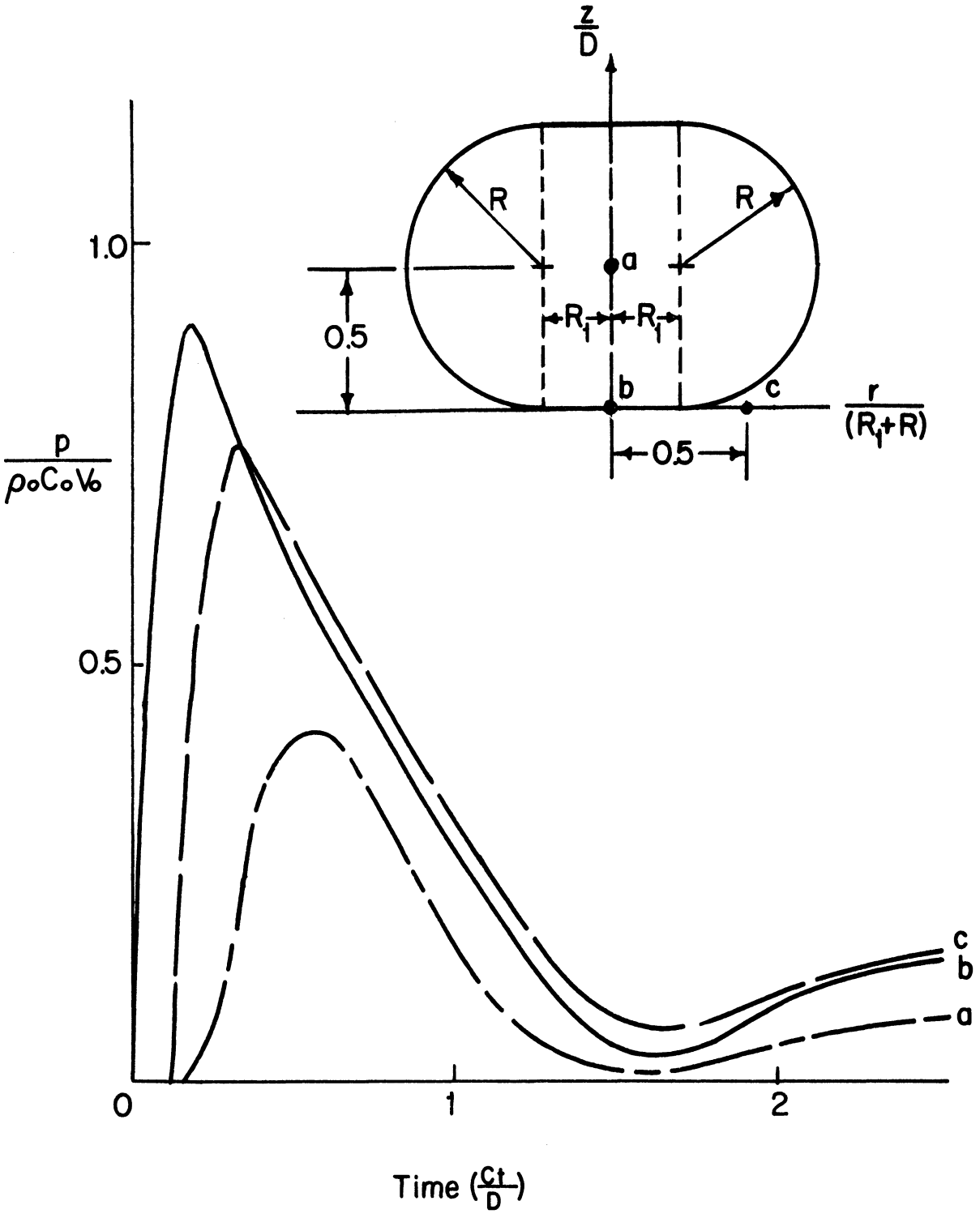

Fig. 24. Local Pressure-Time History at a (r = 0, z = 0.5L), b (r = 0, z = 0), and c (r = 0.75R, z = 0), in an Initially Cylindrical-Spherical Composite Droplet with $R_1/R = 0.25$ and L/D = 1, for Impact Mach Number of 0.2 and for Free-Slip Boundary Condition.

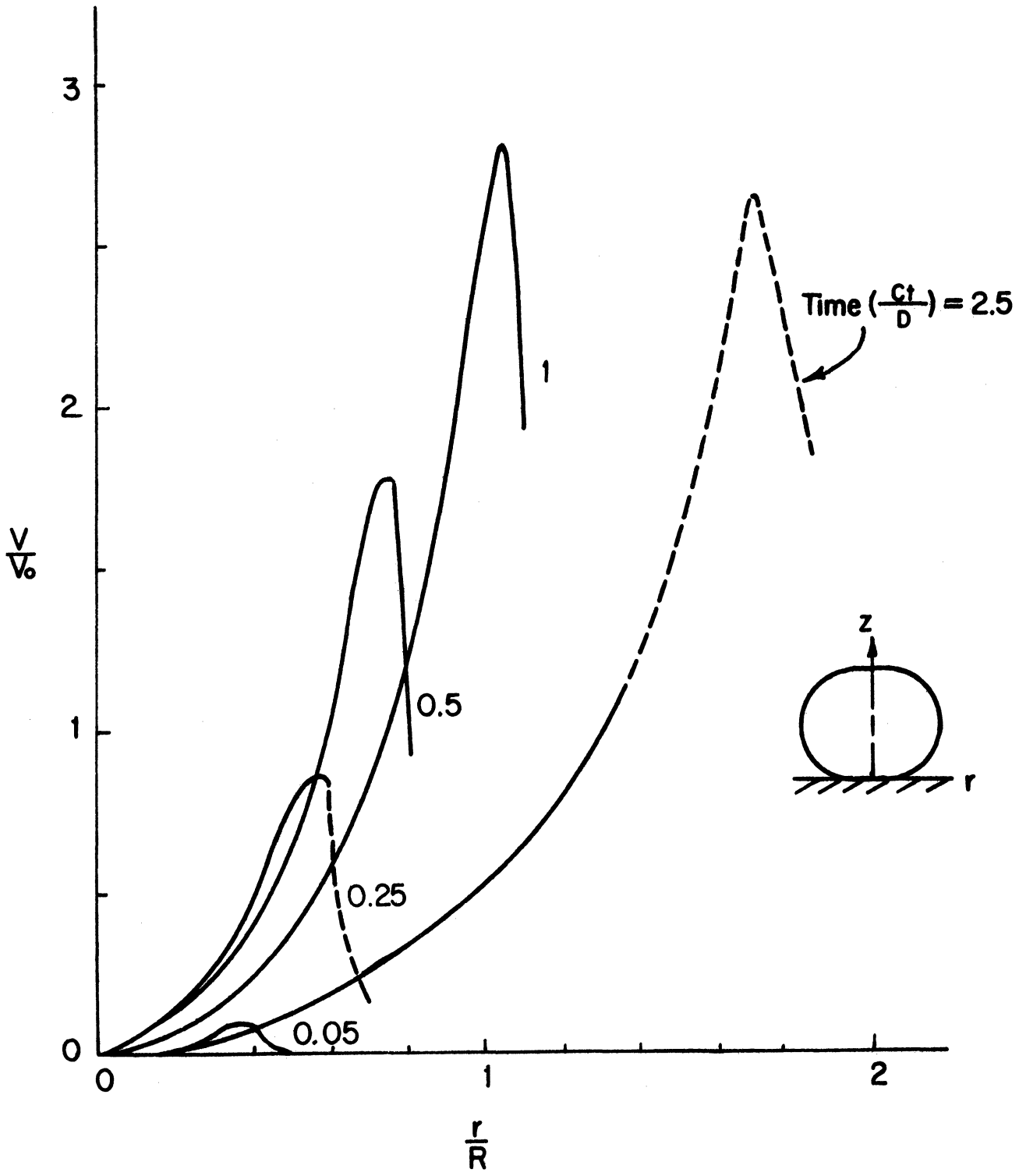

Fig. 25. Radial Velocity-Time History at Liquid-Solid Interface (r = 0) of an Initially Cylindrical-Spherical Composite Droplet with R_1/R = 0.25 and L/D = 1, for Impact Mach Number of 0.2 and for Free-Slip Boundary Condition.

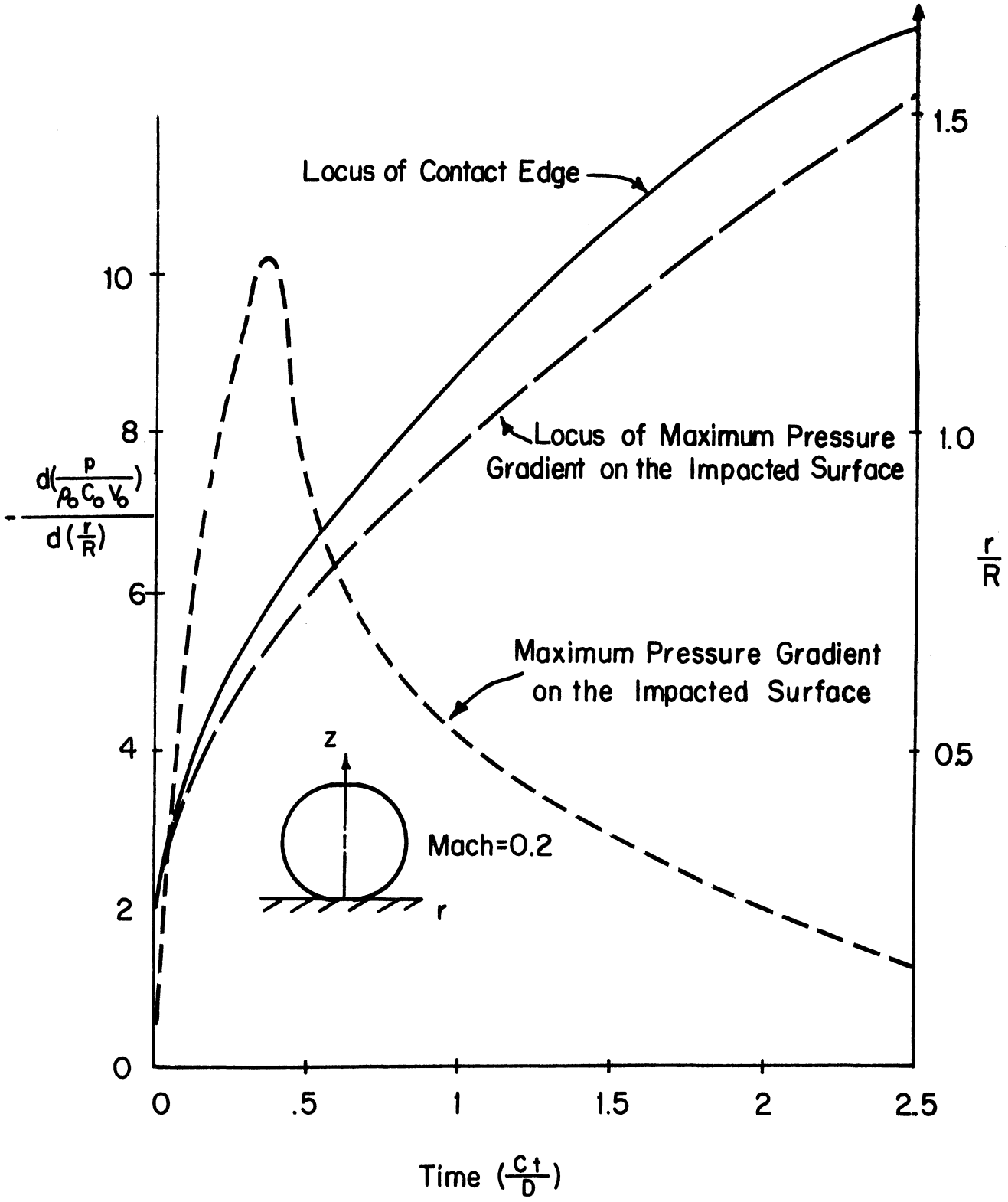

Fig. 26. Maximum Pressure Gradient-Time and -Location Relation and Contact Edge-Time History of an Initially Cylindrical-Spherical Composite Droplet with $R_1/R = 0.25$ and $L/D = 1$, for Impact Mach Number of 0.2 and for Free-Slip Boundary Condition.

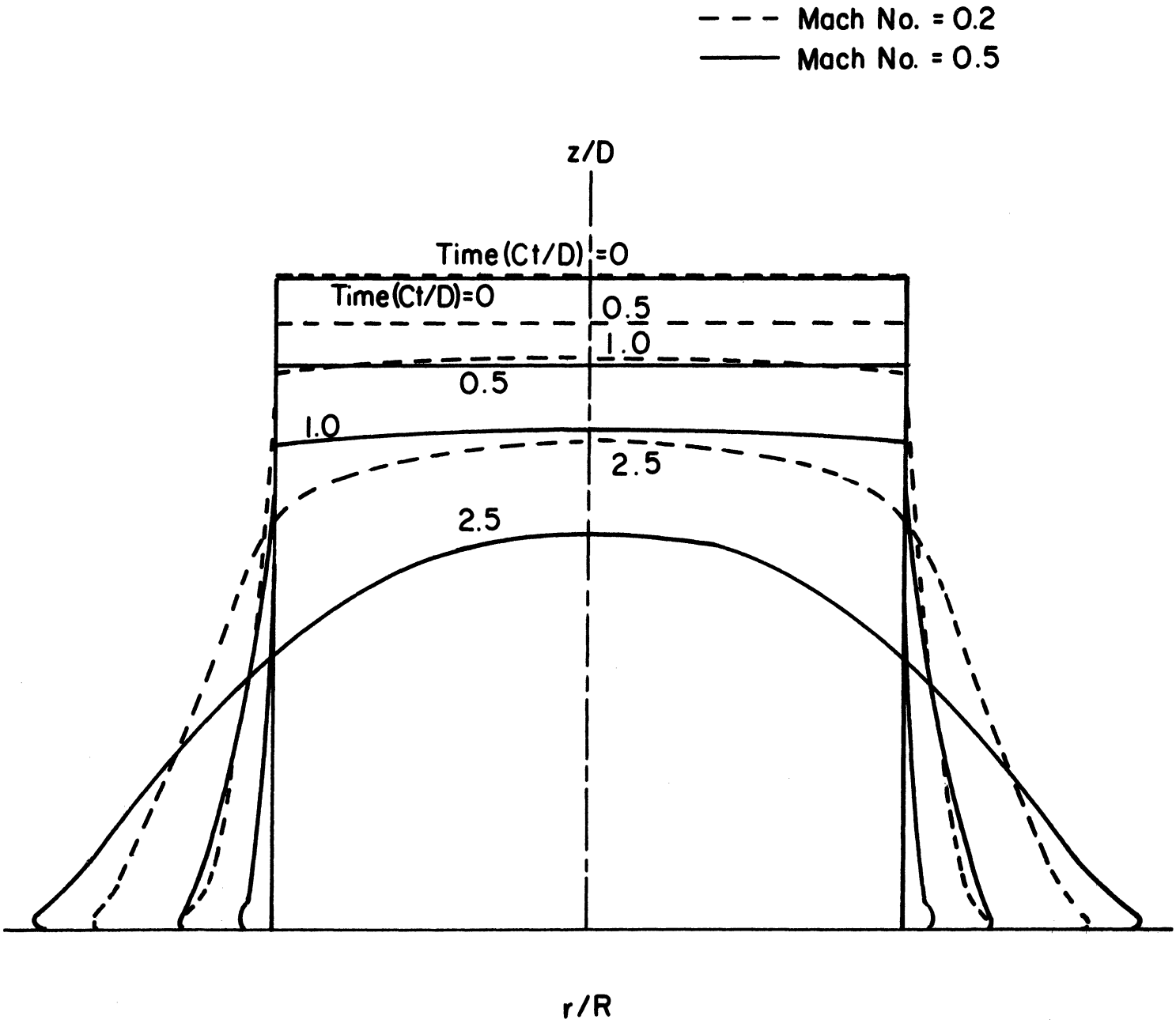

Fig. 27. Shape-Time History of an Initially Cylindrical Droplet with L/D = 1, at Mach Numbers = 0.2 and 0.5 for Non-Slip Boundary Condition.

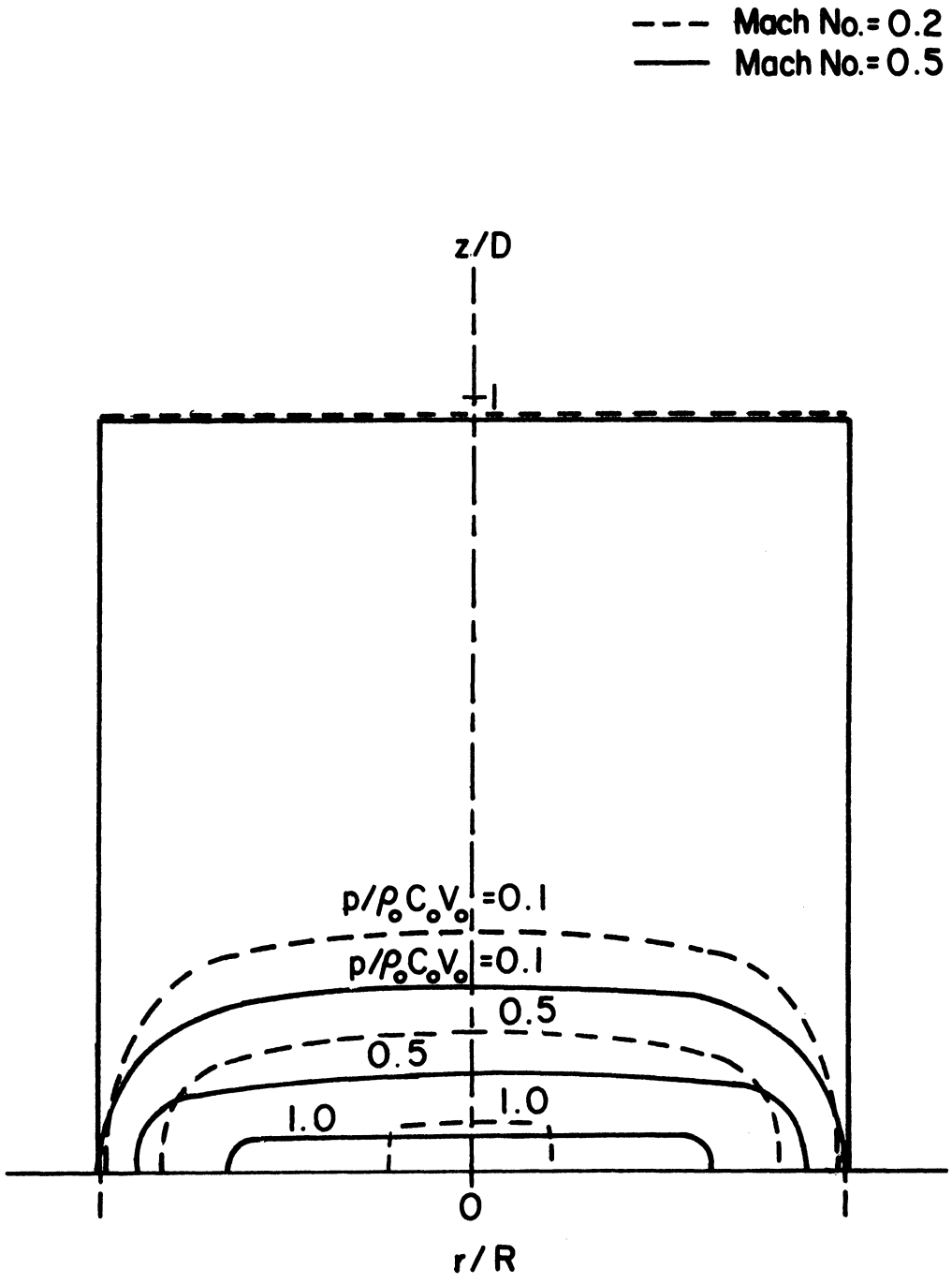

Fig. 28a. Isobar Distribution in an Initially Cylindrical Droplet with L/D = 1, at Time (Ct/D) = 0.125, for Impact Mach Numbers of 0.2 and 0.5. Non-Slip Boundary Condition.

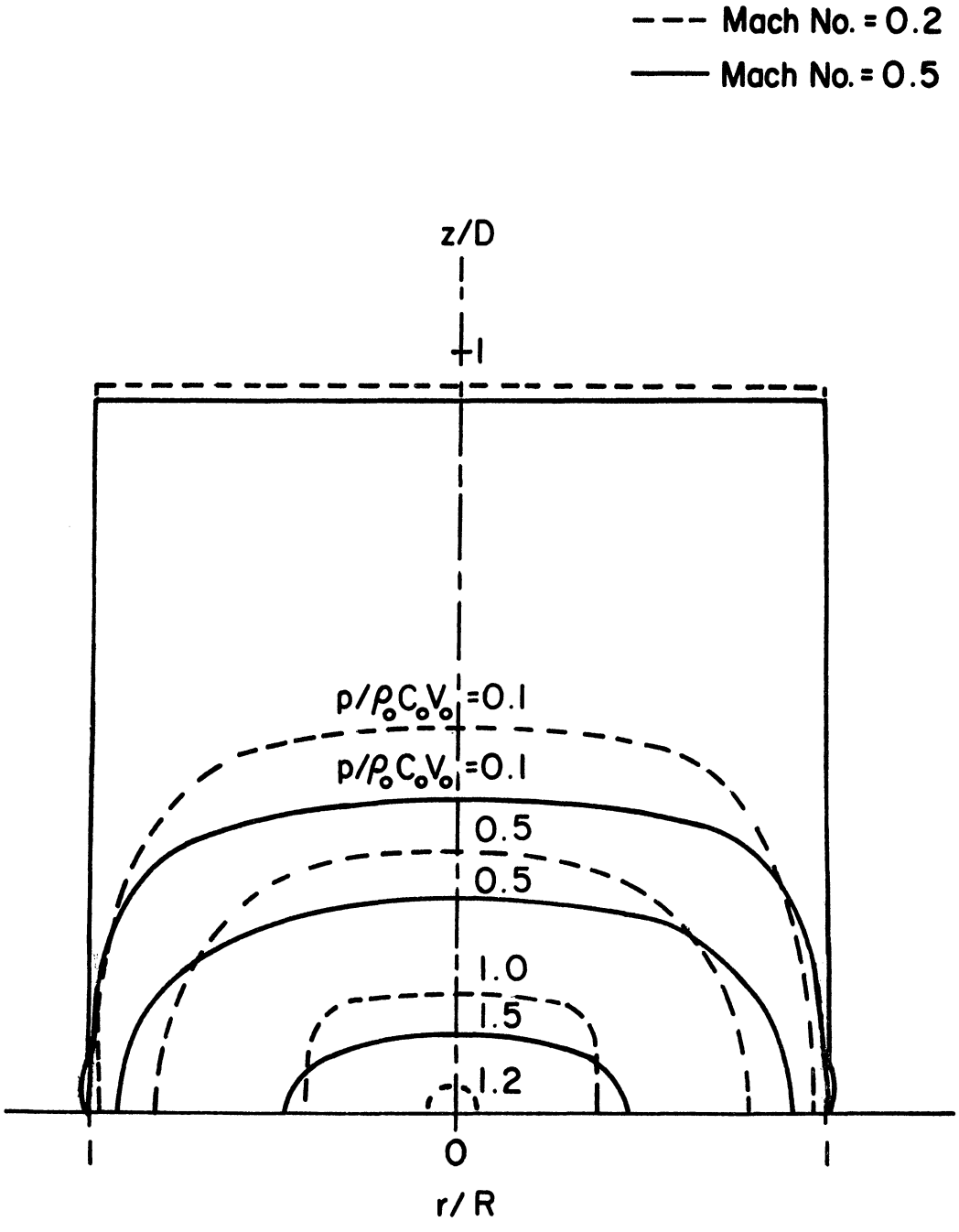

Fig. 28b. Isobar Distribution in an Initially Cylindrical Droplet with L/D = 1, at Time (Ct/D) = 0.25, for Impact Mach Numbers of 0.2 and 0.5. Non-Slip Boundary Condition.

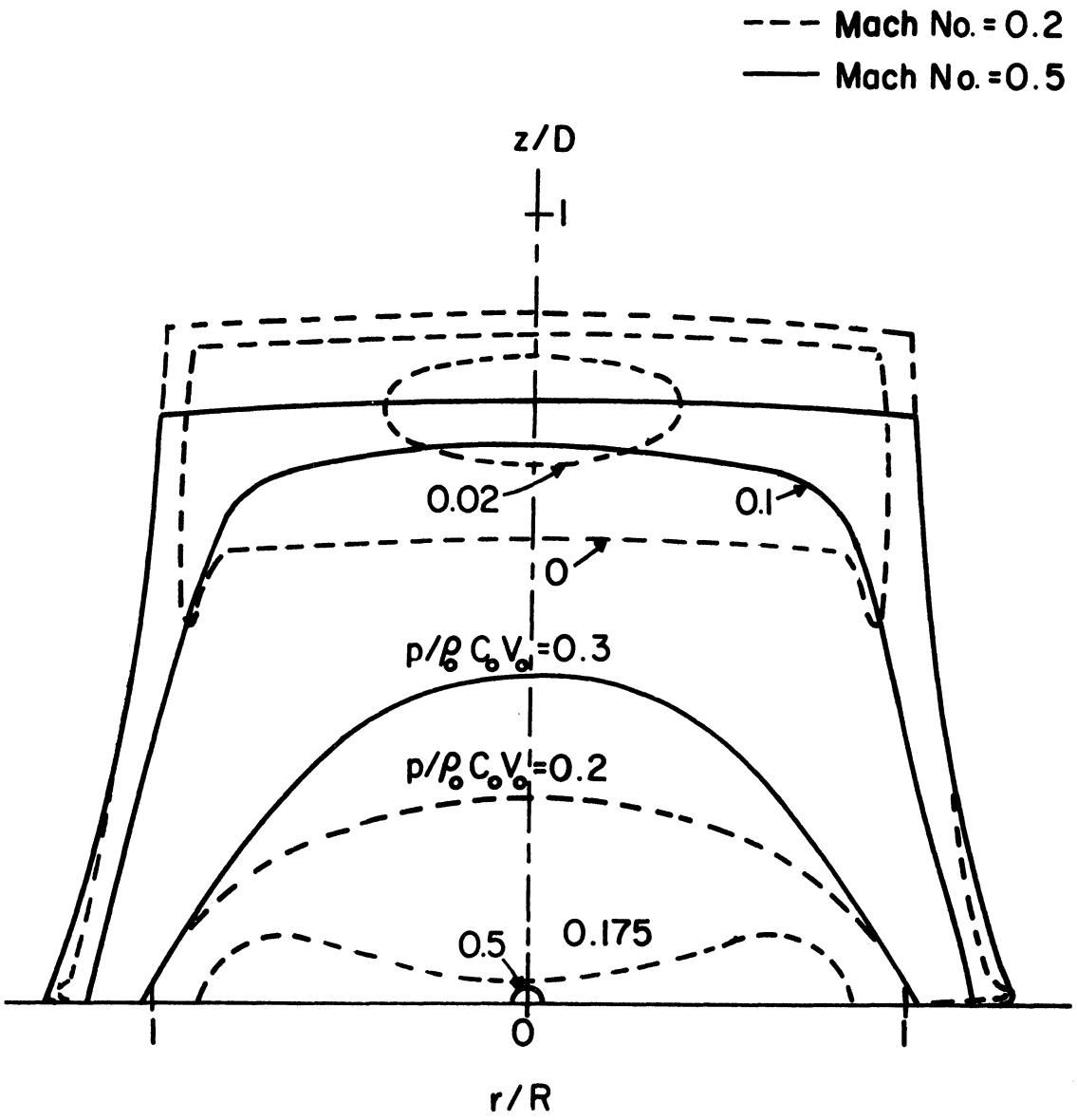

Fig. 28c. Isobar Distribution in an Initially Cylindrical Droplet with L/D = 1, at Time (Ct/D) = 1, for Impact Mach Numbers of 0.2 and 0.5. Non-Slip Boundary Condition.

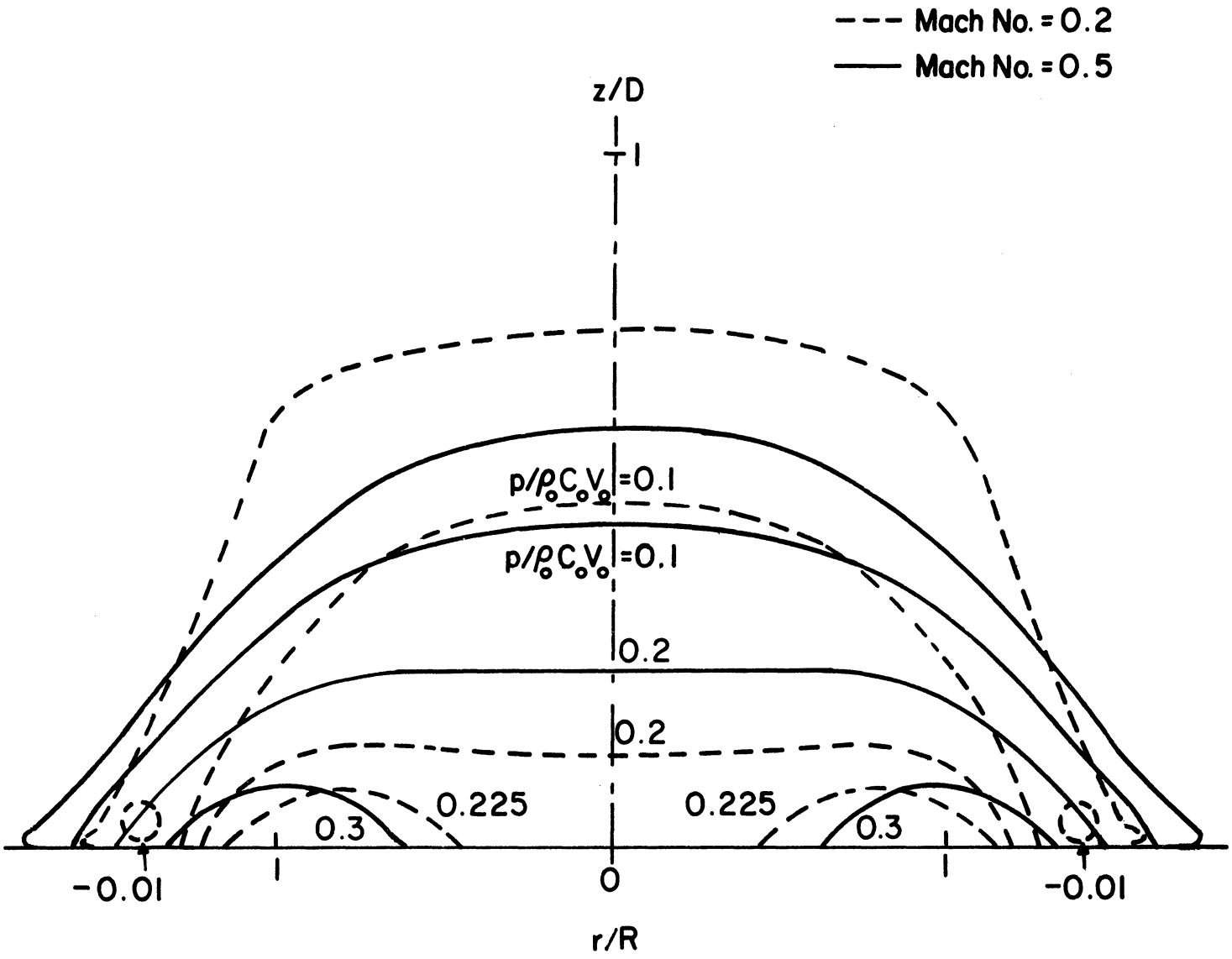

Fig. 28d. Isobar Distribution in an Initially Cylindrical Droplet with L/D = 1, at Time (Ct/D) = 2.5, for Impact Mach Numbers of 0.2 and 0.5. Non-Slip Boundary Condition.

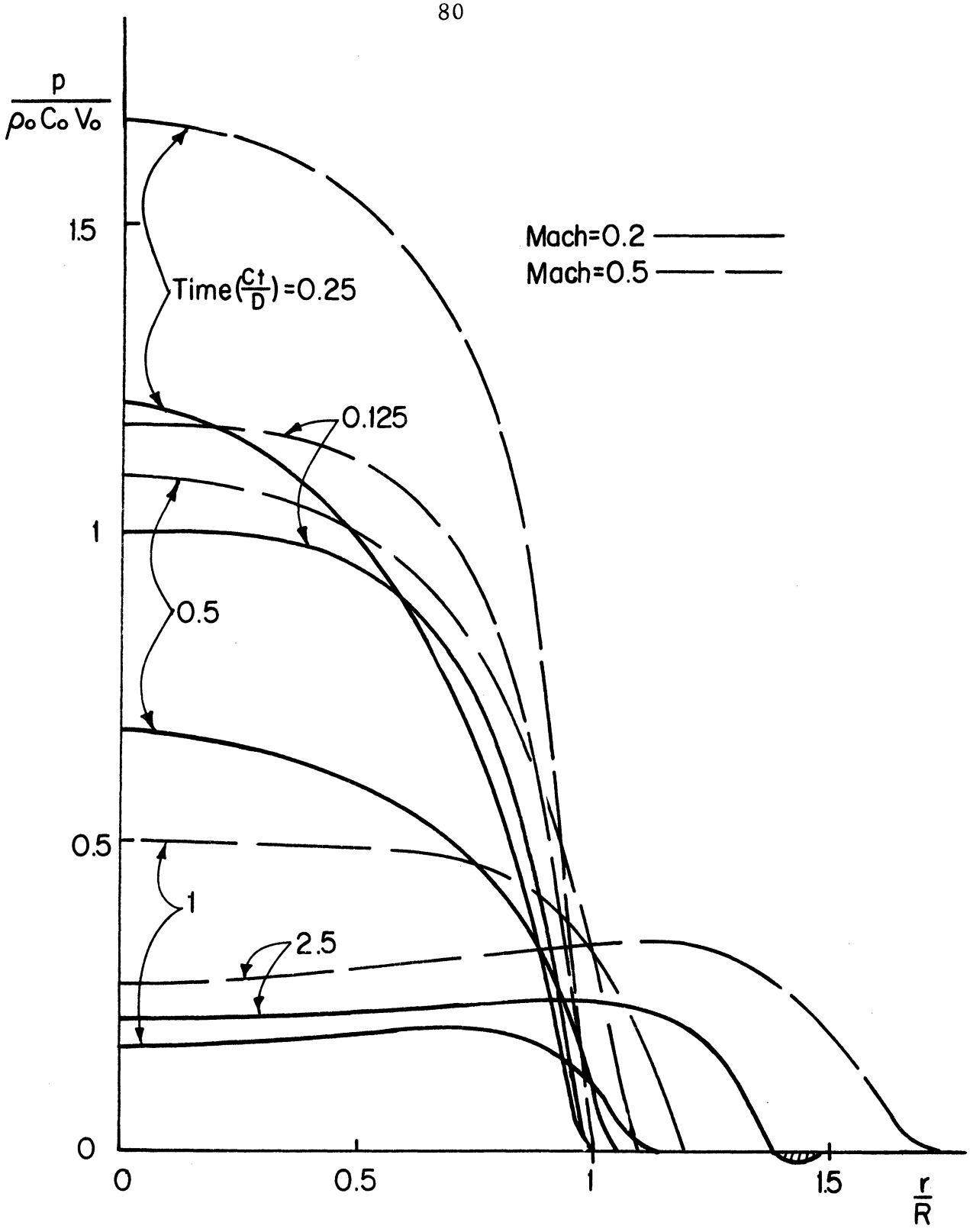

Fig. 29. Pressure-Time History at Liquid-Solid Interface (z = 0) of an Initially Cylindrical Droplet with L/D = 1, for Impact Mach Numbers of 0.2 and 0.5. Non-Slip Boundary Condition.

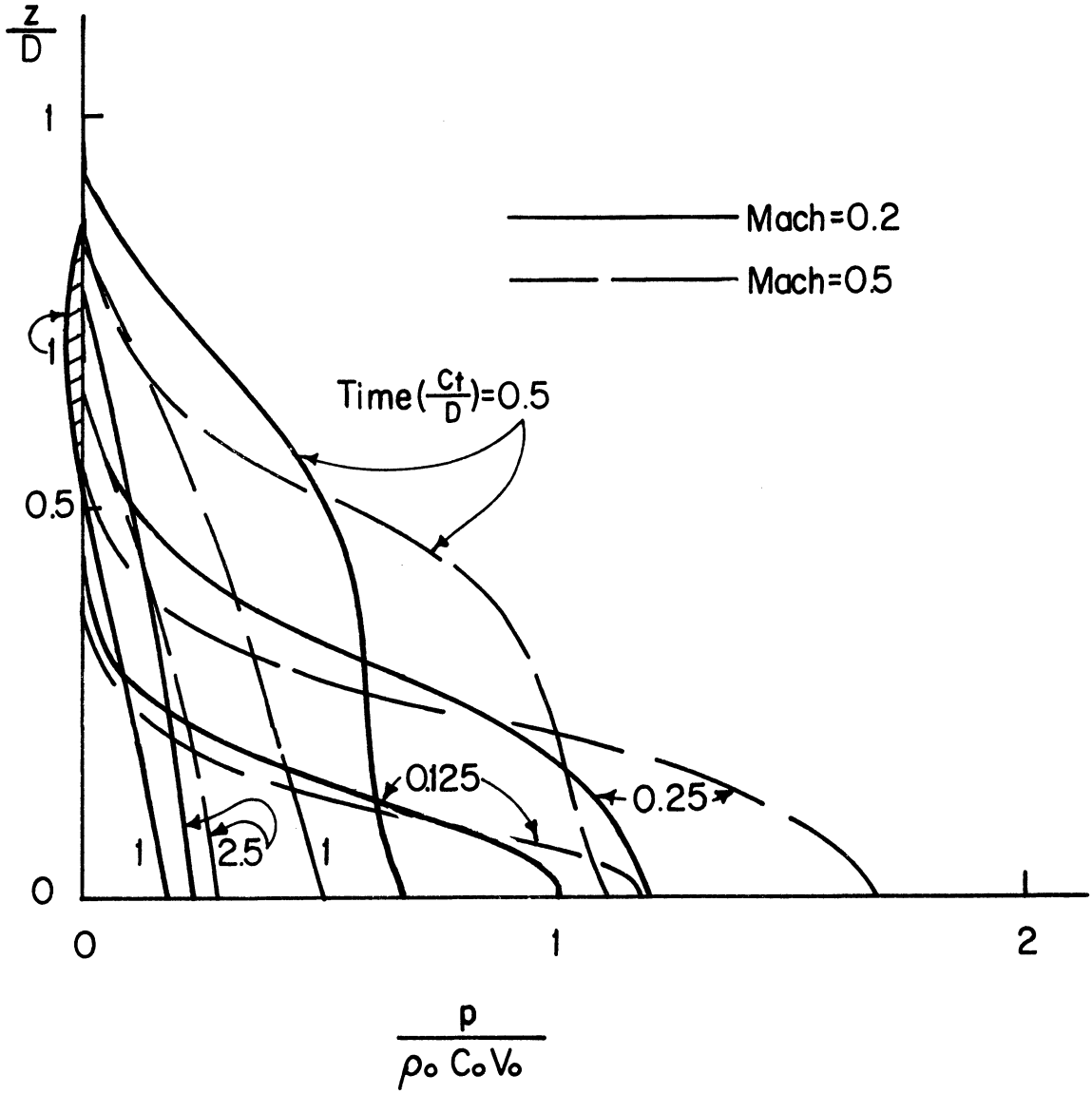

Fig. 30. Pressure-Time History along the Symmetrical Axis (r = 0) of an Initially Cylindrical Droplet with L/D = 1, for Impact Mach Numbers of 0.2 and 0.5. Non-Slip Boundary Condition.

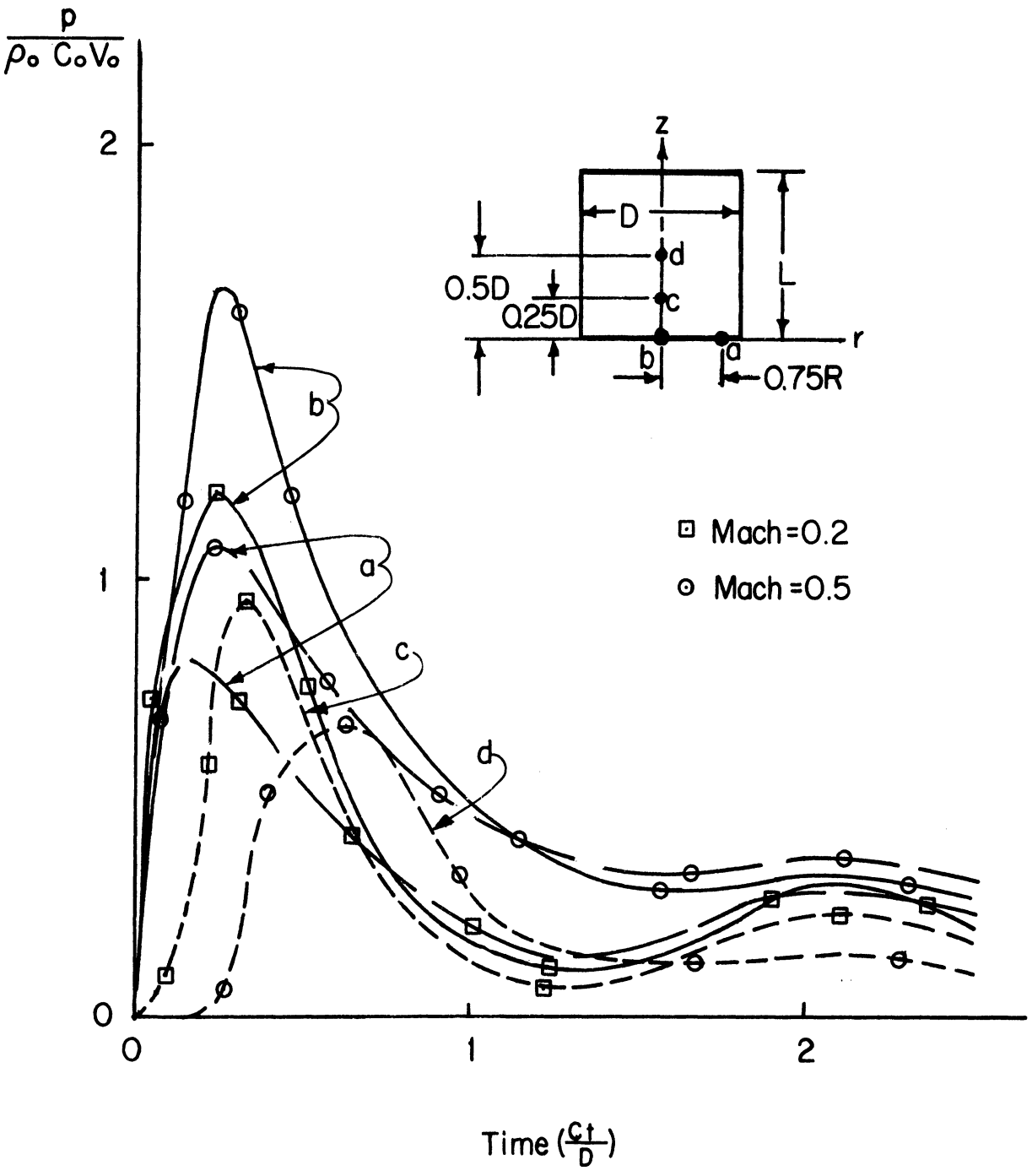

Fig. 31. Local Pressure-Time History at a (r = 0, z = 0.5L), b (r = 0, z = 0), and c (r = 0.75R, z = 0), in an Initially Cylindrical Droplet with L/D = 1, for Impact Mach Numbers of 0.2 and 0.5. Non-Slip Boundary Condition.

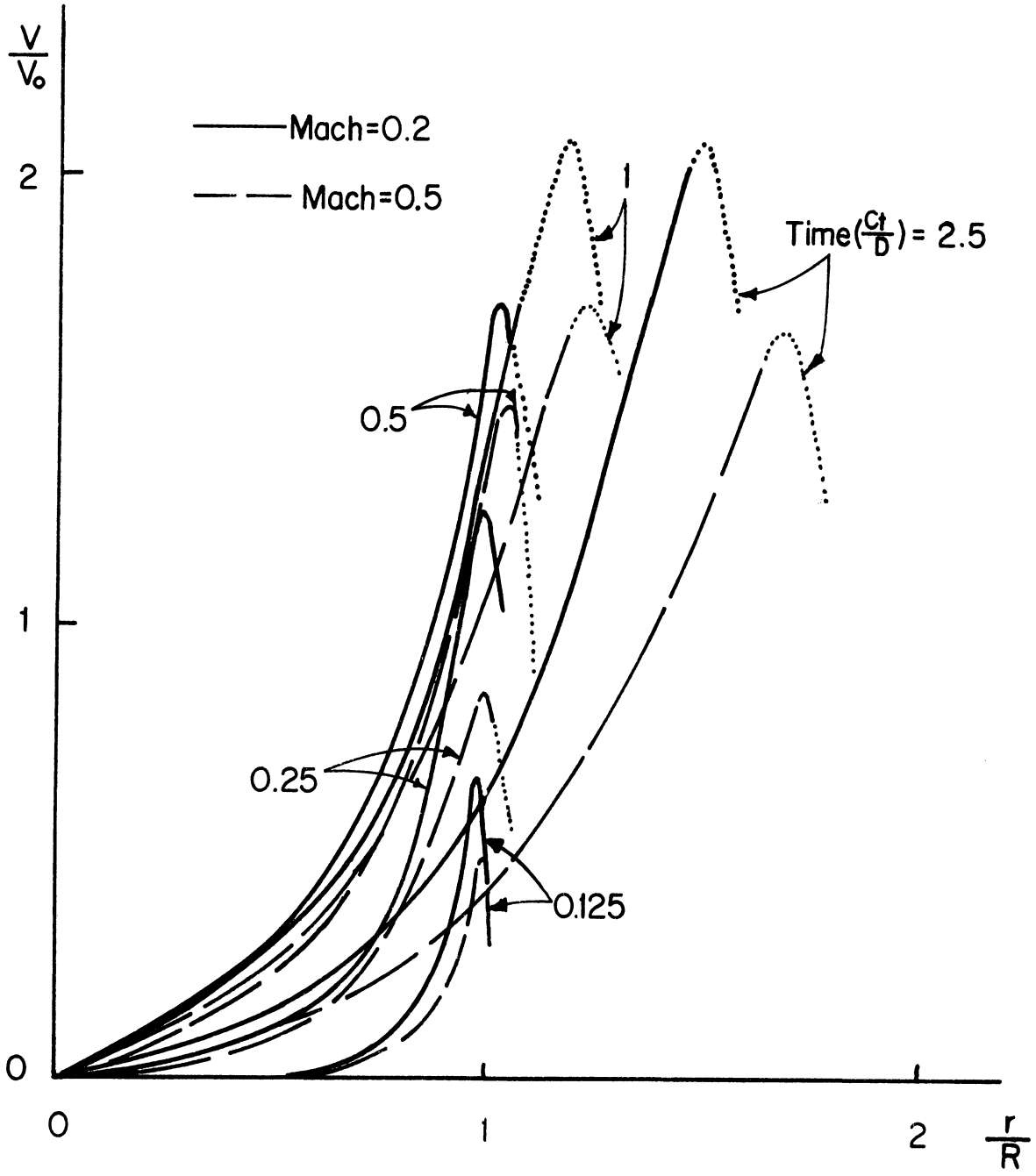

Fig. 32. Radial Velocity-Time History at Liquid-Solid Interface (r = 0) of an Initially Cylindrical Droplet with L/D = 1, for Impact Mach Numbers of 0.2 and 0.5. Non-Slip Boundary Condition.

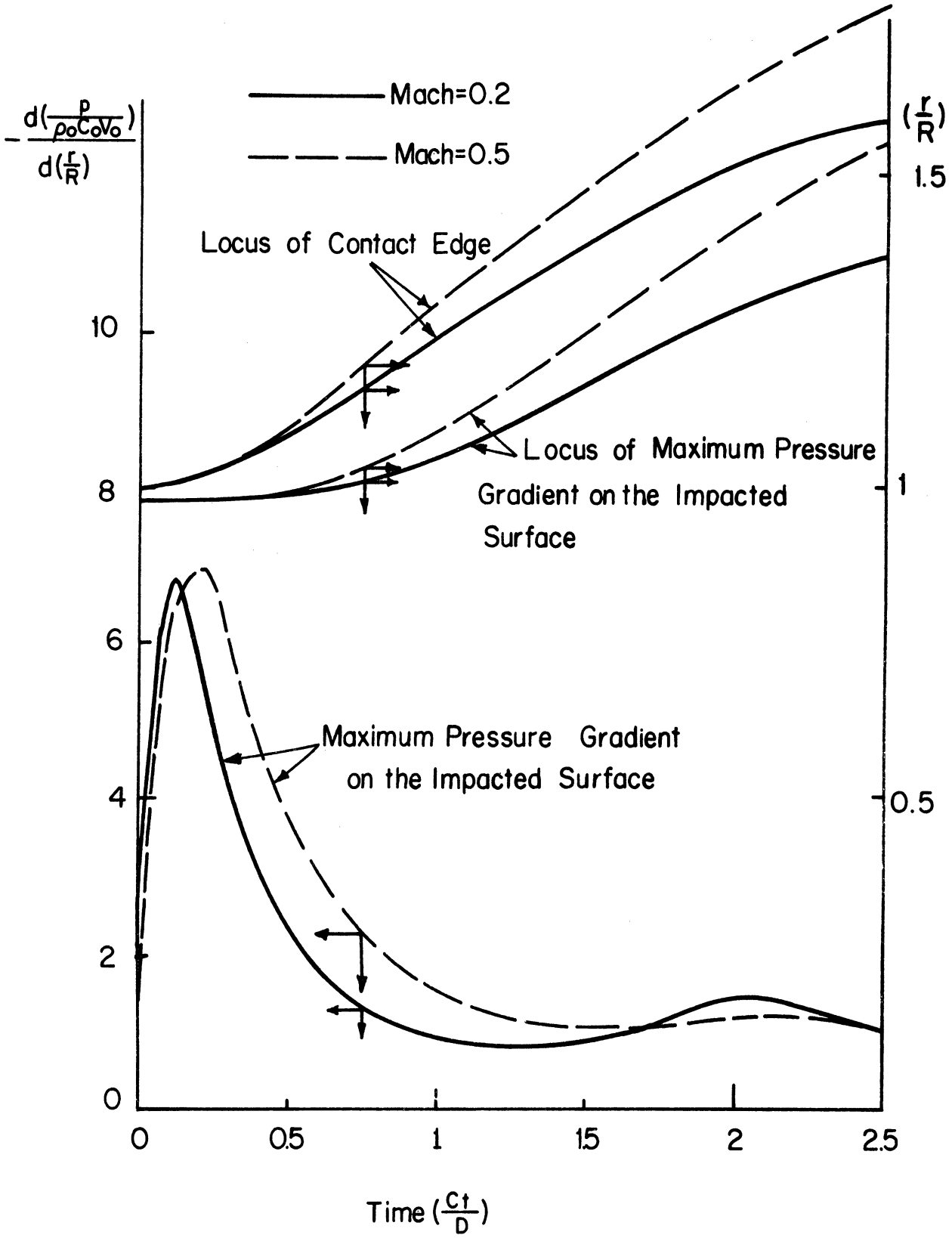

Fig. 33. Maximum Pressure Gradient-Time and -Location Relation and Contact Edge-Time History of an Initially Cylindrical Droplet with L/D = 1, for Impact Mach Numbers of 0.2 and 0.5. Non-Slip Boundary Condition.

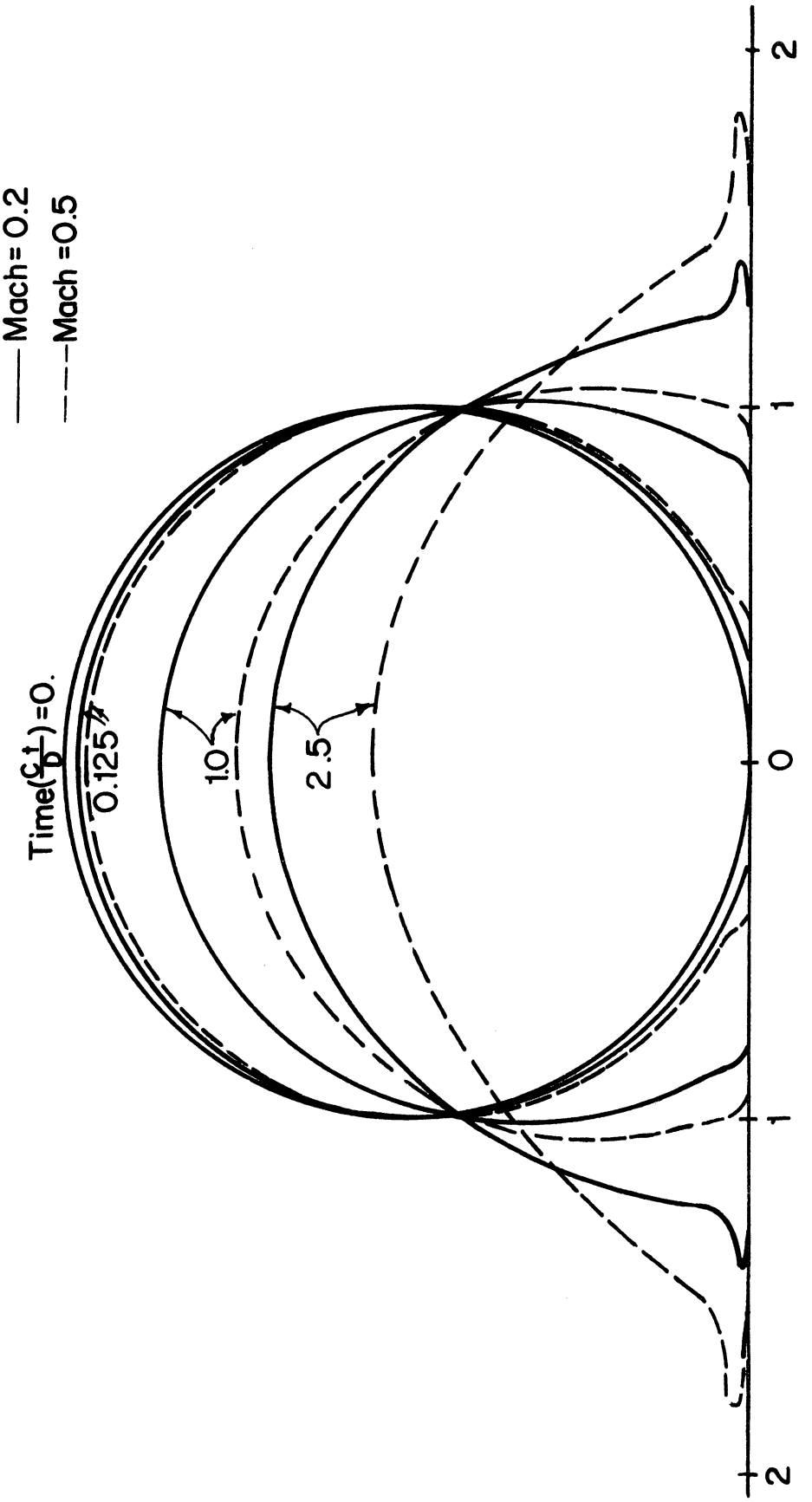

Fig. 34. Shape-Time History of an Initially Spherical Droplet at Mach Numbers = 0.2 and 0.5, for Non-Slip Boundary Condition

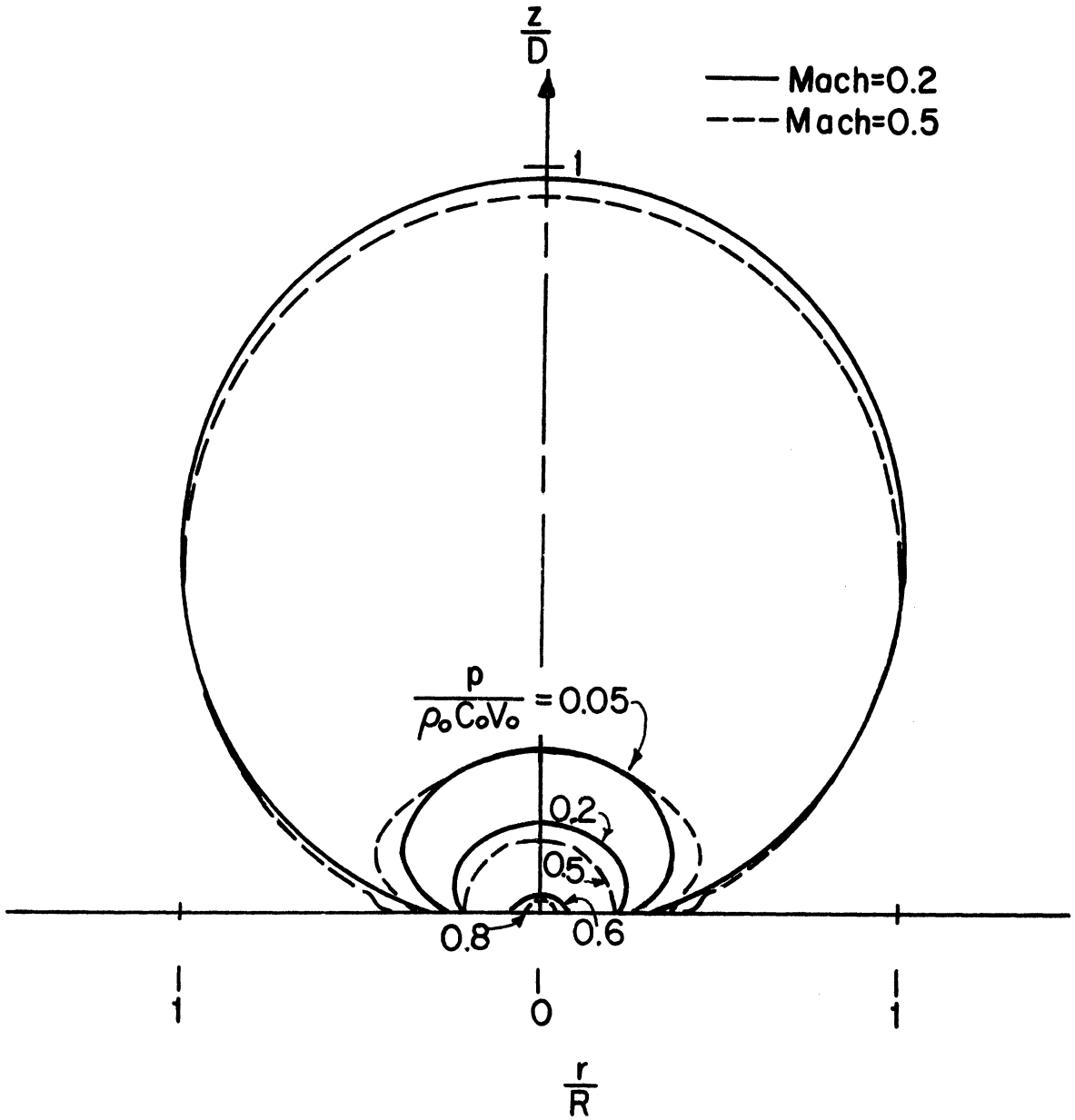

Fig. 35a. Isobar Distribution in an Initially Spherical Droplet at Time (Ct/D) = 0.125, for Impact Mach Numbers of 0.2 and 0.5. Non-Slip Boundary Condition.

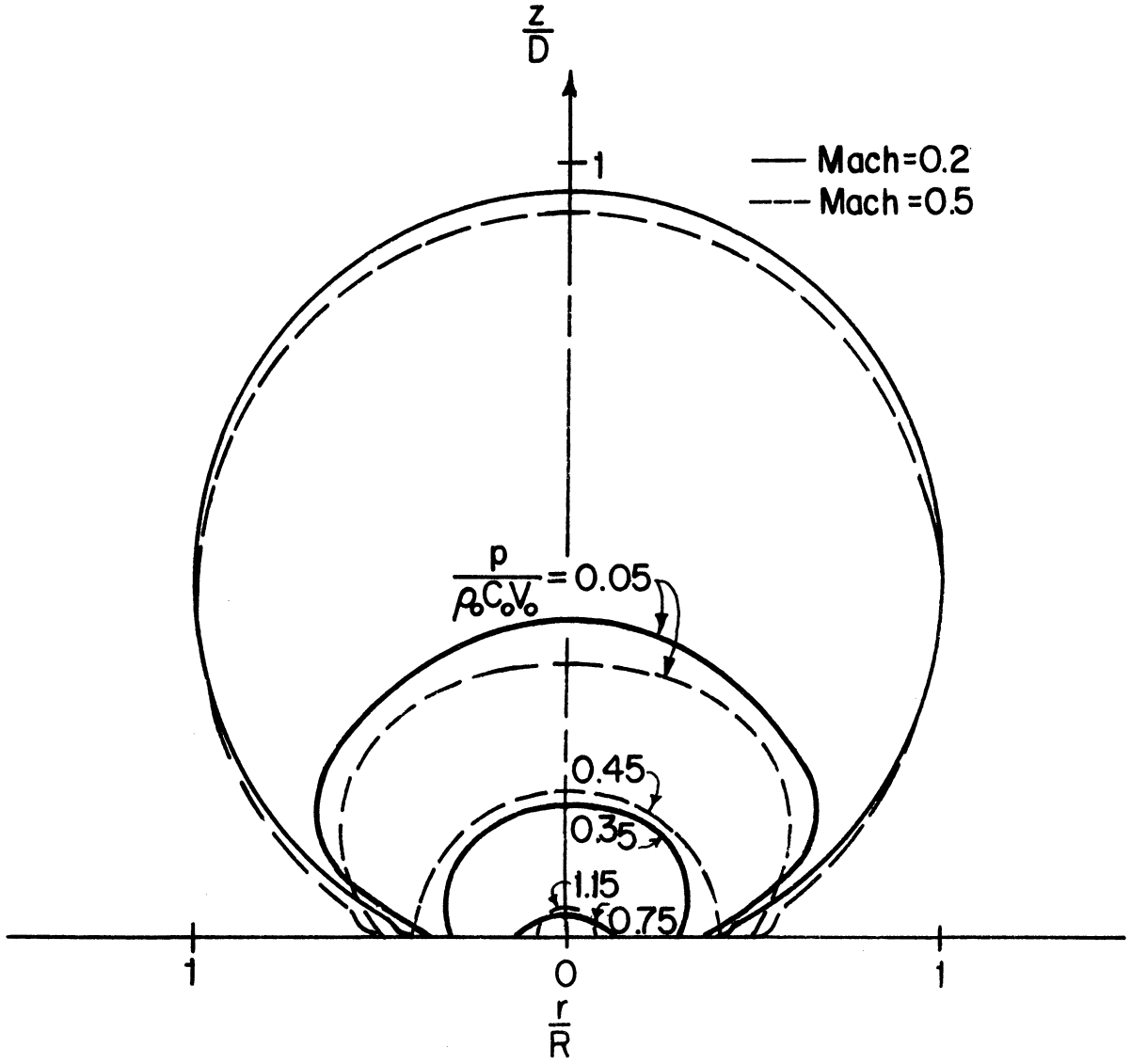

Fig. 35b. Isobar Distribution in an Initially Spherical Droplet at Time (Ct/D) = 0.25, for Impact Mach Numbers of 0.2 and 0.5. Non-Slip Boundary Condition.

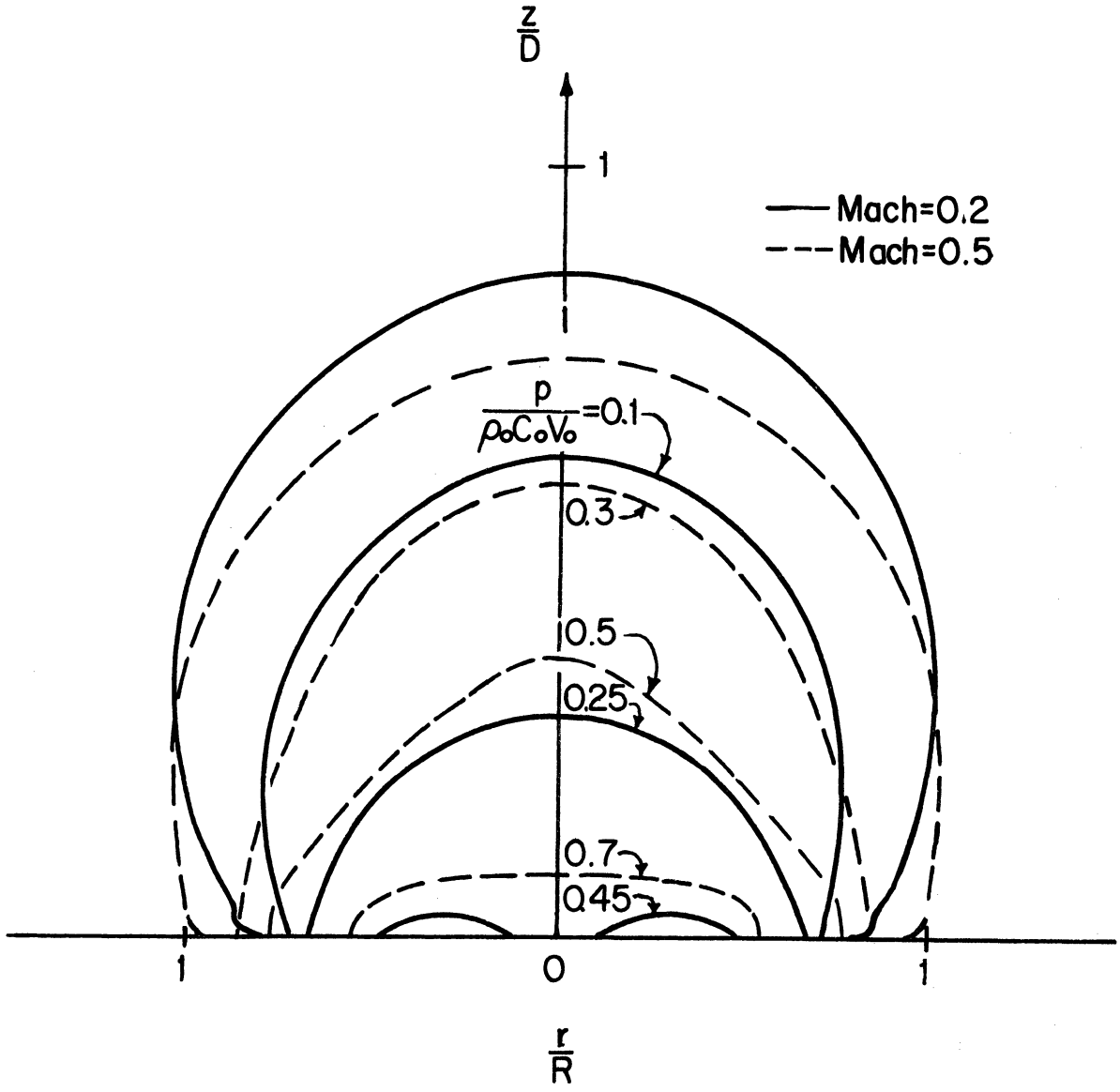

Fig. 35c. Isobar Distribution in an Initially Spherical Droplet at Time (Ct/D) = 1, for Impact Mach Numbers of 0.2 and 0.5. Non-Slip Boundary Condition.

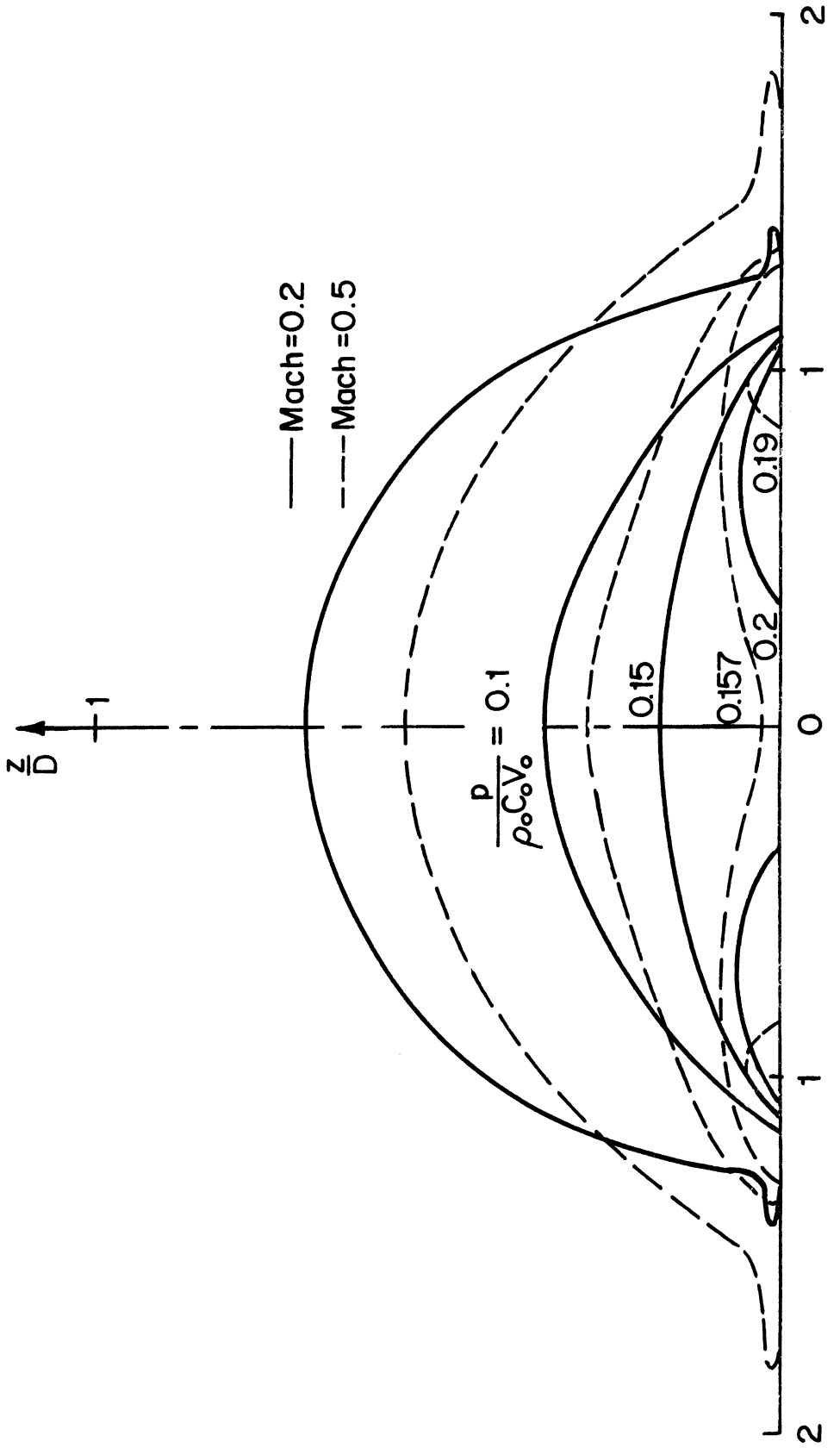

Fig. 35d. Isobar Distribution in an Initially Spherical Droplet at Time (Ct/D) = 2.5, for Impact Mach Numbers of 0.2 and 0.5. Non-Slip Boundary Condition.

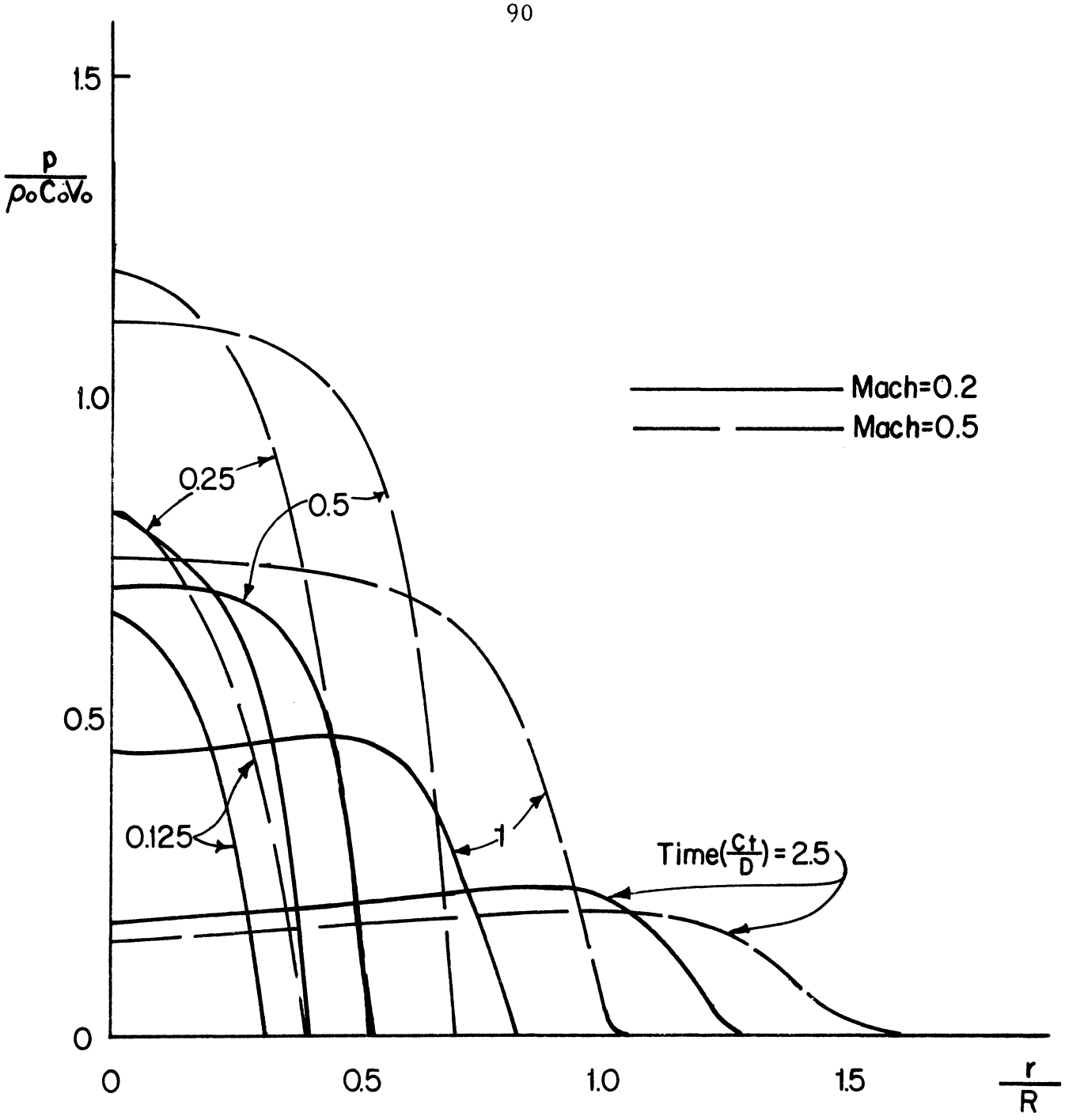

Fig. 36. Pressure-Time History at Liquid-Solid Interface (z = 0) of an Initially Spherical Droplet for Impact Mach Numbers of 0.2 and 0.5. Non-Slip Boundary Condition.

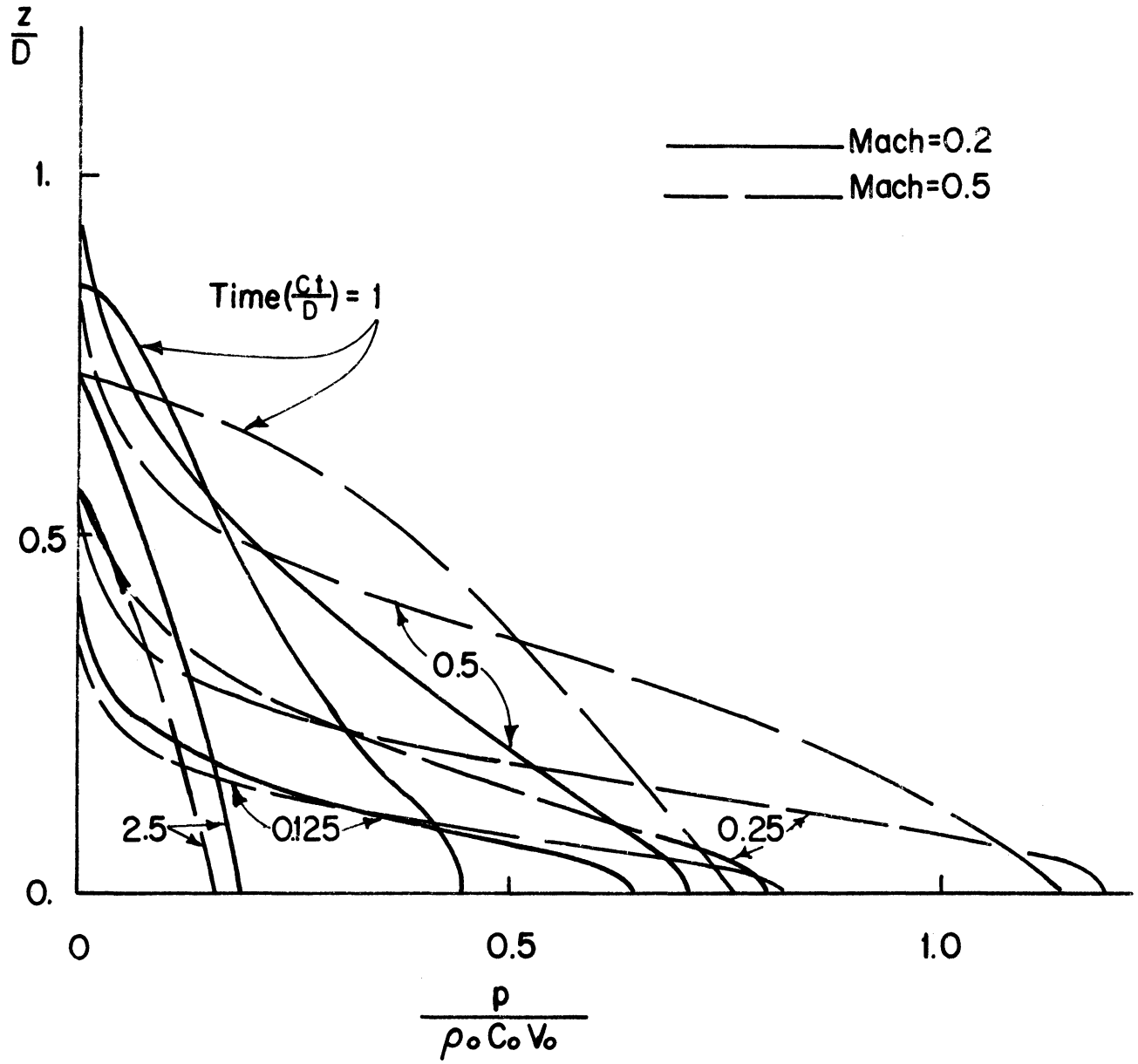

Fig. 37. Pressure-Time History along the Symmetrical Axis (r = 0) of an Initially Spherical Droplet for Impact Mach Numbers of 0.2 and 0.5. Non-Slip Boundary Condition.

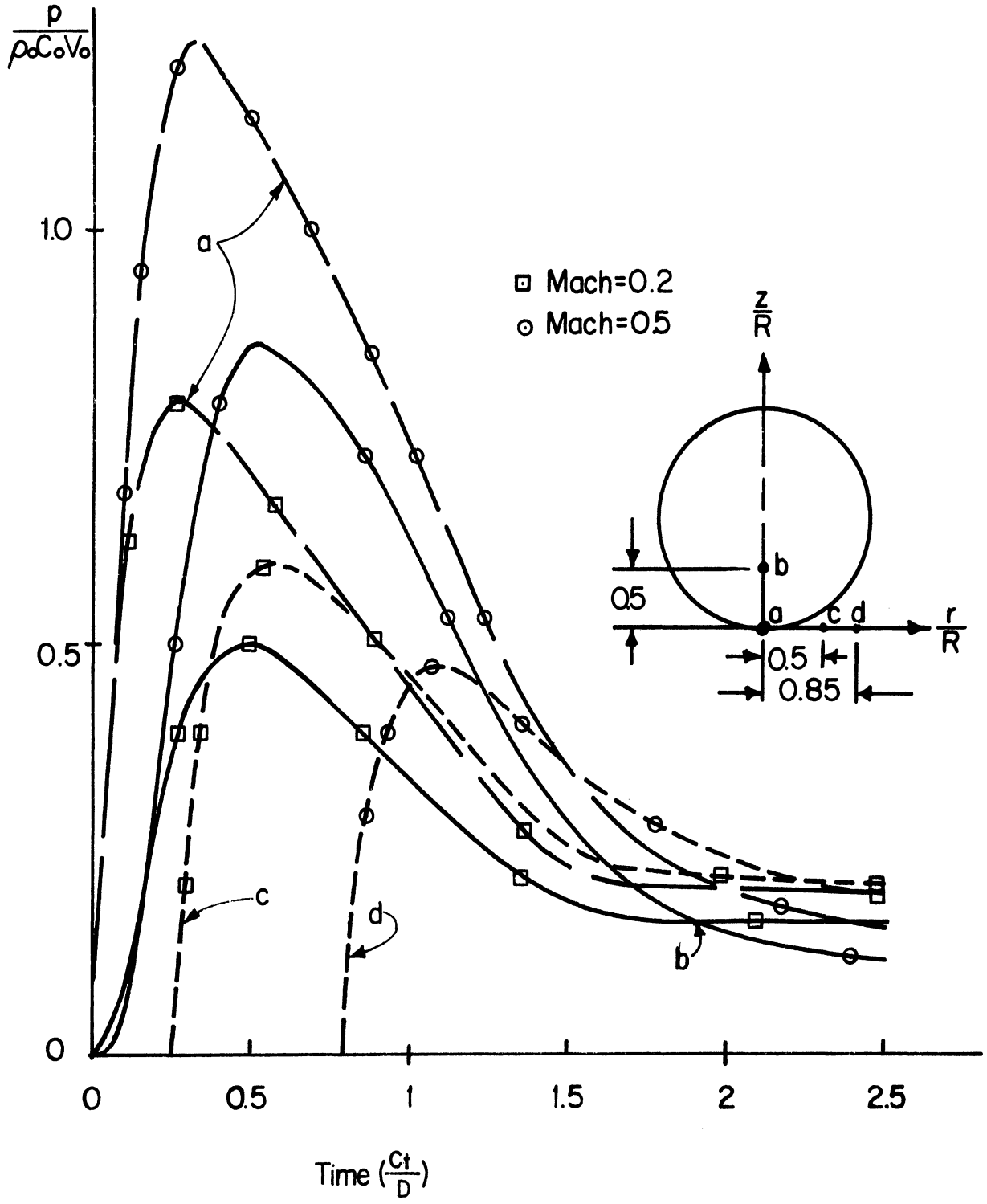

Fig. 38. Local Pressure-Time History at a (r = 0, z = 0.5L), b (r = 0, z = 0), and c (r = 0.75R, z = 0), in an Initially Spherical Droplet for Impact Mach Numbers of 0.2 and 0.5. Non-Slip Boundary Condition.

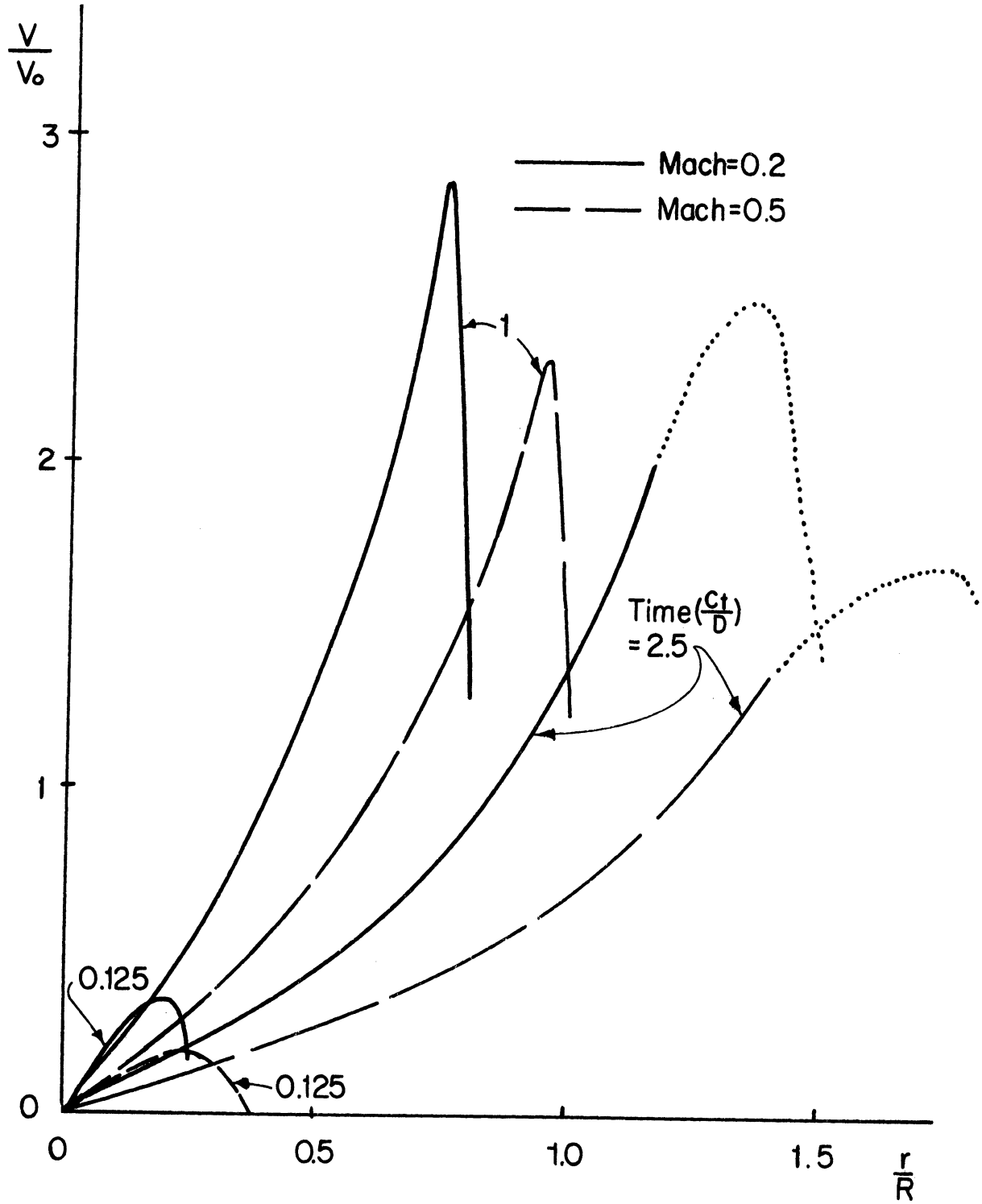

Fig. 39. Radial Velocity-Time History at Liquid-Solid Interface (r = 0) of an Initially Spherical Droplet for Impact Mach Numbers of 0.2 and 0.5. Non-Slip Boundary Condition.

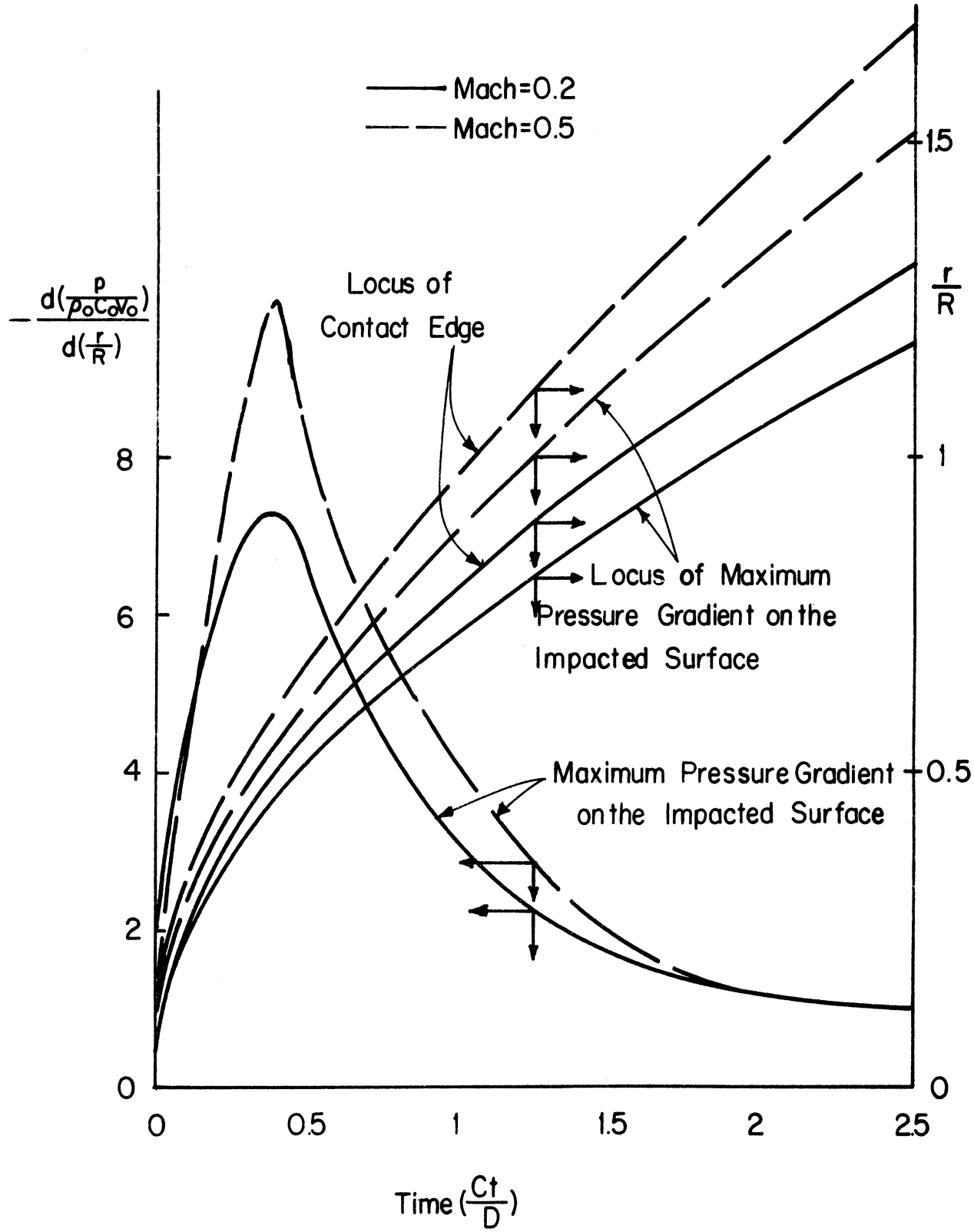

Fig. 40. Maximum Pressure Gradient-Time and -Location Relation and Contact Edge-Time History of an Initially Spheri-Droplet for Impact Mach Numbers of 0.2 and 0.5. Non-Slip Boundary Condition.

CHAPTER IV

CONCLUSIONS

The objective of this study was to investigate numerically the rigorous solution of liquid-solid impact. Effort was directed to seek the pressure and velocity distribution as a function of time. A Compressible-Cell-and-Marker solution method was successfully developed without the problem of numerical oscillation. The effects of drop shape, impact Mach number and non-slip or free-slip boundaries are investigated. Based on the numerical results, the following conclusions in studying the mechanism of liquid impingement on a rigid solid plane can be drawn.

1. One dimensional water hammer pressure corrected with the shock wave velocity represents the theoretical limit for the maximum pressure generated by normal impact of a water droplet on a rigid plane surface.

2. For the impact of a two-dimensional liquid drop bounded by free surface, the lateral flow begins immediately and the pressure build-up is therefore affected from the first instant of contact.

3. For the impact on the end of the cylindrical droplet, the larger the diameter, the closer the impact pressure to the one-dimensional maximum pressure. The critical diameter roughly is four times the cylinder length.

4. A spherical drop has a lower maximum impact pressure than a cylindrical drop does for the same impact velocity.

5. For a given shape of water drop and a given boundary condition, the lower the impact Mach number, the higher the sideway jetting velocity V relative to the impact velocity V_o.

6. The non-slip boundary condition retards the flow, but contributes to a higher pressure build-up and hence an instantaneous peak radial velocity than free-slip boundary condition does.

7. Suggestion by Engel[21] that cavitation may occur as a

result of reflection of the impact wave from the rear surface of the drop is confirmed by Brunton[75] as well as by this study.

8. The central cavitation bubble on the liquid-solid interface will also occur, when sideway jetting velocity exceeds impinging velocity, such that the liquid locally becomes subject to sufficient tension.

9. For a typical spherical water droplet of 2 mm in diameter at an impact Mach number of 0.2, the pressure reaches its peak at 0.25 μ sec. The duration of the first and the most severe pressure pulse is about 1.5 μ sec. This result also agrees with Fyall's photographic observation.[21]

10. The radial pressure gradients on the impacted surface are more severe near the contact edge than in the center. The strong radial pressure gradient remains attached to the edge of the drop. The radial pressure gradients have the peak value at the contact angle of about 12^{o}.

REFERENCES

1. Honegger, E., "Tests on Erosion Caused by Jets," Brown Boveri Review, 14, 4, pp. 95-104, (1927).

2. Cook, S.S., "Erosion by Water-Hammer", Proc. Royal Society, A, 119, pp. 481-488, (1928).

3. Christie, D.G., and Hayward, G.W., "Observation of Events Leading to the Formation of Water Drops Which Cause Turbine Blade Erosion", Phil. Trans. Roy. Soc., A, Part No. 1110, 260, pp. 73-315, (1966).

4. Caldwell, J., "Description of the Damage in Steam Turbine Blading Due to Erosion by Water Droplets", Phil. Trans. Roy. Soc., A, Part No. 1110, 260, pp. 204-208, (1966.)

5. Smith, A., "Physical Aspects of Blade Erosion by Wet Steam in Turbines", Phil. Trans. Roy. Soc., A, Part No. 1110, 260, pp. 209-215, (1966).

6. Schmitt, G.F. Jr., "Current Investigations in Rain Erosion by the U.S. Air Force," ASTM Meeting in Atlantic City, N.J., June 27-July 1, 1966.

7. Wahl, N.E., "Investigation of the Phenomena of Rain Erosion at Subsonic and Supersonic Speeds," Air Force Materials Laboratory Report AFML-TR-65-330, (1966).

8. Fyall, A.A., King, R.B., and Strain, R.N.C., "Rain Erosion Aspects of Aircraft and Guided Missiles", J. Roy. Aero. Soc., 66, pp. 447-453, (1962).

9. Naude, C.F., and Ellis, A.T., "On the Mechanism of Cavitation Damage by Nonhemispherical Cavities Collapsing in Contact with a Solid Boundary," Trans. ASME, J. Basic Engr., December, 1961.

10. Hammitt, F.G., "Observations on Cavitation Damage in a Flowing System", J. Basic Engr., Trans. ASME, 85, D, 3, pp. 347-359, (1963.)

11. Knapp, R.T., Daily, J.W., and Hammitt, F.G., Cavitation, McGraw-Hill, (1970).

12. Pouchot, W.D., et al., "Analytical Investigation of Turbine Erosion Phenomena," Westinghouse Astro-Nuclear Lab. Report PR-(DD)-014, (1966).

13. Zimmerman, W.F., and Rossback, R.J., "Metallurgical and Fluid Dynamic Results of a 2000-hr. Endurance Test on a Two-Stage, 200-horsepower Turbine in a Wet Potassium Vapor", ASME Paper 67-GT-9, (1967.)

14. Wood, G. M., et al., "Cavitation Damage Investigation in Mixed-Flow Liquid Metal Pumps", Symposium on Cavitation in Fluid Machinery, ASME, pp. 196-214, (1965).

15. Hammitt, F. G., "Two-Phase Material Attribution Problems for Rankine-Cycle Liquid Metal Power Plants," Trans. ASME, J. Engr. for Power, 88, A, 4, pp. 388-394, (1966).

16. Wengel, H. G., Jr., and Wang, C. T., "The Mechanics of a Drop After Striking a Stagnant Water Layer", Research Report No. 30, Water Resources Center, University of Illinois, (1970).

17. Worthington, A. M., A Study of Splashes, The MacMillan Company, New York, (1963.)

18. Engel, O. G., "Mechanism of Rain Erosion", WADC Tech. Report 53-192, Part I through XV. (1953).

19. Engel, O. G., "Waterdrop Collisions with Solid Surfaces," J. of Research of the National Bureau of Standards, 54, 5, May 1955.

20. Bowden, F. P., and Brunton, J. H., "The Deformation of Solids by Liquid Impact at Supersonic Speeds", Proc. of the Royal Society, A, 263, pp. 433-450, (1961).

21. Fyall, A. A., "Single Impact Studies of Rain Erosion", Shell Aviation News, 374, (1969).

22. Tait, P. G., "Report on Some of the Physical Properties of Fresh Water and Sea Water", Report on Scienfitic Results of Voy, H. M. S., and Challenger, Phys. Chem., 2, 1-71 (1888).

23. Huang, Y. C., Mitchell, T. M., and Hammitt, F. G., "On Shock Wave Velocity of Water," The University of Michigan, College of Engr., Dept. of Mechanical Engr., Cavitation and Multiphase Flow Lab., ORA Report No. 02643-1-T, (1969).

24. Heymann, F. J., "On the Shock Wave Velocity and Impact Pressure in High-Speed Liquid-Solid Impact," Trans. ASME, J. of Basic Engr., 90, p. 400, July 1968.

25. Kirkwood, J. G., and Bethe, H. A., "The Pressure Wave Produced by an Underwater Explosion; I, Basic Propagation Theory", 588, (1942).

26. Kirkwood, J. G., and Richardson, J. M., "The Pressure Wave Produced by an Underwater Explosion; III, Properties of Salt Water at a Shock Front," OSRD Report 813, (1942).

27. Richardson, J. M., et al., "Hydrodynamic Properties of Sea Water at the Front of a Shock Wave," J. of Chemical Physics, V. 15, 11, pp. 785-794, (1947).

28. Rice, M. H., and Walsh, J. M., "Equation of State for Water to 250 kilobars," J. of Chemical Physics, 26, 4, pp. 825-830, April 1957.

29. Cook, M. A., et al., "Measurements of Detonation Pressure", J. Applied Physics, 33, 12, pp. 3413-3421, Dec. 1962.

30. Savic, P., and Boult, G. T., "The Fluid Flow Associated with the Impact of Liquid Drops with Solid Surfaces", National Research Council of Canada,Report No. MT-26, May 1955.

31. Heymann, F. J., "High-Speed Impact Between a Liquid Drop and a Solid Surface", J. of Applied Physics, 40, 13, pp. 5113-5122, Dec. 1969.

32. Cole, R. H., Underwater Explosions, Dover,(1965.)

33. Amagat, E. N., "Elasticite et Dilatibilite des Fluides," Ann. Chim. Phys., 6, 29, pp. 68-136, 505-574,(1893).

34. Ekman, V. W., "Die Zusammendrisckbarkeit des Meerwassers", Conseil Perm. Int. l'Explor. de la Mer, Publ. de Circon. 43, Copenhagen, 1908.

35. Bridgman, P. W., Proc. Am. Acad. Arts Sci., pp 47, 441, (1912), 74, 399, (1942).

36. Bridgman, P. W., J. Chem. Phys., pp. 3, 597, (1936), 5, 964, (1937), 9, 794, (1941).

37. Kennedy, G. C., Knight, W. L., and Holsen, W. T., "Properties of Water", J. Am. Sci., 256, p. 594, (1958).

38. Newton, M. S., and Kennedy, G. C., "P-V-V-S Relations of Sea Water", J. Marine Res., 23, 88, (1965).

39. Diaz-Pena, M., and McGlashan, M. L., "An Apparatus for Measurement of the Isothermal Compressibility of Liquid", Trans. Faraday Soc., 55, 2018, (1959).

40. Eckart, C., "Properties of Water", J. Am. Soc., 256, pp. 225-240, (1958).

41. Del Grosso, V. A., "The Velocity of Sound in Sea Water at Zero Depth", Naval Res. Lab. Rept. 40002, (1952).

42. Wilson, W., "Speed of Sound in Distilled Water as a Function of Temperature and Pressure,"J. Acoustical Soc. Amer., 31, 1067, (1959).

43. Wilson, W., "Speed of Sound in Sea Water as a Function of Temperature, Pressure and Salinity", J. Acous. Soc. Amer., 38, p. 641, (1960).

44. Briggs, H. B., Johnson, J. B., and Mason, W. P., "Properties of Liquids at High Sound Pressure," J. Acous. Soc. Amer., 19, 664, (1947).

45. Gibson, R. E., and Loeffler, O. H., "P-V-T Relations in Solutions, 5, The Energy-Volume Coefficient of Carbon Tetrachloride, Water, and Ethylene Glycel," J. Am. Chem. Soc., 63, 898, (1941).

46. Kirkwood, J. G., and Montroll, E., "Properties of Pure Water at a Shock Front," U. S. Office of Scientific Research and Development Reports No. 676, (1942).

47. Li, Y.-H., "Equation of State of Water and Sea Water", J. of Geophysical Research, 32, 10, May 1967.

48. Frenkel, I., Kinetic Theory of Liquids, Dover, 1955.

49. Furth, R., "On the Theory of the Liquid State", Proceedings of the Cambridge Philosophical Society, 37, 1941, Part I, p. 252; Part II, p. 276; Part IV, p. 281.

50. Doring, W., "Die Oberhitzungsgrenze und Zerreissfestigkeit von Flussigkeiten", Z. Phys. Chem., B36, 1937, p. 371; B38, p. 292 (1939).

51. Fisher, J. C., "The Fracture of Liquids", J. of Applied Physics, 19, 1948, pp. 1062.

52. Dorsey, N. E., Properties of Ordinary Water-Substance, Reinhold Publishing Corporation, (1940).

53. Reynolds, O., "Papers on Mechanical and Physical Subjects", Vol. 1, pp. 394-398, Cambridge Univ. Press (1900).

54. Briggs, L. J., "Limiting Negative Pressure of Water", J. of Applied Physics, 21, July 1950, pp. 721-722.

55. Blake, F. G., Jr., "The Tensile Strength of Liquids: A Review of the Literature" Technical Memorandum No. 9, Acoustic Research Laboratory, Harvard Univ., June 11, 1949.

56. Harlow, F. G., "Numerical Methods for Fluid Mechanics, An Annotated Bibliography," Los Alamos Scientific Laboratory, Report No. LA-4281, (1969).

57. Welch, J. E., Harlow, F. H., Shannon, J. P., and Daly, B. J., The MAC Methods", Los Alamos Scientific Lab., Report No. LA-3425, (1966).

58. Harlow, F. H., and Welch, J. E., "Numerical Calculation of Time-Dependent Viscous Incompressible Flow of Fluid with Free Surface", Phys. Fluids, 8, 2182, (1965.)

59. Amsden, A. A., "The Particle-in-Cell Method for the Calculation of the Dynamics of Compressible Fluids", Los Alamos Scientific Lab., Report No. LA-3466, (1966).

60. Harlow, F. H., "The Particle-in-Cell Computing Method for Fluid Mechanics," Methods in Computational Physics, 3, 319-343, (1964).

61. Harlow, F. H., and Amsden, A. A., "Numerical Calculation of Almost Incompressible Flow", J. of Computational Physics, 3, 80-93, (1968).

62. Chan, K.-C., and Street, R. L., "A Computer Study of Finite-Amplitude Water Waves", J. of Computational Physics, 6, 68-94, (1970).

63. Noh, W. F., "CEL: A Time-Dependent Two-Space-Dimensional Coupled Eulerian-Lagrangian Code," Methods in Computational Physics, 3, pp. 117-180, (1964).

64. Lax, P., and Wendroff, B., "System of Conservation Laws", Communication on Pure and Applied Mathematics, XIII, pp. 217-237, (1960).

65. Burstein, S. Z., "Finite-Difference Calculations for Hydrodynamic Flows Containing Discontinuities", J. of Computational Physics, 2, 198-222, (1967).

66. Lapidus, A., "A Detached Shock Calculation by Second-Order Finite Differences", J. of Computational Physics, 2, 154-177, (1967).

67. Rubin, E. L., "Difference Methods for the Inviscid and Viscous Equations of a Compressible Gas," J. of Computational Physics, 2, 178-196, (1967).

68. Richtanyer, R. D., and Morton, K. W., Difference Methods for Initial Value Problems, 2nd ed., Inter-Science, (1967).

69. Hirt, C. W., "Heuristic Stability Theory for Finite-Difference Equations", J. of Computational Physics, 2, 399-355, (1968).

70. Mitchell, T. M., "Numerical Studies of Asymmetric and Thermodynamic Effects on Cavitation Bubble Collapse", Ph. D. Thesis, University of Michigan, Dept. of Nuclear Engineering, (1970).

71. Lamb, Sir Horace, Hydrodynamics, 6th Ed., Dover, (1965).

72. Thiruvengadam, A., Ruby, S. L., and Gunasekaran, M., "Experimental and Analytical Investigations on Liquid Impact Erosion", ASTM Special Technical Publication, 474, (1969).

73. Engel, O. G., "Pits in Metals Caused by Collision with Liquid Drops and Rigid Steel Spheres" J. of Research of the National Bureau of Standards, 64A, (1960).
74. Bowden, F. P. and Field, T. F., "The Brittle Fracture of Solids by Liquid Impact, by Solid Impact, and by Shock", Proc. Roy. Soc. (London) A 282, 331 (1964).
75. Brunton, J. H. and Camus, J. J., "The Flow of a Liquid Drop During Impact", 3rd International Congress on Rain Erosion, August 1970.

APPENDIX A

THE MECHANICAL PROPERTIES OF WATER

1. Compression and Tension

Extensive data on the pressure-volume-temperature relationships of fresh water and/or sea water have been collected. To mention some of the more important works, these are: Amagas[33], Ekman[34], Bridgman[35,36], Kennedy[37], Newton and Kennedy[38], and many others[39,40,41,42,43,44,eg.]. The appropriate constant in the Tait's state for water can then be determined. Their values depend upon which experimental data are analyzed. Gibson and Loeffler[45] first found that the constants in Tait's equation are, for the temperature range of $25^{o}C < t < 85^{o}C$,

$$A = 7.31 \qquad \text{(A1)}$$

$$B = 2996.0 + 7.5554\,(t-25) - 0.17814\,(t-25)^{2} + 600\times10^{-6}(t-25)^{3} \text{ bars.}$$

Kirkwood and some of his associates[46,26] using pressure-volume-temperature data of Bridgman for pure water and another slightly different expression of B given by Gibson[26] (through their private communication)

$$B = 2.996 + 7.585 \times 10^{-3}\,(t-25) - 1.790 \times 10^{-4}\,(t-25)^{2} + 6.13 \times 10^{-7}\,(t-25)^{3} \text{ kilobars} \qquad \text{(A2)}$$

finds that A = 7.15 gives less than 4% deviation to fit the Bridgman's data between $20^{o}C$ and $60^{o}C$ up to pressures of 25 kilobars.[32] Li[47], by exhaustive examination of the published experimental data, concluded that the Tait equation represents the pressure-volume-temperature relationship of water very well.

2. Tensile Rupture

Numerous theoretical calculations and experimental measurements of the tensile strength have been made. The simples estimate is the equation of bubble dynamics that the tensile strength, TS,

is equal to the surface tension, S, with the correction of radius R.

$$TS = 2S/R \tag{A3}$$

Thus, for pure water, the equation (A3) gives a tensile strength of approximately 14000 atmospheres corresponding to the situation where the radius would be approximately one-half of the mean intermolecular spacing.[48] More sophisticated approaches give smaller values of tensile strength: 4000 atm by Furth[49] and Doring[50] and about 1300 atm by Fisher.[51] However, at the presence of bubbles of air, 1000A in diameter, a column of water will break at a tension of about 30 atm., no matter how much greater the true tensile strength of water might be.[52]

Many measurements of tension in water have been made by using static or dynamic techniques. Tensile strength was observed at 3 atm. low by Reynolds[53] employing the static method to 250-280 atm, high by Briggs[54], employing a centrifugal method. A review of the literature on the tensile strength of liquids was given by Brake.[70]

APPENDIX B

LISTING OF THE FORTRAN PROGRAM

FOR LIQUID IMPACT PROBLEM

```
"COM11-0-11   &&11&&   JJJAAA            11-0-11   &&11&&   JJJAAA      M 016750
C*****HEAD DEPARTMENT OF ENTIRE PREGRAM **************************
      COMMON DEN(2,100,100),DENU(2,100,100),DENV(2,100,100)
      COMMON U(2,100,100),V(2,100,100),P(2,100,100)
      COMMON /BLRZ/ ZTT(2,200),RTT(2,200),ZT(2,200),RT(2,200)
      COMMON /BLHR/ H(2,200),R(2,200),I(2,200),J(2,200)
      COMMON /AXIS/ RXIS(200),HXISM(2,200),HXISP(2,200)
      COMMON /BLKB/ KBM(2,200),KBP(2,200)
      COMMON /BTOP/ HMAX(500),RMAX(500),HJET(500),RJET(500)
      COMMON /BTOP/ HMIN(500),RMIN(500),HTOP(500),ZA(500),ZB(500)
      COMMON /BTOP/ ZC(500),ZD(500),ZE(500),ZF(500),ZG(500),ZH(500)
      COMMON /BLO/ DENO,DENUO,DENVO,UO,VO,PO,DENP,PP
      COMMON /BLB/ KEND,LEND,LRAD,RDROP,KCORE,LCORE,KSOLID,HSOLID
      COMMON /BLD/ DT,DZ,DR,STAFAC,TDZ,TDR,TDP
      COMMON /BLD/ DINF,UINF,PINF,CINF,UTMACH,PHAMER
      COMMON /BLP/ NPT,NMAX,NJET,NMIN,LMAX,LJET,LMIN,LTIP,NTIP,KTOP
      COMMON /S/ CYCLE,NSTAGE,NPRINT,TIME,TIMEND,CHLEN
      COMMON /BLAB/ A,B,CT,CS
      COMMON /BMAS/ MASS(500),MASSO,PI
      COMMON /JR/ JS(100),RS(100)
      COMMON /BT/ TOUCH(200)
      COMMON /BEND/ KEND2,LEND2,KEND3,LEND3,KLD,NKTT
      COMMON /BCRIT/ PCRIT,DECRIT,CONST
      COMMON /CV/ CO,CP,C1,C2,C3,COEF,ALPHA,COEG
      COMMON /NNP/ N,NP
      COMMON /HAB/ HA,HB,GA,GB,GC,FA,FB,FC,DENB,DMAX,DMIN,NSM,DA,DB
      COMMON /BFL/ JA,JB,JC,JD,JE,JF,JG,JH,JI,JJ,JK,JL,JM,JN
      COMMON /BFL/ JU,JV,JW,JX,JY,JZ
      COMMON /BFL/ JA1,JA2,JA3,JA4,JA5,JA6,JA7,JA8,JA9,JAO
      DIMENSION CHAR(44)
      DIMENSION IMAGE(1500)
      DIMENSION W(500)
      DATA CHAR/'1','2','3','4','5','6','7','8','9','0'
     &,'A','B','C','D','E','F','G','H','K','L','M','N'
     &,'O','P','Q','R','S','T','U','V','W','X','Y','Z'
     &,'#','$','%','&','*','@','<','>','=','+'/
      INTEGER CYCLE,PT,PTM,PTP
      REAL MASS,MASSO
      PI=3.1415927
      PINF=14.70*144.0
C-----INPUT CONSTANTS--------------------------- *
    1 CONTINUE
      READ (5,52) KEND,LEND,LCHARA
      KEND2=KEND-1
      LEND2=LEND-1
      KEND3=KEND-2
      LEND3=LEND-2
      READ (5,52) KCORE,LCORE
      READ (5,52) LRAD
      READ (5,52) KSOLID
      READ (5,52) K1,K3
      READ (5,52) L1,L3
      READ (5,52) KLD,NKTT
      READ (5,52) JA,JB,JC,JD
      READ (5,52) JE,JF,JG,JH,JI,JJ,JK,JL
      READ (5,52) JM,JN,NSM,NSMA,NSMB
      READ (5,52) JU,JV,JW,JX,JY,JZ
      READ (5,52) JA1,JA2,JA3,JA4,JA5,JA6,JA7,JA8,JA9,JAO
      READ (5,58) CSER,CHMS
      READ (5,58) DENB
```

```
      READ (5,58) FB,FC
      READ (5,58) FA,ALPHA
      READ (5,50) GA,GB,GC
      READ (5,50) HA,HB,DA,DB
      READ (5,57) A,B
   57 FORMAT (F5.2,E20.6)
      READ (5,50) UMAK,VMAK
      READ (5,50) CO,DINF
      UO=UMAK*CO
      VO=VMAK*CO
      UINF=SQRT(UO*UO+VO*VO)
      READ (5,50) C1,C2,C3
      READ (5,50) PCRIT
      READ (5,50) PENG,PENH
      READ (5,59) TSTEP,DT
   59 FORMAT (F5.0,E10.2)
      READ (5,52) NHL,NSBH,NVL,NSBV
      READ (5,58) YMAX,YMIN,XMAX,XMIN
      READ (5,52) MHL,MSBH,MVL,MSBV
      READ (5,58) YA,YB,XA,XB
      READ (5,52) IHL,ISBH,IVL,ISBV
      READ (5,58) YC,YD,XC,XD
      READ (5,52) JHL,JSBH,JVL,JSBV
      READ (5,58) YE,YF,XE,XF,YG,YH,XG,XH
      READ (5,58) AMX,AMY
      PREF=DINF*CO*UINF
      PREF=PREF/PINF
      DENO=1.
      UO=UO/UINF
      VO=VO/UINF
      DENUO=UO
      DENVO=VO
      PO=1.
      PO=PO/PREF
      UT=1.
      CINF=SQRT((B+PINF)/DINF)
      COEF=CINF/UINF
      COEG=DINF*UINF*UINF/PINF
      COEG=COEG/PREF
      CP=CO/UINF
      B=B/PINF
      B=B/PREF
      CT=FW(UT)
      CS=CT-UT
      UTMACH=UT/CT
      COMACH=CP/CT
      DENP=DENO*CT/CS
      PHAMER=COEG*DENO*CT*UT
      PP=PO+PHAMER
      DZ=DT*CT*UINF
      DR=DZ
      WMACH=UINF/CO
      SUPSON=CT/CP
      TIMEO=LCHARA*DZ/UINF
      CHLEN=LCHARA*DZ*304.8
      WRITE(6,15) CHLEN,TIMEO,SUPSON,PO,PREF,DENP,PP
   15 FORMAT(/,'CHARACTERISTICS',5E15.6,2F10.5)
      WRITE(6,62) UO,VO,UINF,CS,CT,CP,UMAK,VMAK,UTMACH,COMACH
   62 FORMAT(/,'VELOCITYS',10F10.4)
      PCRIT=PCRIT/PREF
```

```
      DECRIT=((PCRIT+B)/(PO+B))**(1./A)
      CONST=PCRIT/(DENO-DECRIT)
      WRITE (6,73) PCRIT,DECRIT,CONST
   73 FORMAT(/,'NEGATIVE PRESSURE THRESHOLD',3E15.6)
  500 CONTINUE
      READ (5,50) STAFAC
      IF (STAFAC .GT. 1.0) GO TO 500
      IF (STAFAC .LT. 0.) GO TO 999
      ACDT=STAFAC*TSTEP*DT
      TDZ=STAFAC*UTMACH
      TDR=TDZ
      TDP=STAFAC*COMACH
      WRITE(6,60) STAFAC,DT,DZ,DR,TDZ,TDR,TDP
   60 FORMAT(/,'STABILITY FACTOR',F10.4,6E15.5)
      DAVE=GA*DENO+GB*(4.*DENO)+GC*(4.*DENO)
      PO=FP(DAVE)
      NSTAGE=1
      CYCLE=NSTAGE-1
      TIME=0.
      N=1
      NP=2
C-----REQUEST INITIAL CONDITION FOR LAGRANGIAN AND EULERIAN GRID
      CALL SHAPE(ACDT)
      CALL FIRST(DENB)
      CALL CONSER(N)
      WRITE (6,64)
      CALL PLOT1(0,NHL,NSBH,NVL,NSBV)
      CALL PLOT2(IMAGE,XMAX,XMIN,YMAX,YMIN)
      DO 10 PT=1,NPT
      CALL PLOT3('O',R(1,PT),H(1,PT),1,4)
   10 CONTINUE
      CALL PLOT4(1,'H')
      READ (5,52) NPRINT,MX,MY
      IF (CYCLE .GT. MY) GO TO 21
      IF (CYCLE .LT. MX) GO TO 21
      CALL PRIN(N)
   21 CONTINUE
  501 CONTINUE
      NSTAGE=NSTAGE+1
      CYCLE=NSTAGE-1
      TIME=TIME+ACDT
      TIMEND=TIME/TIMEO
C-----CALL LAGRANGIAN AND EULERIAN CALCULATION---------- *
      CALL BOUND(N,NP,TSTEP)
      IF(JN .LE. 0) GO TO 999
      JA=2*NSTAGE+JC
      JB=JS(1)+JA
      KTOPP=KTOP+1
      LTIPP=LTIP+1
      JA=MINO(JA,KTOPP,KEND3)
      JB=MINO(JB,LTIPP,LEND3)
      IF(MOD(JA,2) .EQ. 0) JA=JA+1
      IF(JA .GT. KEND3) JA=JA-2
      CALL FIELD(N,NP,MX,MY,NSMA,NSMB)
   41 CONTINUE
      CALL CONSER(NP)
      IF (CSER .EQ. 0.) GO TO 42
      RATIO=MASS(NSTAGE)/MASS(1)
      CHANGE=RATIO - 1.
      WRITE (6,45) CYCLE,MASS(NSTAGE),RATIO
```

```
   45 FORMAT(/,'CYCLE='I3,10X,'MASS='F10.6,10X,'RATIO='F10.6,/)
      IF (ABS(CHANGE) .LT. CHMS) GO TO 42
      LB=LTIP-1
      DO 43 L=1,LB
      KB=KBP(NP,L)-1
      IF (TOUCH(L)) 46,46,47
   46 KA=1
      GO TO 48
   47 KA=KBM(NP,L)+1
   48 IF (KB .LT. KA) GO TO 43
      DO 44 K=KA,KB
      IF (L .GE. JS(K)) GO TO 44
      DEN(NP,K,L)=DEN(NP,K,L)*RATIO
      DENU(NP,K,L)=DENU(NP,K,L)*RATIO
      DENV(NP,K,L)=DENV(NP,K,L)*RATIO
      P(NP,K,L)=P(NP,K,L)*RATIO
   44 CONTINUE
   43 CONTINUE
      GO TO 41
   42 CONTINUE
      IF (LTIP .GE. LEND2) GO TO 99
      IF (CYCLE .LT. NPRINT) GO TO 510
   99 CONTINUE
C-----PLOTTING THE SHAPE OF IMPACTING LIQUID---------- *
      WRITE(6,56) CYCLE,TIME,NMAX,NMIN,NJET,NTIP
     &,KTOP,TIMEND,LMAX,LMIN,LJET,LTIP
      CALL PLOT1(0,NHL,NSBH,NVL,NSBV)
      CALL PLOT2(IMAGE,XMAX,XMIN,YMAX,YMIN)
      DO 20 PT=1,NPT
      CALL PLOT3('*',R(NP,PT),H(NP,PT),1,4)
   20 CONTINUE
      DO 30 L=L1,JB
      XK=RXIS(L)
      DO 40 K=K1,JA
      KBC=(P(NP,K,L)-PENG)/PENH
      IF (KBC .EQ. JA1) GO TO 40
      KBC=KBC+1
      BCD=CHAR(KBC)
      YK=K-0.5
      CALL PLOT3(BCD,XK,YK,1,4)
   40 CONTINUE
   30 CONTINUE
      CALL PLOT4(1,'H')
      WRITE (6,80)
   80 FORMAT(50X,'R AXIS')
C----- R VS PRESSURE(Z,R)@Z ---------------- *
      WRITE (6,64)
      CALL PLOT1(0,MHL,MSBH,MVL,MSBV)
      CALL PLOT2(IMAGE,XA,XB,YA,YB)
      KBC=0
      K=JA
  170 CONTINUE
      K=K-K3
      KBC=KBC+1
      BCD=CHAR(KBC)
      DO 70 L=L1,JB,L3
      XL=L-1.
      Y=K+P(NP,K,L)*AMY
      CALL PLOT3(BCD,Y,XL,1,4)
   70 CONTINUE
```

```
      IF(K .GT. K1) GO TO 170
      CALL PLOT4(6,'R AXIS')
      WRITE (6,81)
   81 FORMAT (50X,'PRESSURE(Z,R)@Z')
C----- Z VS PRESSURE(Z,R)@R ----------------- *
      WRITE (6,64)
      CALL PLOT1(0,IHL,ISBH,IVL,ISBV)
      CALL PLOT2(IMAGE,XC,XD,YC,YD)
      LBC=0
      DO 72 L=L1,JB,L3
      LBC=LBC+1
      BCD=CHAR(LBC)
      DO 72 K=K1,JA,K3
      YK=K-1.
      X=L+P(NP,K,L)*AMX
      CALL PLOT3(BCD,X,YK,1,4)
   72 CONTINUE
      CALL PLOT4(6,'Z AXIS')
      WRITE (6,82)
   82 FORMAT (50X,'PRESSURE(Z,R)@R')
C----- CALCULATION CONTROL ------------------- *
      IF (LTIP .GE. JN) GO TO 77
      IF (CYCLE .GT. MY) GO TO 22
      IF (CYCLE .LT. MX) GO TO 22
   77 CONTINUE
      CALL PRIN(NP)
      IF (LTIP .GE. JN) GO TO 500
   22 CONTINUE
      READ (5,52) NPRINT,MX,MY
      IF (NPRINT .EQ. 0 ) GO TO 500
      IF (NPRINT .EQ. -1) GO TO 999
  510 CONTINUE
      IF (N .EQ. 1) GO TO 502
      N=1
      NP=2
      GO TO 503
  502 CONTINUE
      N=2
      NP=1
  503 CONTINUE
      GO TO 501
  999 CONTINUE
C----- FINAL RESULTS ------------------------ *
      DO 27 M=1,CYCLE
      W(M)=M
   27 WRITE(6,26) M,MASS(M),HTOP(M),RJET(M)
     &,ZA(M),ZB(M),ZC(M),ZD(M),ZE(M),ZF(M),ZG(M)
   26 FORMAT(I5,F10.4,2E15.4,7F10.4)
      WRITE (6,64)
      CALL PLOT1(0,NHL,NSBH,NVL,NSBV)
      XM=CYCLE
      CALL PLOT2(IMAGE,XM,0.,YMAX,0.)
      DO 24 NCY=JU,CYCLE,JV
      STE=NCY
      CALL PLOT3('T',STE,HTOP(NCY),1,4)
      CALL PLOT3('S',STE,HJET(NCY),1,4)
      CALL PLOT3('R',STE,RJET(NCY),1,4)
   24 CONTINUE
      CALL PLOT4(4,'PATH')
      WRITE (6,64)
```

```
      CALL PLOT1(0,JHL,JSBH,JVL,JSBV)
      CALL PLOT2(IMAGE,XE,XF,YE,YF)
      DO 25 NCY=JU,CYCLE,JV
      STE=NCY
      CALL PLOT3('A',STE,ZA(NCY),1,4)
      CALL PLOT3('B',STE,ZB(NCY),1,4)
      CALL PLOT3('C',STE,ZC(NCY),1,4)
      CALL PLOT3('D',STE,ZD(NCY),1,4)
      CALL PLOT3('E',STE,ZE(NCY),1,4)
   25 CONTINUE
      CALL PLOT4(16,'PRESSURE HISTORY')
      WRITE(6,64)
      CALL STPLT2(IMAGE,W,ZA,NCY,4,'A',5,'P @A ')
      WRITE(6,64)
      CALL STPLT2(IMAGE,W,ZF,NCY,4,'F',5,'DP/DT')
      WRITE(6,64)
      CALL STPLT2(IMAGE,W,ZG,NCY,4,'G',5,'DP/DR')
      WRITE(6,64)
      CALL STPLT2(IMAGE,W,ZH,NCY,4,'H',7,'DP/DT@R')
   64 FORMAT (1H1)
   50 FORMAT(8F10.4)
   53 FORMAT(8I10)
   52 FORMAT (14I5)
   56 FORMAT(1H1,'CYCLE='I3,5X,'TIME='E14.4,10X,'NMAX='I3,5X,
     & 'NMIN='I3,5X,'NJET=',I3,5X,'NTIP='I3,5X,'KTOP='I3,
     & /,12X,'ND TIME='E14.4,10X,
     & 'LMAX='I3,5X,'LMIN=',I3,5X,'LJET=',I3,5X,'LTIP=',I3)
   55 FORMAT (7E10.3)
   58 FORMAT(12F5.1)
      GO TO 1
      END
C*******************************************************************************
      SUBROUTINE FIRST(DENB)
      COMMON DEN(2,100,100),DENU(2,100,100),DENV(2,100,100)
      COMMON U(2,100,100),V(2,100,100),P(2,100,100)
      COMMON /BLKB/ KBM(2,200),KBP(2,200)
      COMMON /BEND/ KEND2,LEND2,KEND3,LEND3,KLD,NKTT
      COMMON /BLO/ DENO,DENUO,DENVO,UO,VO,PO,DENP,PP
      COMMON /BLB/ KEND,LEND,LRAD,RDROP,KCORE,LCORE,KSOLID,HSOLID
      COMMON /BLP/ NPT,NMAX,NJET,NMIN,LMAX,LJET,LMIN,LTIP,NTIP,KTOP
      COMMON /BFL/ JA,JB,JC,JD,JE,JF,JG,JH,JI,JJ,JK,JL,JM,JN
      DIMENSION DENZ(20000),DENUZ(20000),DENVZ(20000)
      DIMENSION UZ(20000),VZ(20000),PZ(20000)
      EQUIVALENCE (DEN,DENZ),(DENU,DENUZ),(DENV,DENVZ)
      EQUIVALENCE (U,UZ),(V,VZ),(P,PZ)
      N=1
      DO 30 L=1,LMAX
      KLO=KBM(N,L)
      KHI=KBP(N,L)
      KBMM=KLO-1
      KBPP=KHI+1
      IF(KBMM .LT. KSOLID) GO TO 50
      DO 60 K=KSOLID,KBMM
      NKL=N+(K-1)*2+(L-1)*NKTT
      DENZ(NKL)=DENB
      DENUZ(NKL)=DENUO
      DENVZ(NKL)=DENVO
      UZ(NKL)=UO
      VZ(NKL)=VO
      PZ(NKL)=PO
```

```
   60 CONTINUE
   50 CONTINUE
C
      IF (KBPP .GT. KEND) GO TO 55
      DO 70 K=KBPP,KEND
      NKL=N+(K-1)*2+(L-1)*NKTT
      DENZ(NKL)=DENB
      DENUZ(NKL)=DENUO
      DENVZ(NKL)=DENVO
      UZ(NKL)=UO
      VZ(NKL)=VO
      PZ(NKL)=PO
   70 CONTINUE
   55 CONTINUE
      DO 80 K=KLO,KHI
      NKL=N+(K-1)*2+(L-1)*NKTT
      DENZ(NKL)=DENO
      DENUZ(NKL)=DENUO
      DENVZ(NKL)=DENVO
      UZ(NKL)=UO
      VZ(NKL)=VO
      PZ(NKL)=PO
   80 CONTINUE
   30 CONTINUE
      LMAXP=LMAX+1
      DO 90 L=LMAXP,LEND
      DO 90 K=2,KEND
      NKL=N+(K-1)*2+(L-1)*NKTT
      DENZ(NKL)=DENB
       DENUZ(NKL)=DENUO
      DENVZ(NKL)=DENVO
      UZ(NKL)=UO
      VZ(NKL)=VO
      PZ(NKL)=PO
   90 CONTINUE
      K=1
      KP=K+1
      DO 20 L=1,LEND
      NKL=N+(K-1)*2+(L-1)*NKTT
      NKPL=NKL+2
      DENZ(NKL)=DENO
      DENUZ(NKL)=DENUZ(NKPL)
      DENVZ(NKL)=DENVZ(NKPL)
      UZ(NKL)=UZ(NKPL)
      VZ(NKL)=VZ(NKPL)
      PZ(NKL)=PZ(NKPL)
   20 CONTINUE
      NP=2
      DO 75 L=1,LEND
      DO 75 K=1,KEND
      NKL=N+(K-1)*2+(L-1)*NKTT
      NPKL=NP+(K-1)*2+(L-1)*NKTT
      DENZ(NPKL)=DENZ(NKL)
      DENUZ(NPKL)=DENUZ(NKL)
      DENVZ(NPKL)=DENVZ(NKL)
      UZ(NPKL)=UZ(NKL)
      VZ(NPKL)=VZ(NKL)
      PZ(NPKL)=PO
   75 CONTINUE
      RETURN
```

```
      END
C*********************************************************************
      SUBROUTINE SHAPE(ACDT)
      COMMON DEN(2,100,100),DENU(2,100,100),DENV(2,100,100)
      COMMON U(2,100,100),V(2,100,100),P(2,100,100)
      COMMON /BLRZ/ ZTT(2,200),RTT(2,200),ZT(2,200),RT(2,200)
      COMMON /BLHR/ H(2,200),R(2,200),I(2,200),J(2,200)
      COMMON /AXIS/ RXIS(200),HXISM(2,200),HXISP(2,200)
      COMMON /BLKB/ KBM(2,200),KBP(2,200)
      COMMON /BTOP/ HMAX(500),RMAX(500),HJET(500),RJET(500)
      COMMON /BTOP/ HMIN(500),RMIN(500),HTOP(500)
      COMMON /BLO/ DENO,DENUO,DENVO,UO,VO,PO,DENP,PP
      COMMON /BLB/ KEND,LEND,LRAD,RDROP,KCORE,LCORE,KSOLID,HSOLID
      COMMON /BLD/ DT,DZ,DR,STAFAC,TDZ,TDR,TDP
      COMMON /BLD/ DINF,UINF,PINF,CINF,UTMACH,PHAMER
      COMMON /BLP/ NPT,NMAX,NJET,NMIN,LMAX,LJET,LMIN,LTIP,NTIP,KTOP
      COMMON /BLAB/ A,B,CT,CS
      COMMON /BT/ TOUCH(200)
      COMMON /BMAS/ MASS(500),MASSO,PI
      COMMON /JR/ JS(100),RS(100)
      INTEGER PT,PTM,PTP,PTU
      REAL MASS,MASSO
      PT=0
      N=1
      RDROP=LRAD-0.5
      IF(RDROP .LT. 0.) RDROP=0.
      DDROP=2.*RDROP
      HSOLID=KSOLID-0.5
      LMAX=LCORE+LRAD
      LMIN=LMAX
      LTIP=LMAX
      LJET=LCORE
      LCOREP=LCORE+1
      BK=HSOLID+RDROP
      HCENTR=BK+KCORE
      KCENTR=HCENTR+1.
      RRMAX=RDROP*RDROP
      HHCNTR=2.*HCENTR
      KTOP=HHCNTR
      RTIP=LTIP-0.5
      HCORE=KCORE
      RCORE=LCORE
      MASSO=0.
      MASSO=MASSO+PI*RCORE*RCORE*RDROP
      MASSO=MASSO+PI*RTIP*RTIP*HCORE
      MASSO=MASSO+2.*PI*(RDROP*RDROP*RDROP/3.+PI*RDROP*RDROP*LCORE/4.)
      MASSO=2.*MASSO
      WRITE(6,21) KSOLID,KTOP,LTIP,HSOLID,HHCNTR,RTIP,RCORE,HCORE
     &,RDROP,MASSO
   21 FORMAT(/,'GEOMETRY',3I4,6F10.4,E15.5)
      NMAX=1
      DO 20 L=1,LEND
      TOUCH(L)=0.
      RXIS(L)=L-0.5
   20 CONTINUE
      IF(LCORE .EQ. 0) GO TO 14
      DO 12 L=1,LCORE
      PT=PT+1
      R(N,PT)=L-0.5
      H(N,PT)=HSOLID
```

```
      I(N,PT)=KSOLID
      J(N,PT)=L
      HXISM(N,L)=HSOLID
      HXISP(N,L)=HHCNTR-HXISM(N,L)
      KBM(N,L)=KSOLID
      KBP(N,L)= HXISP(N,L)+1.0
   12 CONTINUE
      NMAX=PT
   14 CONTINUE
      IF (RDROP .LE. 0.) GO TO 77
      DO 1 L=LCOREP,LMAX
      PT=PT+1
      PTM=PT-1
      R(1,PT)=L-0.5
      DRI=R(N,PT)-LCORE
      IF(DRI-RDROP) 4,5,5
    5 RZ=0.0
      GO TO 7
    4 RZ=SQRT(RRMAX-DRI*DRI)
    7 CONTINUE
      H(N,PT)=BK-RZ
      HXISM(1,L)=H(1,PT)
      I(1,PT)=H(1,PT)+1.0
      J(1,PT)=L
      KBM(1,L)=I(1,PT)
      IF (PT .EQ. 1) GO TO 1
      IDF=I(1,PT)-I(1,PTM)
      IF (PT .EQ. 1) GO TO 2

      IF (IDF .LE. 1) GO TO 2
      PTP=PTM+IDF
      R(1,PTP)=R(1,PT)
      H(1,PTP)=H(1,PT)
       I(1,PTP)= I(1,PT)
       J(1,PTP)= J(1,PT)
      NR=PT
      NS=PTP-1
      DO 3 PT=NR,NS
      I(1,PT)=I(1,PTM)+PT-PTM
      H(1,PT)=I(1,PT)-0.5
      RZ=BK-H(N,PT)
      R(N,PT)=SQRT(RRMAX-RZ*RZ)+LCORE
      J(1,PT)=R(1,PT)+1.0
    3 CONTINUE
      HXISM(N,L)=H(N,NR)
      KBM(N,L)=HXISM(N,L)+1.0
      PT=PTP
      IF (NMAX .LT. PT) NMAX=PT
    2 CONTINUE
      HXISP(N,L)=HHCNTR-HXISM(N,L)
      KBP(1,L)=HXISP(1,L)+1.0
    1 CONTINUE
      NMAX=PT
   77 CONTINUE
      IF(KCORE .EQ. 0) GO TO 6
      NCO=NMAX
      INCO=I(N,NCO)
      IK=INCO+1
      DO 22 K=IK,KCENTR
      PT=PT+1
```

```
      KD=K-INCO
      R(N,PT)=R(N,NCO)
      H(N,PT)=H(N,NCO)+KD
      I(N,PT)=H(N,PT)+1.
      J(N,PT)=R(N,PT)+1.
   22 CONTINUE
      NMAX=PT
    6 CONTINUE
      NMIN=NMAX
      NJET=LCORE
      NTIP=NMAX
      NPT=2*NMAX-1
      NMAXM=NMAX-1
      ZT(1,NMAX)=UO
      RT(1,NMAX)=VO
C     10
      DO 10 PT=1,NMAXM
      PTU=NPT-PT+1
      H(N,PTU)=HHCNTR-H(N,PT)
      R(1,PTU)=R(1,PT)
      I(1,PTU)=H(1,PTU)+1.0
      J(1,PTU)=J(1,PT)
      ZT(1,PT)=UO
      RT(1,PT)=VO
      ZT(1,PTU)=UO
      RT(1,PTU)=VO
   10 CONTINUE
      ZCRIT=UTMACH*UTMACH*DDROP
      RCRIT=SQRT((DDROP-ZCRIT)*ZCRIT)+LCORE
      TDUR=RDROP*DR/UINF*(1.-SQRT(1.-UTMACH*UTMACH))
      CYDUR=TDUR/ACDT
      WRITE(6,50) UTMACH,RDROP,ZCRIT,RCRIT,CYDUR,TDUR
   50 FORMAT(/,'COMPRESSIBLE AREA',5F10.4,E15.5,/)
      JS(1)=1
      RS(1)=0.5
      DO 92 K=KSOLID,KEND
      JS(K)=1
      RS(K)=0.
      DO 92 PT=1,NPT
      IF (I(N,PT) .NE. K) GO TO 92
      IF (R(N,PT) .LE. RS(K)) GO TO 92
      JS(K)=J(N,PT)
      RS(K)=R(N,PT)
   92 CONTINUE
      RETURN
      END
C*******************************************************************************
      SUBROUTINE FIELD(N,NP,MX,MY,NSMA,NSMB)
      COMMON DEN(2,100,100),DENU(2,100,100),DENV(2,100,100)
      COMMON U(2,100,100),V(2,100,100),P(2,100,100)
      COMMON /Q/ QU(2,100,100),QV(2,100,100)
      COMMON /BLRZ/ ZTT(2,200),RTT(2,200),ZT(2,200),RT(2,200)
      COMMON /BLHR/ H(2,200),R(2,200),I(2,200),J(2,200)
      COMMON /AXIS/ RXIS(200),HXISM(2,200),HXISP(2,200)
      COMMON /BLKB/ KBM(2,200),KBP(2,200)
      COMMON /JR/ JS(100),RS(100)
      COMMON /BTOP/ HMAX(500),RMAX(500),HJET(500),RJET(500)
      COMMON /BTOP/ HMIN(500),RMIN(500),HTOP(500),ZA(500),ZB(500)
      COMMON /BTOP/ ZC(500),ZD(500),ZE(500),ZF(500),ZG(500),ZH(500)
      COMMON /BLO/ DENO,DENUO,DENVO,UO,VO,PO,DENP,PP
```

```
      COMMON /BLB/ KEND,LEND,LRAD,RDROP,KCORE,LCORE,KSOLID,HSOLID
      COMMON /BLD/ DT,DZ,DR,STAFAC,TDZ,TDR,TDP
      COMMON /BLD/ DINF,UINF,PINF,CINF,UTMACH,PHAMER
      COMMON /BLP/ NPT,NMAX,NJET,NMIN,LMAX,LJET,LMIN,LTIP,NTIP,KTOP
      COMMON /S/ CYCLE,NSTAGE,NPRINT,TIME
      COMMON /BLAB/ A,B,CT,CS
      COMMON /BT/ TOUCH(200)
      COMMON /BMAS/ MASS(500),MASSO,PI
      COMMON /BEND/ KEND2,LEND2,KEND3,LEND3,KLD,NKTT
      COMMON /BCRIT/ PCRIT, DECRIT,CONST
      COMMON /CV/ CO,CP,C1,C2,C3,COEF,ALPHA,COEG
      COMMON /HAB/ HA,HB,GA,GB,GC,FA,FB,FC,DENB,DMAX,DMIN,NSM,DA,DB
      COMMON /BFL/ JA,JB,JC,JD,JE,JF,JG,JH,JI,JJ,JK,JL,JM,JN
      COMMON /BFL/ JU,JV,JW,JX,JY,JZ
      DIMENSION DENZ(20000),DENUZ(20000),DENVZ(20000)
      DIMENSION UZ(20000),VZ(20000),PZ(20000)
      EQUIVALENCE (DEN,DENZ),(DENU,DENUZ),(DENV,DENVZ)
      EQUIVALENCE (U,UZ),(V,VZ),(P,PZ)
      DIMENSION QUZ(20000),QVZ(20000)
      EQUIVALENCE (QU,QUZ),(QV,QVZ)
      REAL MASS,MASSO
      INTEGER CYCLE
      INTEGER PT,PTM,PTP
   81 FORMAT (2I3,F10.4,7E15.4)
      DMAX=PCRIT
      DMIN=1.
      DPT=0.
      DPR=0.
      KDPT=1
      LDPT=1
      KDPR=1
      LDPR=1
      DO 15 PT=1,NPT
      K=I(NP,PT)
      L=J(NP,PT)
      NPKL=NP+(K-1)*2+(L-1)*NKTT
      IF (K .EQ. KSOLID .AND. L .LE. JS(1)) GO TO 16
      DENZ(NPKL)=DENO
      PZ(NPKL)=PO
      UZ(NPKL)=ZT(NP,PT)
      VZ(NPKL)=RT(NP,PT)
      DENUZ(NPKL)=DENZ(NPKL)*UZ(NPKL)
      DENVZ(NPKL)=DENZ(NPKL)*VZ(NPKL)
      GO TO 15
   16 CONTINUE
      KP=K+1
      KM=K-1
      LP=L+1
      LM=L-1
      IF(L .NE. 1) GO TO 18
      LP=1
      LM=1
   18 CONTINUE
      KR=(K-1)*2
      LR=(L-1)*NKTT
      NKL=N+KR+LR
      NKPL=NKL+2
      NKML=NKL-2
      NKLP=N+(K-1)*2+(LP-1)*NKTT
      NKLM=N+(K-1)*2+(LM-1)*NKTT
```

```
      RO=L
      RI=L-1
      RDR=(RO+RI)/2.
      TRDR=TDR/RDR
      DAVE=GA*DENZ(NKL)
     &+GB*(DENZ(NKML)+DENZ(NKPL)+DENZ(NKLM)+DENZ(NKLP))
     &+GC*(DEN(N,KP,LM)+DEN(N,KM,LM)+DEN(N,KP,LP)+DEN(N,KM,LP))
      IF(ALPHA .EQ. 0.) GO TO 2
      DU=UZ(NKPL)-UZ(NKML)
      DV=VZ(NKLM)-VZ(NKLP)
      QUZ(NPKL)=FQ(DAVE,DU)
      QVZ(NPKL)=FQ(DAVE,DV)
      GO TO 4
    2 QUZ(NPKL)=0.
      QVZ(NPKL)=0.
    4 CONTINUE
      DENZ(NPKL)=DAVE
     &+(DENUZ(NKPL)-DENUZ(NKML))*TDZ
     &+(DENVZ(NKLM)*RI-DENVZ(NKLP)*RO)*TRDR
      DE=DENZ(NPKL)
      IF (DE .LE. DMAX) GO TO 7
      DMAX=DE
      KDMAX=K
      LDMAX=L
    7 CONTINUE
      IF (DE .GE. DMIN) GO TO 9
      DMIN=DE
      KDMIN=K
      LDMIN=L
    9 CONTINUE
      DENUZ(NPKL)=GA*DENUZ(NKL)
     &+GB*(DENUZ(NKPL)+DENUZ(NKML)+DENUZ(NKLM)+DENUZ(NKLP))
     &+GC*(DENU(N,KP,LM)+DENU(N,KM,LM)+DENU(N,KP,LP)+DENU(N,KM,LP))
     &+(DENUZ(NKPL)*UZ(NKPL)-DENUZ(NKML)*UZ(NKML))*TDZ
     &+(DENVZ(NKLM)*UZ(NKLM)*RI-DENVZ(NKLP)*UZ(NKLP)*RO)*TRDR
     &+FA*(PZ(NKPL)-PZ(NKML))*TDP
     &-QUZ(NPKL)*TDP
      DENVZ(NPKL)=GA*DENVZ(NKL)
     &+GB*(DENVZ(NKPL)+DENVZ(NKML)+DENVZ(NKLM)+DENVZ(NKLP))
     &+GC*(DENV(N,KP,LM)+DENV(N,KM,LM)+DENV(N,KP,LP)+DENV(N,KM,LP))
     &+(DENUZ(NKPL)*VZ(NKPL)-DENUZ(NKML)*VZ(NKML))*TDZ
     &+(DENVZ(NKLM)*VZ(NKLM)*RI-DENVZ(NKLP)*VZ(NKLP)*RO)*TRDR
     &+FA*(PZ(NKLM)-PZ(NKLP))*TDP
     &-QVZ(NPKL)*TDP
      IF (DE .LT. DECRIT) DE=DECRIT
      UZ(NPKL)=DENUZ(NPKL)/DE
      VZ(NPKL)=DENVZ(NPKL)/DE
      PZ(NPKL)=FP(DENZ(NPKL))
      IF (L .LT. JS(1)) GO TO 17
      DENZ(NPKL)=DENO
      PZ(NPKL)=PO
   17 CONTINUE
   15 CONTINUE
C------GET SUBROUTINES
      CALL PARTA(N,NP,KDMAX,LDMAX,KDMIN,LDMIN)
      IF(KLD .EQ. 1) GO TO 69
      CALL PARTB(N,NP,KDMAX,LDMAX,KDMIN,LDMIN)
      CALL PARTC(N,NP,KDMAX,LDMAX,KDMIN,LDMIN)
   69 CONTINUE
      IF(DMIN .GE. 0.) GO TO 79
```

```
      WRITE(6,78) CYCLE,DMAX,KDMAX,LDMAX,DMIN,KDMIN,LDMIN
   78 FORMAT(/,'***NEGATIVE DENSITY***',I5,2(F10.4,2I4))
      GO TO 77
   79 CONTINUE
      WRITE (6,65) CYCLE,DMAX,KDMAX,LDMAX,DMIN,KDMIN,LDMIN
   65 FORMAT(I5,2(F10.4,2I4))
   77 CONTINUE
C*****DOMAIN BOUNDARY CELLS CONDITIONS
      CALL DOMAIN(N,NP,DENO,NSMA,NSMB)
      IF(NSMA .NE. 1) GO TO 39
      KLD=1
      CALL PRIN(NP)
      KLD=2
   39 CONTINUE
      CALL AVE(N,NP)
      K=2
      DO 35 L=1,JB,KLD
      LP=L+1
      LM=L-1
      DP=P(NP,K,L)-P(N,K,L)
      IF(ABS(DP) .LE. DPT) GO TO 36
      DPT=DP
      KDPT=K
      LDPT=L
   36 CONTINUE
      DP=P(NP,K,L)-P(NP,K,LP)
      IF(ABS(DP) .LE. DPR) GO TO 37
      DPR=DP
      KDPR=K
      LDPR=L
   37 CONTINUE
   35 CONTINUE
      WRITE(6,38) CYCLE,KDPT,LDPT,DPT,KDPR,LDPR,DPR
   38 FORMAT(I5,'  DP/DT  ',2I3,E15.5,'  DP/DR  ',2I3,E15.5)
      DPT=P(NP,K,JX)-P(N,K,JX)
      DPR=P(NP,K,JY)-P(NP,K,JZ)
      DPRT=P(NP,K,JY)-P(N,K,JY)
   20 CONTINUE
      IF (NSMB .EQ. 1) GO TO 67
C*****PHASE BOUNDARY CELLS CONDITIONS
    5 CONTINUE
      DO 70 PT=2,NPT
      PTM=PT-1
      IF (I(NP,PTM) .EQ. I(NP,PT)) GO TO 70
      IF (J(NP,PTM)-J(NP,PT)) 71,72,73
   71 DENV(NP,I(NP,PTM),J(NP,PT))=DENV(NP,I(NP,PTM),J(NP,PTM))
         V(NP,I(NP,PTM),J(NP,PT))=   V(NP,I(NP,PTM),J(NP,PTM))
      GO TO 70
   72 DENV(NP,I(NP,PTM),(J(NP,PTM)+1))=DENV(NP,I(NP,PTM),J(NP,PTM))
         V(NP,I(NP,PTM),(J(NP,PTM)+1))=   V(NP,I(NP,PTM),J(NP,PTM))
      DENV(NP,I(NP,PT ),(J(NP,PT )+1))=DENV(NP,I(NP,PT ),J(NP,PT ))
         V(NP,I(NP,PT ),(J(NP,PT )+1))=   V(NP,I(NP,PT ),J(NP,PT ))
      GO TO 70
   73 DENV(NP,I(NP,PT),J(NP,PTM))=DENV(NP,I(NP,PT ),J(NP,PT ))
         V(NP,I(NP,PT),J(NP,PTM))=   V(NP,I(NP,PT ),J(NP,PT ))
   70 CONTINUE
   67 CONTINUE
      NH=CYCLE
      ZA(NH)=P(NP,1,1)
      ZB(NH)=P(NP,JE,JF)
```

```
      ZC(NH)=P(NP,JG,JH)
      ZD(NH)=P(NP,JI,JJ)
      ZE(NH)=P(NP,JK,JL)
      ZF(NH)=DPT
      ZG(NH)=DPR
      ZH(NH)=DPRT
      WRITE(6,21) NH,ZA(NH),ZB(NH),ZC(NH).ZD(NH),ZE(NH)
   21 FORMAT(I5,8E15.4)
      RETURN
      END
C*****HISTORY OF LIQUOD BOUNDARY ***************************************
      SUBROUTINE BOUND(N,NP,TSTEP)
      COMMON DEN(2,100,100),DENU(2,100,100),DENV(2,100,100)
      COMMON U(2,100,100),V(2,100,100),P(2,100,100)
      COMMON /BLRZ/ ZTT(2,200),RTT(2,200),ZT(2,200),RT(2,200)
      COMMON /BLHR/ H(2,200),R(2,200),I(2,200),J(2,200)
      COMMON /AXIS/ RXIS(200),HXISM(2,200),HXISP(2,200)
      COMMON /BLKB/ KBM(2,200),KBP(2,200)
      COMMON /JR/ JS(100),RS(100)
      COMMON /BTOP/ HMAX(500),RMAX(500),HJET(500),RJET(500)
      COMMON /BTOP/ HMIN(500),RMIN(500),HTOP(500)
      COMMON /BLO/ DENO,DENUO,DENVO,UO,VO,PO,DENP,PP
      COMMON /BLB/ KEND,LEND,LRAD,RDROP,KCORE,LCORE,KSOLID,HSOLID
      COMMON /BEND/ KEND2,LEND2,KEND3,LEND3,KLD
      COMMON /BLD/ DT,DZ,DR,STAFAC,TDZ,TDR,TDP
      COMMON /BLD/ DINF,UINF,PINF,CINF,UTMACH,PHAMER
      COMMON /BLP/ NPT,NMAX, NJET,NMIN,LMAX,LJET,LMIN,LTIP,NTIP,KTOP
      COMMON /S/ CYCLE,NSTAGE,NPRINT,TIME
      COMMON /HAB/ HA,HB,GA,GB,GC,FA,FB,FC,DENB,DMAX,DMIN,NSM,DA,DB
      COMMON /BFL/ JA,JB,JC,JD,JE,JF,JG,JH,JI,JJ,JK,JL,JM,JN
      COMMON /BFL/ JU,JV,JW,JX,JY,JZ
      COMMON /BLAB/ A,B,CT,CS
      COMMON /BT/ TOUCH(200)
      COMMON /BMAS/ MASS(500),MASSO,PI
      REAL MASS,MASSO
      INTEGER CYCLE
      INTEGER PT,PTM,PTP
C     1
      M=0
      DO 1 PT=1,NPT
      PTM=PT-1
      K=I(N,PT)
      KM=K-1
      KP=K+1
      L=J(N,PT)
      LM=L-1
      LP=L+1
      DE=DEN(N,K,L)
      IF (L .NE. 1) GO TO 11
      RTT(N,PT)=0.
      RTT(NP,PT)=0.
      RT(NP,PT)=0.
      R(NP,PT)=0.5
      GO TO 12
   11 CONTINUE
      RTT(N,PT)=(P(N,K,LM)-P(N,K,LP))
      RTT(N,PT)=RTT(N,PT)/DE
      RT(NP,PT)=RT(N,PT)+RTT(N,PT)*TDP
      R(NP,PT)=R(N,PT)+(RT(NP,PT)+RT(N,PT))*TDR*TSTEP/2.
      IF (R(NP,PT) .GT. 0.5) GO TO 12
```

```
      R(NP,PT)=0.5
      RT(NP,PT)=0.
   12 CONTINUE
      ZTT(N,PT)=(P(N,KP,L)-P(N,KM,L))
      ZTT(N,PT)=ZTT(N,PT)/DE
      ZT(NP,PT)=ZT(N,PT)+ZTT(N,PT)*TDP
      H(NP,PT)=H(N,PT)-(ZT(NP,PT)+ZT(N,PT))*TDZ*TSTEP/2.
      IF(H(NP,PT) .GT. HSOLID) GO TO 2
      IF(H(NP,PT) .EQ. H(N,PT)) GO TO 3
      PCT=(HSOLID-H(NP,PT))/(H(N,PT)-H(NP,PT))
      GO TO 4
    3 PCT=1.0
    4 CONTINUE
      M=M+1
      H(NP,PT)=HSOLID
      ZT(NP,PT)=0.0
      ZTT(NP,PT)=(-ZTT(N,PT)-ZT(N,PT)/TDP)*PCT
      DENU(N,KM,L)=0.
      DENU(NP,KM,L)=0.
      DENU(N,K,L)=DA*DENU(N,K,L)
      U(N,KM,L)=0.
      U(NP,KM,L)=0.
      U(N,K,L)=DENU(N,K,L)/DE
    2 CONTINUE
      I(NP,PT)=H(NP,PT)+1.0
      J(NP,PT)=R(NP,PT)+1.0
    1 CONTINUE
      PT=0
    7 CONTINUE
      PT=PT+1
      MH=PT
      IF (PT .GE. M) GO TO 9
      MM=1
    8 CONTINUE
      PT=MH+MM
      IF (PT .GT. M) GO TO 17
      IF (R(NP,PT) .GT. R(NP,MH)) GO TO 17
      MM=MM+1
      GO TO 8
   17 IF (MM .EQ. 1) GO TO 7
      DRR=R(NP,PT)-R(NP,MH)
      DRT=RT(NP,MH)-RT(NP,PT)
      IF (DRT .EQ. 0.) GO TO 7
      TMET=DRR/DRT
      RMET=R(NP,PT)+RT(NP,PT)*TMET
      IF (RMET .LT. 0.5) RMET=0.5
      RTMET=(RT(NP,PT)+RT(NP,MH))/2.
      DO 18 MJ=MH,PT
      R(NP,MJ)=RMET
      RT(NP,MJ)=RTMET
   18 CONTINUE
      IF(PT .LT. M) GO TO 7
    9 CONTINUE
      HTOP(CYCLE)=H(NP,NPT)
      HMAX(CYCLE)=H(NP,NMAX)
      RMAX(CYCLE)=R(NP,NMAX)
      HJET(CYCLE)=H(NP,NJET)
      RJET(CYCLE)=R(NP,NJET)
      PT=1
   10 CONTINUE
```

```
      PT=PT+1
      IF(PT .GE. NPT) GO TO 35
      PTM=PT-1
      IDF=IABS(I(NP,PT)-I(NP,PTM))
      JDF=IABS(J(NP,PT)-J(NP,PTM))
      IF(IDF .LE. 1 .AND. JDF .LE. 1) GO TO 10
      KDF=IDF
      IF(JDF .GT. KDF) KDF=JDF
      KDFM=KDF-1
      IF(KDFM .LT. JW) GO TO 36
      WRITE(6,37) PT,I(NP,PT),J(NP,PT),I(NP,PTM),J(NP,PTM)
   37 FORMAT(/,'**CHECK**',6I5)
      JN=0
   36 CONTINUE
      M=NPT
   15 CONTINUE
      MP=M+KDFM
      I(NP,MP)=I(NP,M)
      J(NP,MP)=J(NP,M)
      H(NP,MP)=H(NP,M)
      R(NP,MP)=R(NP,M)
      ZT(NP,MP)=ZT(NP,M)
      RT(NP,MP)=RT(NP,M)
      M=M-1
      IF(M .GE. PT) GO TO 15
      MPM=MP-1
      DO 16 MB=PT,MPM
      KDG=MB-PTM
      R(NP,MB)=R(NP,PTM)+(R(NP,MP)-R(NP,PTM))*KDG/KDF
      H(NP,MB)=H(NP,PTM)+(H(NP,MP)-H(NP,PTM))*KDG/KDF
      I(NP,MB)=H(NP,MB)+1.0
      J(NP,MB)=R(NP,MB)+1.0
      RT(NP,MB)=RT(NP,PTM)+(RT(NP,MP)-RT(NP,PTM))*KDG/KDF
      ZT(NP,MB)=ZT(NP,PTM)+(ZT(NP,MP)-ZT(NP,PTM))*KDG/KDF
      WRITE(6,52) MB,I(NP,MB),J(NP,MB),H(NP,MB),R(NP,MB)
     & ,ZT(NP,MB),RT(NP,MB)
   52 FORMAT ('NEW POINT', I3,5X,2I3,4F10.4)
   16 CONTINUE
      IF(KDFM .LE. JW) GO TO 39
      CALL PRIN(NP)
      GO TO 71
   39 CONTINUE
      IF(NMAX .GT. PTM) NMAX=NMAX+KDFM
      IF(NJET .GT. PTM) NJET=NJET+KDFM
      IF(NMIN .GT. PTM) NMIN=NMIN+KDFM
      IF(NTIP .GT. PTM) NTIP=NTIP+KDFM
      NPT=NPT+KDFM
      PT=PT+KDFM
      GO TO 10
   35 CONTINUE
      PT=0
   80 CONTINUE
      PT=PT+1
      IF (PT .GE. NPT) GO TO 90
      M=1
   82 CONTINUE
      MPT=PT+M
      IF (MPT .GT. NPT) GO TO 84
      IF (I(NP,MPT) .NE. I(NP,PT)) GO TO 84
      IF (J(NP,MPT) .NE. J(NP,PT)) GO TO 84
```

```
      M=M+1
      GO TO 82
   84 IF (M .EQ. 1) GO TO 80
      MM=M-1
      DO 86 MG=1,MM
      MGPT=PT+MG
      R(NP,PT)=R(NP,PT)+R(NP,MGPT)
      H(NP,PT)=H(NP,PT)+H(NP,MGPT)
      RT(NP,PT)=RT(NP,PT)+RT(NP,MGPT)
      ZT(NP,PT)=ZT(NP,PT)+ZT(NP,MGPT)
   86 CONTINUE
      R(NP,PT)=R(NP,PT)/M
      H(NP,PT)=H(NP,PT)/M
      I(NP,PT)=H(NP,PT)+1.
      J(NP,PT)=R(NP,PT)+1.
      RT(NP,PT)=RT(NP,PT)/M
      ZT(NP,PT)=ZT(NP,PT)/M
      WRITE (6,87) M,I(NP,PT),J(NP,PT),H(NP,PT),R(NP,PT)
     &,ZT(NP,PT),RT(NP,PT)
   87 FORMAT('GROUPING',I4,5X,2I3,4F10.4)
   88 CONTINUE
      NB=MPT-MM
      I(NP,NB)=I(NP,MPT)
      J(NP,NB)=J(NP,MPT)
      H(NP,NB)=H(NP,MPT)
      R(NP,NB)=R(NP,MPT)
      ZT(NP,NB)=ZT(NP,MPT)
      RT(NP,NB)=RT(NP,MPT)
      MPT=MPT+1
      IF (MPT .LE. NPT) GO TO 88
      NPT=NPT-MM
      IF (NMAX .GT. PT) NMAX=NMAX-MM
      IF (NJET .GT. PT) NJET=NJET-MM
      IF (NMIN .GT. PT) NMIN=NMIN-MM
      IF (NTIP .GT. PT) NTIP=NTIP-MM
      GO TO 80
   90 CONTINUE
      DO 6 PT=2,NMAX
      PTM=PT-1
      IF (R(NP,PT) .GE. R(NP,PTM)) GO TO 6
      IF (R(NP,PTM) .GT. R(NP,NJET)) NJET=PTM
      IF(R(NP,PT) .LT. R(NP,NMIN)) NMIN=PT
    6 CONTINUE
      IF(R(NP,NMAX) .GT. R(NP,NTIP)) NTIP=NMAX
      IF(R(NP,NJET) .GT. R(NP,NTIP)) NTIP=NJET
      LMAX=R(NP,NMAX)+1.0
      LJET=R(NP,NJET)+1.0
      LMIN=R(NP,NMIN)+1.0
      LTIP=R(NP,NTIP)+1.0
      NTIPM=NTIP-1
      NJETM=NJET-1
      NMAXM=NMAX-1
      NPTM=NPT-1
      NMINM=NMIN-1
      HXISM(NP,1)=H(NP,1)
      IF(HXISM(NP,1) .LE. 1.5) TOUCH(1)=1.0
      HXISP(NP,1)=H(NP,NPT)
      IF(HXISP(NP,1) .LE. 1.5) TOUCH(1)=2.0
      KBM(NP,1)=I(NP,1)
      KBP(NP,1)=I(NP,NPT)
```

```
      LF=LTIP
      IF(R(NP,NTIP) .LT. RXIS(LTIP)) LF=LTIP-1
      DO 20 L=2,LF
      DO 22 PT=1,NTIPM
      PTP=PT+1
      IF(RXIS(L) .GT. R(NP,PT) .AND. RXIS(L) .LE. R(NP,PTP)) GO TO 24
      GO TO 22
   24 HXISM(NP,L)=H(NP,PT)+(RXIS(L)-R(NP,PT))*(H(NP,PTP)-H(NP,PT))/
     & (R(NP,PTP)-R(NP,PT))
      KBM(NP,L)=HXISM(NP,L)+1.
      IF(HXISM(NP,L) .LE. 1.5) TOUCH(L)=1.0
   22 CONTINUE
   54 FORMAT(2I3,F10.4)
   20 CONTINUE
      DO 26 L=2,LF
      DO 28 PT=NTIP,NPTM
      PTP=PT+1
      IF(RXIS(L) .GT. R(NP,PTP) .AND. RXIS(L) .LE. R(NP,PT)) GO TO 30
      GO TO 28
   30 HXISP(NP,L)=H(NP,PT)+
     & (RXIS(L)-R(NP,PT))*(H(NP,PTP)-H(NP,PT))/(R(NP,PTP)-R(NP,PT))
      KBP(NP,L)=HXISP(NP,L)+1.
      IF(HXISP(NP,L) .LE. 1.5) TOUCH(L)=2.0
   28 CONTINUE
      IF(TOUCH(L) .GT. 0.) JS(1)=L
   26 CONTINUE
      RS(1)=JS(1)
      L=LTIP
      M=0
      KTOP=HTOP(CYCLE)+1.0
      DO 70 PT=1,NPT
      IF (I(NP,PT) .GT. KTOP) KTOP=I(NP,PT)
      IF (J(NP,PT) .NE. L) GO TO 70
      M=M+1
      IF (M .GT. 1) GO TO 72
      HXISM(NP,L)=H(NP,PT)
      KBM(NP,L)=I(NP,PT)
      HXISP(NP,L)=H(NP,PT)
      KBP(NP,L)=I(NP,PT)
      GO TO 70
   72 CONTINUE
      HXISP(NP,L)=H(NP,PT)
      KBP(NP,L)=I(NP,PT)
   70 CONTINUE
      DO 91 K=KSOLID,KEND2
      JS(K)=1
      RS(K)=0.
      DO 92 PT=1,NPT
      IF (I(NP,PT) .NE. K) GO TO 92
      IF (R(NP,PT) .LE. RS(K)) GO TO 92
      JS(K)=J(NP,PT)
      RS(K)=R(NP,PT)
   92 CONTINUE
   91 CONTINUE
      WRITE(6,93) CYCLE,NPT,KTOP,LTIP
   93 FORMAT(/,4I5)
   76 FORMAT(3I3,2F10.4)
   71 CONTINUE
      RETURN
      END
```

```
C*****PRINT*************************************************************
      SUBROUTINE PRIN(NP)
      COMMON DEN(2,100,100),DENU(2,100,100),DENV(2,100,100)
      COMMON U(2,100,100),V(2,100,100),P(2,100,100)
      COMMON /Q/ QU(2,100,100),QV(2,100,100)
      COMMON /BLRZ/ ZTT(2,200),RTT(2,200),ZT(2,200),RT(2,200)
      COMMON /BLHR/ H(2,200),R(2,200),I(2,200),J(2,200)
      COMMON /AXIS/ RXIS(200),HXISM(2,200),HXISP(2,200)
      COMMON /BLKB/ KBM(2,200),KBP(2,200)
      COMMON /BTOP/ HMAX(500),RMAX(500),HJET(500),RJET(500)
      COMMON /BTOP/ HMIN(500),RMIN(500),HTOP(500)
      COMMON /JR/ JS(100),RS(100)
      COMMON /BLO/ DENO,DENUO,DENVO,UO,VO,PO,DENP,PP
      COMMON /BLB/ KEND,LEND,LRAD,RDROP,KCORE,LCORE,KSOLID,HSOLID
      COMMON /BEND/ KEND2,LEND2,KEND3,LEND3,KLD
      COMMON /BLD/ DT,DZ,DR,STAFAC,TDZ,TDR,TDP
      COMMON /BLD/ DINF,UINF,PINF,CINF,UTMACH,PHAMER
      COMMON /BLP/ NPT,NMAX,NJET,NMIN,LMAX,LJET,LMIN,LTIP,NTIP
      COMMON /S/ CYCLE,NSTAGE,NPRINT,TIME,TIMEND,CHLEN
      COMMON /BLAB/ A,B,CT,CS
      COMMON /BT/ TOUCH(200)
      COMMON /BMAS/ MASS(500),MASSO,PI
      COMMON /CV/ CO,CP,C1,C2,C3,COEF,ALPHA,COEG
      COMMON /BFL/ JA,JB,JC,JD,JE,JF,JG,JH,JI,JJ,JK,JL,JM,JN
      COMMON /BFL/ JU,JV,JW,JX,JY,JZ
      REAL MASS,MASSO
      INTEGER CYCLE
      INTEGER PT
      P1=PO*1.01
      P2=PO*0.99
      LTIPP=LTIP+1
      WRITE (6,64) CYCLE,TIME,TIMEND,MASS(NSTAGE)
      WRITE (6,62)
      DO 14 PT=1,NPT
      WRITE(6,70) PT,I(NP,PT),J(NP,PT),H(NP,PT),R(NP,PT)
     & ,ZT(NP,PT),RT(NP,PT)
   14 CONTINUE
      WRITE(6,72)
      WRITE(6,70)(L,KBM(NP,L),KBP(NP,L),HXISM(NP,L),HXISP(NP,L),
     & RXIS(L),TOUCH(L),L=1,LTIP)
      WRITE(6,74)
      WRITE(6,76) (K,JS(K),RS(K),K=1,KEND2)
   74 FORMAT(//,4X,'K    JS    RS'/)
   76 FORMAT(2I5,F10.3)
      K=KSOLID
      WRITE(6,22) K
   22 FORMAT(//,'K=',I3,/,'  L     DENSITY      DEN*U',
     & 10X,'DEN*V',10X,'U',15X,'V',15X,'P',/)
      DO 32 L=1,LTIPP,KLD
      WRITE (6,54) L,DEN(NP,K,L),DENU(NP,K,L),DENV(NP,K,L),
     & U(NP,K,L),V(NP,K,L),P(NP,K,L)
   32 CONTINUE
      DO 20 L=1,LTIPP,KLD
      I1=MOD(L,2)
      WRITE (6,66) L
      KBPP=KBP(NP,L)+1
      IF (L .EQ. LTIPP) KBPP=I(NP,NPT)+1
      K2=JA
      IF(K2 .GT. KBPP) K2=KBPP
      DO 12 K=1,K2,KLD
```

```
      IF (ALPHA .EQ. 0.) GO TO 16
      I2=MOD(K,2)
      IF (I1 .EQ. I2) GO TO 21
   16 CONTINUE
      WRITE (6,54) K,DEN(NP,K,L),DENU(NP,K,L),DENV(NP,K,L),
     & U(NP,K,L),V(NP,K,L),P(NP,K,L)
      GO TO 12
   21 CONTINUE
      IF (QU(NP,K,L) .LT. 0. .OR. QV(NP,K,L) .LT. 0.) GO TO 16
      WRITE (6,54) K,DEN(NP,K,L),DENU(NP,K,L),DENV(NP,K,L)
     &,U(NP,K,L),V(NP,K,L),P(NP,K,L),QU(NP,K,L),QV(NP,K,L)
   12 CONTINUE
   20 CONTINUE
   54 FORMAT (I4,F10.4,7E15.6)
   58 FORMAT (I3)
   60 FORMAT(3I5,2E15.6,2F10.4)
   62 FORMAT(3X,'PT    I    J',T20,'H',T30,'R',T40,'ZT',T50,'RT')
   64 FORMAT(1H1,/,'CYCLE='I3,5X,'TIME='E12.5,10X,
     & 'TIME ND =',E12.5,10X,'MASS=',F9.6)
   66 FORMAT(//,'L=',I3,/,'  K    DENSITY      DEN*U',
     & 10X,'DEN*V',10X,'U',15X,'V',15X,'P',/)
   72 FORMAT(//,4X,'L  KBM  KBP',T20,'HXISM     HXISP      RXIS',
     & 6X,'TOUCH',/)
   70 FORMAT(3I5,4F10.4)
      RETURN
      END
C*****CONSERVATION OF TOTAL MASS **********************************
      SUBROUTINE CONSER(NP)
      COMMON DEN(2,100,100),DENU(2,100,100),DENV(2,100,100)
      COMMON U(2,100,100),V(2,100,100),P(2,100,100)
      COMMON /BLKB/ KBM(2,200),KBP(2,200)
      COMMON /JR/ JS(100),RS(100)
      COMMON /BLHR/ H(2,200),R(2,200),I(2,200),J(2,200)
      COMMON /AXIS/ RXIS(200),HXISM(2,200),HXISP(2,200)
      COMMON /BLO/ DENO,DENUO,DENVO,UO,VO,PO,DENP,PP
      COMMON /BLB/ KEND,LEND,LRAD,RDROP,KCORE,LCORE,KSOLID,HSOLID
      COMMON /BLP/ NPT,NMAX,NJET,NMIN,LMAX,LJET,LMIN,LTIP,NTIP
      COMMON /S/ CYCLE,NSTAGE,NPRINT,TIME
      COMMON /BMAS/ MASS(500),MASSO,PI
      REAL MASS,MASSO
      INTEGER CYCLE,PT,PTM,PTP
      LIMIT=LCORE+LRAD
      LIMITM=LIMIT-1
      AMASS=0.
      L2=LIMITM
      DO 20 L=1,L2
      RO=L
      RI=L-1
      RDR=(RO+RI)/2.
      K1=KBM(NP,L)+1
      K2=KBP(NP,L)-1
      K=KBM(NP,L)
      AMASS=AMASS+DEN(NP,K,L)*2.*PI*RDR*
     & (K1-1-HXISM(NP,L))
      DO 22 K=K1,K2
      IF (L .GT. JS(K)) GO TO 22
      AMASS=AMASS+DEN(NP,K,L)*2.*PI*RDR
   22 CONTINUE
      K=KBP(NP,L)
      AMASS=AMASS+DEN(NP,K,L)*2.*PI*RDR*
```

```
     & (HXISP(NP,L)-K2)
  20 CONTINUE
     RTEP=LIMIT-0.5
     IF (L2 .GE. LTIP) GO TO 50
     L3=L2+1
     L4=LTIP-1
     IF(L4 .LT. L3) GO TO 50
     DO 30 L=L3,L4
     RDR=RTEP*L/LTIP
     K1=KBM(NP,L)+1
     K2=KBP(NP,L)-1
     K=KBM(NP,L)
     AMASS=AMASS+DEN(NP,K,L)*2.*PI*RDR*
    & (K1-1-HXISM(NP,L))
     DO 32 K=K1,K2
     IF (L .GT. JS(K)) GO TO 32
     AMASS=AMASS+DEN(NP,K,L)*2.*PI*RDR
  32 CONTINUE
     K=KBP(NP,L)
     AMASS=AMASS+DEN(NP,K,L)*2.*PI*RDR*
    & (HXISP(NP,L)-K2)
  30 CONTINUE
  50 CONTINUE
     XL=LIMITM
     RTEP=(RTEP+XL)/2.
     L=LTIP
     LG=0
     DO 40 PT=1,NPT
     IF(J(NP,PT) .LT. LTIP) GO TO 40
     PTM=PT-1
     PTP=PT+1
     LG=LG+1
     K=I(NP,PT)
     RDR=RTEP
     IF(LG .GT. 1) GO TO 42
     RDR=RDR*(K-H(NP,PT))
     GO TO 44
  42 CONTINUE
     IF(I(NP,PT) .EQ. I(NP,PTM)) GO TO 40
     IF(J(NP,PTP) .LT. LTIP) RDR=RDR*(H(NP,PT)+1-K)
  44 CONTINUE
     AMASS=AMASS+DEN(NP,K,L)*2.*PI*RDR
    & *(R(NP,PT)+1.-J(NP,PT))
  40 CONTINUE
 100 CONTINUE
     MASS(NSTAGE)=AMASS/MASSO
     WRITE(6,24) CYCLE,AMASS,MASSO,MASS(NSTAGE)
  24 FORMAT(I5,3E20.5)
     RETURN
     END
C*****SUBFUNCTION TO EVALUATE SHOCK WAVE VELOCITY **********************
     FUNCTION FW(V)
     COMMON /BLAB/ A,B,CT,CS
     COMMON /CV/ CO,CP,C1,C2,C3,COEF,ALPHA,COEG
     COMMON /NNP/ N,NP
     VCP=V/CP
     CE=(C1+C2*VCP+C3*VCP*VCP)*CP
     VC=V/CE
     IF (1.-VC) 1,1,2
   1 WRITE (6,3) V,CP,VCP,CE,VC
```

```
    3 FORMAT('FW CHECK',5E15.6)
      CALL PRIN(N)
      CALL PRIN(NP)
    2 CONTINUE
      T3=(1.-VC)**A
      T1=1.-T3
      T2=VC*T3
      FW=COEF*SQRT(T1/T2)
      RETURN
      END
C*****SUBFUNCTION TO EVALUATE ARTIFICIAL VISCOSITY ******************
      FUNCTION FQ(DEN,W)
      COMMON /BLAB/ A,B,CT,CS
      COMMON /CV/ CQ,CP,C1,C2,C3,COEF,ALPHA,COEG
      IF (ALPHA) 1,1,4
    4 IF (W) 1,1,2
    1 FQ=0.
      GO TO 3
    2 FQ=COEG*DEN*FW(W)*W
      FQ=ALPHA*FQ
    3 CONTINUE
      RETURN
      END
C*****SUBFUNCTION : EQUATION OF STATE OF WATER ******************
      FUNCTION FP(DEN)
      COMMON /BLO/ DENO,DENUO,DENVO,UO,VO,PO,DENP,PP
      COMMON /BLAB/ A,B,CT,CS
      COMMON /BCRIT/ PCRIT,DECRIT,CONST
      IF (DEN .GT. DECRIT) GO TO 9
      FP=PCRIT
      GO TO 5
    9 CONTINUE
      FP=DEN**A*(B+PO)-B
    5 CONTINUE
      RETURN
      END
C*****SUBFUNCTION TO CALCULATE DENSITY BY KNOWING PRESSURE*******************
      FUNCTION FD(P)
      COMMON /BLO/ DENO,DENUO,DENVO,UO,VO,PO,DENP,PP
      COMMON /BLAB/ A,B,CT,CS
      COMMON /BCRIT/ PCRIT,DECRIT,CONST
      IF (P .GT. PCRIT) GO TO 1
      FD=DECRIT
      GO TO 2
    1 CONTINUE
      FD=((P+B)/(PO+B))**(1.0/A)
    2 CONTINUE
      RETURN
      END
C*******************************************************************************
C*****  EULERIAN CALCULATION PART A  ***********************************
      SUBROUTINE PARTA(N,NP,KDMAX,LDMAX,KDMIN,LDMIN)
      COMMON DEN(2,100,100),DENU(2,100,100),DENV(2,100,100)
      COMMON U(2,100,100),V(2,100,100),P(2,100,100)
      COMMON /Q/ QU(2,100,100),QV(2,100,100)
      COMMON /BLKB/ KBM(2,200),KBP(2,200)
      COMMON /BLB/ KEND,LEND,LRAD,RDROP,KCORE,LCORE,KSOLID,HSOLID
      COMMON /BLD/ DT,DZ,DR,STAFAC,TDZ,TDR,TDP
      COMMON /BEND/ KEND2,LEND2,KEND3,LEND3,KLD,NKTT
      COMMON /BLO/ DENO,DENUO,DENVO,UO,VO,PO,DENP,PP
```

```
      COMMON /BCRIT/ PCRIT,DECRIT,CONST
      COMMON /JR/ JS(100),RS(100)
      COMMON /BLP/ NPT,NMAX,NJET,NMIN,LMAX,LJET,LMIN,LTIP,NTIP,KTOP
      COMMON /S/ CYCLE,NSTAGE,NPRINT,TIME,TIMEND,CHLEN
      COMMON /HAB/ HA,HB,GA,GB,GC,FA,FB,FC,DENB,DMAX,DMIN
      COMMON /BFL/ JA,JB,JC,JD,JE,JF,JG,JH,JI,JJ,JK,JL,JM,JN
      DIMENSION DENZ(20000),DENUZ(20000),DENVZ(20000)
      DIMENSION UZ(20000),VZ(20000),PZ(20000)
      EQUIVALENCE (DEN,DENZ),(DENU,DENUZ),(DENV,DENVZ)
      EQUIVALENCE (U,UZ),(V,VZ),(P,PZ)
      DIMENSION QUZ(20000),QVZ(20000)
      EQUIVALENCE (QU,QUZ),(QV,QVZ)
C------PRELIMINARY CALCULATIONS
C  107
      JBP=JB+1
      DO 107 L=2,JBP,KLD
      LM=L-1
      LP=L+1
      RO=L
      RI=L-1
      RDR=(RO+RI)/2.
      IRDR=IDR/RDR
      KHI=KBP(NP,L)
      KLO=KBM(NP,L)
      LR=(L-1)*NKTT
      KLOL=NP+(KLO-1)*2+LR
      KHIL=NP+(KHI-1)*2+LR
C------FIRST STEP CALCULATION
C  101
      JAP=JA+1
      DO 101 K=2,JAP,KLD
      KM=K-1
      KP=K+1
      KR=(K-1)*2
      NPKL=NP+KR+LR
      NKL=N+KR+LR
      NKPL=NKL+2
      NKML=NKL-2
      NKLP=NKL+NKTT
      NKLM=NKL-NKTT
      NPKPL=NPKL+2
      NPKML=NPKL-2
      NPKLP=NPKL+NKTT
      NPKLM=NPKL-NKTT
      IF (L .GT. JS(K)) GO TO 104
      IF (L .EQ. JS(K)) GO TO 101
      IF(K .LT. KLO) GO TO 105
      IF(K .EQ. KLO) GO TO 101
      IF(K .EQ. KHI) GO TO 101
      IF (K .GT. KHI) GO TO 106
      GO TO 102
  104 CONTINUE
      DENZ(NPKL)=DENB
      DENUZ(NPKL)=DENUZ(NKL)
      DENVZ(NPKL)=DENVZ(NKL)
      UZ(NPKL)=UZ(NKL)
      VZ(NPKL)=VZ(NKL)
      PZ(NPKL)=PO
      GO TO 101
  105 CONTINUE
```

```
      DENZ(NPKL)=DENB
      DENUZ(NPKL)=DENUZ(KLOL)
      DENVZ(NPKL)=DENVZ(KLOL)
      UZ(NPKL)=UZ(KLOL)
      VZ(NPKL)=VZ(KLOL)
      PZ(NPKL)=PO
      GO TO 101
  106 CONTINUE
      DENZ(NPKL)=DENB
      DENUZ(NPKL)=DENUZ(KHIL)
      DENVZ(NPKL)=DENVZ(KHIL)
      UZ(NPKL)=UZ(KHIL)
      VZ(NPKL)=VZ(KHIL)
      PZ(NPKL)=PO
      GO TO 101
  102 CONTINUE
      DAVE=GA*DENZ(NKL)
     &+GB*(DENZ(NKML)+DENZ(NKPL)+DENZ(NKLM)+DENZ(NKLP))
     &+GC*(DEN(N,KP,LM)+DEN(N,KM,LM)+DEN(N,KP,LP)+DEN(N,KM,LP))
      IF(ALPHA .EQ. 0.) GO TO 2
      DU=UZ(NKPL)-UZ(NKML)
      DV=VZ(NKLM)-VZ(NKLP)
      QUZ(NPKL)=FQ(DAVE,DU)
      QVZ(NPKL)=FQ(DAVE,DV)
      GO TO 4
    2 QUZ(NPKL)=0.
      QVZ(NPKL)=0.
    4 CONTINUE
      DENZ(NPKL)=DAVE
     &+(DENUZ(NKPL)-DENUZ(NKML))*TDZ
     &+(DENVZ(NKLM)*RI-DENVZ(NKLP)*RO)*TRDR
      DE=DENZ(NPKL)
      IF (DE .LE. DMAX) GO TO 7
      DMAX=DE
      KDMAX=K
      LDMAX=L
    7 CONTINUE
      IF (DE .GE. DMIN) GO TO 9
      DMIN=DE
      KDMIN=K
      LDMIN=L
    9 CONTINUE
      DENUZ(NPKL)=GA*DENUZ(NKL)
     &+GB*(DENUZ(NKPL)+DENUZ(NKML)+DENUZ(NKLM)+DENUZ(NKLP))
     &+GC*(DENU(N,KP,LM)+DENU(N,KM,LM)+DENU(N,KP,LP)+DENU(N,KM,LP))
     &+(DENUZ(NKPL)*UZ(NKPL)-DENUZ(NKML)*UZ(NKML))*TDZ
     &+(DENVZ(NKLM)*UZ(NKLM)*RI-DENVZ(NKLP)*UZ(NKLP)*RO)*TRDR
     &+FA*(PZ(NKPL)-PZ(NKML))*TDP
     &-QUZ(NPKL)*TDP
      DENVZ(NPKL)=GA*DENVZ(NKL)
     &+GB*(DENVZ(NKPL)+DENVZ(NKML)+DENVZ(NKLM)+DENVZ(NKLP))
     &+GC*(DENV(N,KP,LM)+DENV(N,KM,LM)+DENV(N,KP,LP)+DENV(N,KM,LP))
     &+(DENUZ(NKPL)*VZ(NKPL)-DENUZ(NKML)*VZ(NKML))*TDZ
     &+(DENVZ(NKLM)*VZ(NKLM)*RI-DENVZ(NKLP)*VZ(NKLP)*RO)*TRDR
     &+FA*(PZ(NKLM)-PZ(NKLP))*TDP
     &-QVZ(NPKL)*TDP
      IF (DE .LT. DECRIT) DE=DECRIT
      UZ(NPKL)=DENUZ(NPKL)/DE
      VZ(NPKL)=DENVZ(NPKL)/DE
      PZ(NPKL)=FP(DENZ(NPKL))
```

```
  101 CONTINUE
  107 CONTINUE
      RETURN
      END
C****  PART B EULERIAN CALCULATION ****************************************
      SUBROUTINE PARTB(N,NP,KDMAX,LDMAX,KDMIN,LDMIN)
      COMMON DEN(2,100,100),DENU(2,100,100),DENV(2,100,100)
      COMMON U(2,100,100),V(2,100,100),P(2,100,100)
      COMMON /Q/ QU(2,100,100),QV(2,100,100)
      COMMON /BLKB/ KBM(2,200),KBP(2,200)
      COMMON /BLO/ DENO,DENUO,DENVO,UO,VO,PO,DENP,PP
      COMMON /BLD/ DT,DZ,DR,STAFAC,TDZ,TDR,TDP
      COMMON /BLB/ KEND,LEND,LRAD,RDROP,KCORE,LCORE,KSOLID,HSOLID
      COMMON /BEND/ KEND2,LEND2,KEND3,LEND3,KLD,NKTT
      COMMON /BCRIT/ PCRIT,DECRIT,CONST
      COMMON /JR/ JS(100),RS(100)
      COMMON /BLP/ NPT,NMAX,NJET,NMIN,LMAX,LJET,LMIN,LTIP,NTIP,KTOP
      COMMON /S/ CYCLE,NSTAGE,NPRINT,TIME,TIMEND,CHLEN
      COMMON /HAB/ HA,HB,GA,GB,GC,FA,FB,FC,DENB,DMAX,DMIN
      COMMON /BFL/ JA,JB,JC,JD,JE,JF,JG,JH,JI,JJ,JK,JL,JM,JN
      DIMENSION DENZ(20000),DENUZ(20000),DENVZ(20000)
      DIMENSION UZ(20000),VZ(20000),PZ(20000)
      EQUIVALENCE (DEN,DENZ),(DENU,DENUZ),(DENV,DENVZ)
      EQUIVALENCE (U,UZ),(V,VZ),(P,PZ)
      DIMENSION QUZ(20000),QVZ(20000)
      EQUIVALENCE (QU,QUZ),(QV,QVZ)
C------SECOND STEP CALCULATION
C  120
      JBP=JB+1
      DO 120 L=2,JBP,KLD
      KLO=KBM(NP,L)
      KHI=KBP(NP,L)
      LR=(L-1)*NKTT
      KLOL=NP+(KLO-1)*2+LR
      KHIL=NP+(KHI-1)*2+LR
      DO 121 K=3,JA,KLD
      KP=K+1
      KM=K-1
      KR=(K-1)*2
      NPKL=NP+KR+LR
      NKL=N+KR+LR
      NPKPL=NPKL+2
      NPKML=NPKL-2
      IF(L .GT. JS(K)) GO TO 144
      IF (L .EQ. JS(K)) GO TO 121
      IF (K .LT. KLO) GO TO 145
      IF (K .EQ. KLO) GO TO 121
      IF (K .EQ. KHI) GO TO 121
      IF (K .GT. KHI) GO TO 146
      GO TO 142
  144 CONTINUE
      DENZ(NPKL)=DENB
      DENUZ(NPKL)=DENUZ(NKL)
      DENVZ(NPKL)=DENVZ(NKL)
      UZ(NPKL)=UZ(NKL)
      VZ(NPKL)=VZ(NKL)
      PZ(NPKL)=PO
      GO TO 121
  145 CONTINUE
      DENZ(NPKL)=DENB
```

```
      DENUZ(NPKL)=DENUZ(KLOL)
      DENVZ(NPKL)=DENVZ(KLOL)
      UZ(NPKL)=UZ(KLOL)
      VZ(NPKL)=VZ(KLOL)
      PZ(NPKL)=PO
      GO TO 121
  146 CONTINUE
      DENZ(NPKL)=DENB
      DENUZ(NPKL)=DENUZ(KHIL)
      DENVZ(NPKL)=DENVZ(KHIL)
      UZ(NPKL)=UZ(KHIL)
      VZ(NPKL)=VZ(KHIL)
      PZ(NPKL)=PO
      GO TO 121
  142 CONTINUE
      DENZ(NPKL)=(DENZ(NPKPL)+DENZ(NPKML))/2.
      PZ(NPKL)=FP(DENZ(NPKL))
      DE=DENZ(NPKL)
      DENUZ(NPKL)=(DENUZ(NPKPL)+DENUZ(NPKML))/2.
      DENVZ(NPKL)=(DENVZ(NPKPL)+DENVZ(NPKML))/2.
      IF (DE .LT. DECRIT) DE=DECRIT
      UZ(NPKL)=DENUZ(NPKL)/DE
      VZ(NPKL)=DENVZ(NPKL)/DE
  121 CONTINUE
  120 CONTINUE
      DO 122 L=3,JB,KLD
      LP=L+1
      LM=L-1
      KLO=KBM(NP,L)
      KHI=KBP(NP,L)
      LR=(L-1)*NKTT
      KLOL=NP+(KLO-1)*2+LR
      KHIL=NP+(KHI-1)*2+LR
      JAP=JA+1
      DO 123 K=2,JAP,KLD
      KR=(K-1)*2
      NPKL=NP+KR+LR
      NKL=N+KR+LR
      NPKLP=NPKL+NKTT
      NPKLM=NPKL-NKTT
      IF (L .GT. JS(K)) GO TO 154
      IF (L .EQ. JS(K)) GO TO 123
      IF (K .LT. KLO) GO TO 155
      IF (K .EQ. KLO) GO TO 123
      IF (K .EQ. KHI) GO TO 123
      IF (K .GT. KHI) GO TO 156
      GO TO 152
  154 CONTINUE
      DENZ(NPKL)=DENB
      DENUZ(NPKL)=DENUZ(NKL)
      DENVZ(NPKL)=DENVZ(NKL)
      UZ(NPKL)=UZ(NKL)
      VZ(NPKL)=VZ(NKL)
      PZ(NPKL)=PO
      GO TO 123
  155 CONTINUE
      DENZ(NPKL)=DENB
      DENUZ(NPKL)=DENUZ(KLOL)
      DENVZ(NPKL)=DENVZ(KLOL)
      UZ(NPKL)=UZ(KLOL)
```

```
      VZ(NPKL)=VZ(KLOIL)
      PZ(NPKL)=PO
      GO TO 123
  156 CONTINUE
      DENZ(NPKL)=DENB
      DENUZ(NPKL)=DENUZ(KHIL)
      DENVZ(NPKL)=DENVZ(KHIL)
      UZ(NPKL)=UZ(KHIL)
      VZ(NPKL)=VZ(KHIL)
      PZ(NPKL)=PO
      GO TO 123
  152 CONTINUE
      DENZ(NPKL)=(DENZ(NPKLM)+DENZ(NPKLP))/2.
      PZ(NPKL)=FP(DENZ(NPKL))
      DE=DENZ(NPKL)
      DENUZ(NPKL)=(DENUZ(NPKLM)+DENUZ(NPKLP))/2.
      DENVZ(NPKL)=(DENVZ(NPKLM)+DENVZ(NPKLP))/2.
      IF (DE .LT. DECRIT) DE=DECRIT
      UZ(NPKL)=DENUZ(NPKL)/DE
      VZ(NPKL)=DENVZ(NPKL)/DE
  123 CONTINUE
  122 CONTINUE
      RETURN
      END
C*****  EULERIAN CALCULATION PART C ************************************
      SUBROUTINE PARTC(N,NP,KDMAX,LDMAX,KDMIN,LDMIN)
      COMMON DEN(2,100,100),DENU(2,100,100),DENV(2,100,100)
      COMMON U(2,100,100),V(2,100,100),P(2,100,100)
      COMMON /Q/ QU(2,100,100),QV(2,100,100)
      COMMON /BLKB/ KBM(2,200),KBP(2,200)
      COMMON /BLD/ DT,DZ,DR,STAFAC,TDZ,TDR,TDP
      COMMON /BLB/ KEND,LEND,KB,LB,KCORE,LCORE,KSOLID,HSOLID
      COMMON /BEND/ KEND2,LEND2,KEND3,LEND3,KLD,NKTT
      COMMON /BLO/ DENO,DENUO,DENVO,UO,VO,PO,DENP,PP
      COMMON /CV/ CO,CP,C1,C2,C3,COEF,ALPHA,COEG
      COMMON /BCRIT/ PCRIT,DECRIT,CONST
      COMMON /BLP/ NPT,NMAX,NJET,NMIN,LMAX,LJET,LMIN,LTIP,NTIP,KTOP
      COMMON /S/ CYCLE,NSTAGE,NPRINT,TIME,TIMEND,CHLEN
      COMMON /HAB/ HA,HB,GA,GB,GC,FA,FB,FC,DENB,DMAX,DMIN
      COMMON /BFL/ JA,JB,JC,JD,JE,JF,JG,JH,JI,JJ,JK,JL,JM,JN
      DIMENSION DENZ(20000),DENUZ(20000),DENVZ(20000)
      DIMENSION UZ(20000),VZ(20000),PZ(20000)
      EQUIVALENCE (DEN,DENZ),(DENU,DENUZ),(DENV,DENVZ)
      EQUIVALENCE (U,UZ),(V,VZ),(P,PZ)
      DIMENSION QUZ(20000),QVZ(20000)
      EQUIVALENCE (QU,QUZ),(QV,QVZ)
      COMMON /JR/ JS(100),RS(100)
C-----THIRD STEP CALCULATION
      DO 117 L=3,JB,KLD
      LM=L+1
      LP=L+1
      LMM=L-2
      LPP=L+2
      RO=L
      RI=LM
      ROO=RO+1
      RII=RI-1
      RDR=(RO+RI)/2
      TRDR=TDR/RDR
      KLO=KBM(NP,L)
```

```
      KHI=KBP(NP,L)
      LR=(L-1)*NKTT
      KLOL=NP+(KLO-1)*2+LR
      KHIL=NP+(KHI-1)*2+LR
      DO 111 K=3,JA,KLO
      KM=K-1
      KP=K+1
      KMM=K-2
      KPP=K+2
      KR=(K-1)*2
      NPKL=NP+KR+LR
      NKL=N+KR+LR
      NKPL=NKL+2
      NKML=NKL-2
      NKLP=NKL+NKTT
      NKLM=NKL-NKTT
      NPKPL=NPKL+2
      NPKML=NPKL-2
      NPKLP=NPKL+NKTT
      NPKLM=NPKL-NKTT
      IF (L .GT. JS(K)) GO TO 114
      IF (L .EQ. JS(K)) GO TO 111
      IF (K .LT. KLO) GO TO 115
      IF (K .EQ. KLO) GO TO 111
      IF (K .EQ. KHI) GO TO 111
      IF (K .GT. KHI) GO TO 116
      GO TO 112
  114 CONTINUE
      DENZ(NPKL)=DENB
      DENUZ(NPKL)=DENUZ(NKL)
      DENVZ(NPKL)=DENVZ(NKL)
      UZ(NPKL)=UZ(NKL)
      VZ(NPKL)=VZ(NKL)
      PZ(NPKL)=PO
      GO TO 111
  115 CONTINUE
      DENZ(NPKL)=DENB
      DENUZ(NPKL)=DENUZ(KLOL)
      DENVZ(NPKL)=DENVZ(KLOL)
      UZ(NPKL)=UZ(KLOL)
      VZ(NPKL)=VZ(KLOL)
      PZ(NPKL)=PO
      GO TO 111
  116 CONTINUE
      DENZ(NPKL)=DENB
      DENUZ(NPKL)=DENUZ(KHIL)
      DENVZ(NPKL)=DENVZ(KHIL)
      UZ(NPKL)=UZ(KHIL)
      VZ(NPKL)=VZ(KHIL)
      PZ(NPKL)=PO
      GO TO 111
  112 CONTINUE
C -----ESSENTIAL CALCULATION
      IF(ALPHA .EQ. 0.) GO TO 2
      DU=(UZ(NPKPL)-UZ(NPKML)+FC*(U(N,KPP,L)-U(N,KMM,L)))*FB
      DV=(VZ(NPKLM)-VZ(NPKLP)+FC*(V(N,K,LMM)-V(N,K,LPP)))*FB
      QUZ(NPKL)=FQ(DENZ(NKL),DU)
      QVZ(NPKL)=FQ(DENZ(NKL),DV)
      GO TO 4
    2 QUZ(NPKL)=0.
```

```
      QVZ(NPKL)=0.
    4 CONTINUE
      EA=GA*DENZ(NKL)
     &+HA*(DENZ(NPKPL)+DENZ(NPKML)+DENZ(NPKLM)+DENZ(NPKLP))
     &+HB*(DEN(N,KPP,L)+DEN(N,KMM,L)+DEN(N,K,LMM)+DEN(N,K,LPP))
      EB=GA*DENUZ(NKL)
     &+HA*(DENUZ(NPKPL)+DENUZ(NPKML)+DENUZ(NPKLM)+DENUZ(NPKLP))
     &+HB*(DENU(N,KPP,L)+DENU(N,KMM,L)+DENU(N,K,LMM)+DENU(N,K,LPP))
      EC=GA*DENVZ(NKL)
     &+HA*(DENVZ(NPKPL)+DENVZ(NPKML)+DENVZ(NPKLM)+DENVZ(NPKLP))
     &+HB*(DENV(N,KPP,L)+DENV(N,KMM,L)+DENV(N,K,LMM)+DENV(N,K,LPP))
      DENZ(NPKL)=EA+
     &(FB*(DENUZ(NPKPL)-DENUZ(NPKML))
     &+FC*(DENU(N,KPP,L)-DENU(N,KMM,L))
     & )*TDZ+
     &(FB*(DENVZ(NPKLM)*RI-DENVZ(NPKLP)*RO)
     & +FC*(DENV(N,K,LMM)*RII-DENV(N,K,LPP)*ROO)
     & )*TRDR
      DE=DENZ(NPKL)
      IF (DE .LE. DMAX) GO TO 7
      DMAX=DE
      KDMAX=K
      LDMAX=L
    7 CONTINUE
      IF (DE .GE. DMIN) GO TO 9
      DMIN=DE
      KDMIN=K
      LDMIN=L
    9 CONTINUE
      DENUZ(NPKL)=EB+
     &(FB*(DENUZ(NPKPL)*UZ(NPKPL)-DENUZ(NPKML)*UZ(NPKML))
     & +FC*(DENU(N,KPP,L)*U(N,KPP,L)-DENU(N,KMM,L)*U(N,KMM,L))
     & )*TDZ+
     &(FB*(DENVZ(NPKLM)*UZ(NPKLM)*RI-DENVZ(NPKLP)*UZ(NPKLP)*RO)
     & +FC*(DENV(N,K,LMM)*U(N,K,LMM)*RII-DENV(N,K,LPP)*U(N,K,LPP)*ROO)
     & )*TRDR+
     &(FB*(PZ(NPKPL)-PZ(NPKML))
     & +FC*(P(N,KPP,L)-P(N,KMM,L))
     & )*TDP*FA
     &-QUZ(NPKL)*TDP
      DENVZ(NPKL)=EC+
     &(FB*(DENUZ(NPKPL)*VZ(NPKPL)-DENUZ(NPKML)*VZ(NPKML))
     & +FC*(DENU(N,KPP,L)*V(N,KPP,L)-DENU(N,KMM,L)*V(N,KMM,L))
     & )*TDZ+
     &(FB*(DENVZ(NPKLM)*VZ(NPKLM)*RI-DENVZ(NPKLP)*VZ(NPKLP)*RO)
     & +FC*(DENV(N,K,LMM)*V(N,K,LMM)*RII-DENV(N,K,LPP)*V(N,K,LPP)*ROO)
     & )*TRDR+
     &(FB*(PZ(NPKLM)-PZ(NPKLP))
     & +FC*(P(N,K,LMM)-P(N,K,LPP))
     & )*TDP*FA
     &-QVZ(NPKL)*TDP
      IF (DE .LT. DECRIT) DE=DECRIT
      UZ(NPKL)=DENUZ(NPKL)/DE
      VZ(NPKL)=DENVZ(NPKL)/DE
      PZ(NPKL)=FP(DENZ(NPKL))
  111 CONTINUE
  117 CONTINUE
      RETURN
      END
C***** AVERAGE ON THE CELL BOUNDARY ********************************
```

```
      SUBROUTINE AVE(N,NP)
      COMMON DEN(2,100,100),DENU(2,100,100),DENV(2,100,100)
      COMMON U(2,100,100),V(2,100,100),P(2,100,100)
      COMMON /BLB/ KEND,LEND,LRAD,RDROP,KCORE,LCORE,KSOLID,HSOLID
      COMMON /BEND/ KEND2,LEND2,KEND3,LEND3,KLD,NKTT
      COMMON /BLP/ NPT,NMAX,NJET,NMIN,LMAX,LJET,LMIN,LTIP,NTIP,KTOP
      COMMON /JR/ JS(100),RS(100)
      COMMON /BLKB/ KBM(2,200),KBP(2,200)
      COMMON /BT/ TOUCH(200)
      DIMENSION PEN(20000),PENU(20000),PENV(20000)
      DIMENSION AAU(20000),AAV(20000),AAP(20000)
      EQUIVALENCE (DEN(1,1,1),PEN(1)),(DENU(1,1,1),PENU(1))
      EQUIVALENCE (DENV(1,1,1),PENV(1)),(U(1,1,1),AAU(1))
      EQUIVALENCE (V(1,1,1),AAV(1)),(P(1,1,1),AAP(1))
      COMMON /BFL/ JA,JB,JC,JD,JE,JF,JG,JH,JI,JJ,JK,JL,JM,JN
      COMMON /BFL/ JU,JV,JW,JX,JY,JZ
      LTIPM=LTIP-1
      DO 3 L=2,LTIPM,2
      K1=KBM(NP,L)+1
      IF(MOD(K1,2) .EQ. 0) K1=K1+1
      IF(TOUCH(L) .GT. 0.) K1=1
      K2=KBP(NP,L)-1
      IF(K2 .LT. K1) GO TO 3
      LB=NP+(L-1)*NKTT
      DO 1 K=K1,K2,2
      IF(L .GE. JS(K)) GO TO 1
      M=LB+(K-1)*2
      I=M-NKTT
      J=M+NKTT
      PEN(M)=(PEN(I)+PEN(J))/2.
      PENU(M)=(PENU(I)+PENU(J))/2.
      PENV(M)=(PENV(I)+PENV(J))/2.
      AAU(M)=(AAU(I)+AAU(J))/2.
      AAV(M)=(AAV(I)+AAV(J))/2.
      AAP(M)=(AAP(I)+AAP(J))/2.
    1 CONTINUE
    3 CONTINUE
      DO 4 L=1,LTIPM
      K1=KBM(NP,L)+1
      IF(MOD(K1,2) .EQ. 1) K1=K1+1
      IF(TOUCH(L) .GT. 0.) K1=2
      K2=KBP(NP,L)-1
      IF(K2 .LT. K1) GO TO 4
      LB=NP+(L-1)*NKTT
      DO 2 K=K1,K2,2
      IF(L .GE. JS(K)) GO TO 2
      M=LB+(K-1)*2
      I=M-2
      J=M+2
      PEN(M)=(PEN(I)+PEN(J))/2.
      PENU(M)=(PENU(I)+PENU(J))/2.
      PENV(M)=(PENV(I)+PENV(J))/2.
      AAU(M)=(AAU(I)+AAU(J))/2.
      AAV(M)=(AAV(I)+AAV(J))/2.
      AAP(M)=(AAP(I)+AAP(J))/2.
    2 CONTINUE
    4 CONTINUE
      RETURN
      END
C*****SUBROUTINE FOR DOMAIN BOUNDARY CONDITION **************************
```

```
      SUBROUTINE DOMAIN(N,NP,DENO,NSMA,NSMB)
      COMMON DEN(2,100,100),DENU(2,100,100),DENV(2,100,100)
      COMMON U(2,100,100),V(2,100,100),P(2,100,100)
      COMMON /BLB/ KEND,LEND,LRAD,RDROP,KCORE,LCORE,KSOLID,HSOLID
      COMMON /BT/ TOUCH(200)
      COMMON /JR/ JS(100),RS(100)
      COMMON /BEND/ KEND2,LEND2,KEND3,LEND3,KLD,NKTT
      DIMENSION PEN(20000),PENU(20000),PENV(20000)
      DIMENSION AAU(20000),AAV(20000),AAP(20000)
      EQUIVALENCE (DEN(1,1,1),PEN(1)),(DENU(1,1,1),PENU(1))
      EQUIVALENCE (DENV(1,1,1),PENV(1)),(U(1,1,1),AAU(1))
      EQUIVALENCE (V(1,1,1),AAV(1)),(P(1,1,1),AAP(1))
      COMMON /BFL/ JA,JB,JC,JD,JE,JF,JG,JH,JI,JJ,JK,JL,JM,JN
      COMMON /BFL/ JU,JV,JW,JX,JY,JZ
      L1=1+JM
      DO 1 L=L1,JB,JM
      NPO=NP+(L-1)*NKTT
      NPI=NPO+JM*2
      IF (L .GT. JS(1)) GO TO 8
      PEN(NPO)=PEN(NPI)
      IF (PEN(NPO) .LT. DENO) PEN(NPO)=DENO
      AAP(NPO)=AAP(NPI)
      PENU(NPO)=0.
      AAU(NPO)=0.
      GO TO 1
    8 CONTINUE
      PEN(NPO)=PEN(NPI)
      AAP(NPO)=AAP(NPI)
      PENU(NPO)=PENU(NPI)
      AAU(NPO)=AAU(NPI)
    1 CONTINUE
    2 CONTINUE
      DO 3 K=L1,JA,JM
      NPO=NP+(K-1)*2
      NPI=NPO+JM*NKTT
       PEN(NPO)=PEN(NPI)
      PENU(NPO)=PENU(NPI)
      AAU(NPO)=AAU(NPI)
      AAP(NPO)=AAP(NPI)
    3 CONTINUE
    4 CONTINUE
      DEN(NP,1,1)=DEN(NP,L1,1)
      P(NP,1,1)=P(NP,L1,1)
    6 CONTINUE
      RETURN
      END
$SIGNOFF
```

1847 LINES PRINTED